Univerzita Karlova v Praze

Přírodovědecká fakulta

Vývojová a buněčná biologie

Mgr. Ilona Kalasová

Localization and function of phosphoinositides in the cell nucleus

Lokalizace a funkce fosfoinositidů v buněčném jádře

Disertační práce

Školitel: Prof. RNDr. Pavel Hozák, DrSc.

Praha 2016

Prohlášení:

Prohlašuji, že jsem závěrečnou práci zpracovala samostatně a že jsem uvedla všechny použité informační zdroje a literaturu. Tato práce ani její podstatná část nebyla předložena k získání jiného nebo stejného akademického titulu.

V Praze, 16.02.2016

Podpis

In the first place, I have to thank my supervisor Pavel Hozák, who gave me the opportunity to join the project and thought me how to be an independent researcher.

I am very grateful especially to Bětka Kalendová, Sukriye Yildirim and Janka Rohožková, my wise peers and dear friends, who were always very kind to me and helped me from the very beginning of my PhD studies. My special thanks go also to Margarita Sobol, Lívia Uličná and Pavel Kříž, who were always more than willing to help me with literally anything. Thank you for never letting me down.

I am very thankful to Martin Petr and Lenka Jarolímová, who shared our lab corner with me and made it a very special place. I was always looking forward to enjoy their company and our late discussions.

I would like to thank all the other people, namely Veronika Fáberová, Pavel Marášek, Irina Studenyak, Tomáš Venit, Rasťo Dzijak, Lukáš Pastorek, Iva Jelínková, Lenka Pišlová, Ivana Nováková, Zuzka Lubovská, Markéta Morská, Karel Janoušek, Jindřiška Fišerová, Lenka Augustová, Bětka Darašová, and Vlada Filimonenko, for helping me with the experiments and creating a friendly atmosphere.

Most of all, I would like to thank to my dear parents, my little sister and my bellowed Michal for their never-ending support.

I cannot thank you all enough for your help, your support and your friendship. Although I often struggled with my experiments and my determination, these past five years made me the person I am today and I would not change any of it.

Thank you!

ABBREVIATIONS

Akt, protein kinase B

Arp, actin-related protein

B23, nuclephosmin

BASP1, brain acid soluble proten 1

BIK, Bcl2-interacting killer

DAG, diacylglycerol

EN-actin, EYEP-NLS actin

ENTH, epsin N-terminal homology domain

F-actin, filamentous actin

FERM, 4.1/ezrin/radixin/moesin domain

FYVE, Fab1/YOTB/Vac1/EEA domain

G-actin, globular actin

HDAC1, histone deacetylase 1

IMPK, inositol multiphosphate kinase

ING2, ihibitor of growth protein 2

Ins(1,4,5)P3, inositol 1,4,5-trisphosphate

LSD1, lysine-specific histone demethylase 1

NADPH, nicotinamide adenine dinucleotide phosphate-oxidase

NGF, nerve growth factor

NM1, nuclear myosin 1

Osh4p, oxysterol-binding protein 4

PH, pleckstrin homology domain

PHD, plant homeodomain

PI(3)P, phosphatidylinositol 3-phosphate

PI(3,4)P2, phosphatidylinositol 3,4-bisphosphate

PI(3,4,5)P3, phosphatidylinositol 3,4,5-trisphosphate

PI(3,5)P2, phosphatidylinositol 3,5-bisphosphate

PI(4)P, phosphatidylinositol 4-phosphate

PI(4,5)P2 4-Ptase I, phosphatidylinositol 4,5-bisphosphate 4-phosphatase

PI(4,5)P2, phosphatidylinositol 4,5-bisphosphate

PI(5)P, phosphatidylinositol 5-phosphate

PI, phosphatidylinositol

PI3KC2α, phosphatidylinositol 3-kinase type IIα

PI3KC2β, phosphatidylinositol 3-kinase type IIβ

PI3Kβ, phosphatidylinositol 3-kinase type Iβ

PI3Kγ, phosphatidylinositol 3-kinase type Iγ

PI4Kα, phosphatidylinositol 4-kinase α

PI4Kβ, phosphatidylinositol 4-kinase β

PIKfyve, FYVE finger-containing phosphoinositide kinase

PIP4KIIα, phosphatidylinositol 5-phosphate 4-kinase type IIα

PIP4KIIβ, phosphatidylinositol 5-phosphate 4-kinase type IIβ

PIP5KIα, phosphatidylinositol 4-phosphate 5-kinase type Iα

PIP5KIγ, phosphatidylinositol 4-phosphate 5-kinase I γ

PIP5KIγ_i4, phosphatidylinositol 4-phosphate 5-kinase type Iγ_i4

PI-PLC, phosphatidylinositol-specific phospholipase C

PIPTs, PI transfer proteins

PIs, phosphoinositides

PKCδ, protein kinase C δ

PTEN, phosphatase and tensin homolog

PX, phox homology domain

RING finger domain, really interesting new gene finger domain

RNA Pol I and II, RNA polymerase I and II

ROS, reactive oxygen species

SARA, Smad anchor for receptor activation

SF-1, steroidogenic factor 1

SHIP-1, Src-homology 2-containing inositol 5-phosphatase 1

SHIP-2, Src-homology 2-containing inositol 5-phosphatase 2

Star-PAP, speckle targeted PIP5KIα regulated poly(A) polymerase

TAPP1 and TAPP2, tandem PH-domain containing protein 1 and 2

TGF-β, transforming growth factor-β

UBF, upstream binding factor 1

UHFR1, ubiquitin-like PHD and RING finger domain-containing protein 1

TABLE OF CONTENTS

ABSTRACT (ENGLISH)

Phosphoinositides (PIs) are negatively charged glycerol-based phospholipids. Their inositol head can be phosphorylated at three positions generating seven differently phosphorylated species. Cytoplasmic phosphoinositides regulate membrane and cytoskeletal dynamics, vesicular trafficking, ion channels and transporters and generate second messengers. In the nucleus, PIs are implicated in pre-mRNA processing, DNA transcription and chromatin remodelling. However, their nuclear functions are still poorly understood. Here we focus on nuclear phosphatidylinositol 4-phosphate (PI(4)P) and phosphatidylinositol 4,5-bisphosphate (PI(4,5)P2). We describe their localization and interaction with proteins involved in regulation of DNA transcription.

PI(4)P localizes to the nuclear membrane, nuclear speckles and nucleoplasm. The majority of nuclear PI(4)P is associated with chromatin and colocalizes with H3K4me2. PI(4,5)P2 localizes to nucleoli and nuclear speckles. Besides, 30 % of nuclear PI(4,5)P2 forms small nucleoplasmic PI(4,5)P2 islets. They have carbon rich core, which is probably formed by lipids, and are surrounded by proteins and nucleic acids. The active form of RNA polymerase II associates with PI(4,5)P2 islets and DNA is actively transcribed in the vicinity of PI(4,5)P2 islets. Moreover, nuclear myosin 1 (NM1) binds PI(4,5)P2 in the nucleus. This interaction targets NM1 to PI(4,5)P2 islets and is essential for NM1 interaction with transcription machinery and active DNA transcription. Therefore, we suggest that PI(4,5)P2 islets facilitate a spatial-temporal arrangement of transcription complexes assembly.

Moreover, we demonstrate that lysine-specific histone demethylase 1 (LSD1), enzyme that demethylates H3K4me2, interacts with both PI(4)P and PI(4,5)P2. While the interaction with PI(4)P leads to an inhibition of LSD1, the interaction with PI(4,5)P2 stimulates LSD1 H3K4me2 demethylase activity *in vitro*. Thus, PI(4)P and PI(4,5)P2 could regulate transcription at the epigenetic level also *in vivo*.

Another PI(4,5)P2 binding protein, actin, exists in the cytoplasm in monomeric form that can polymerize to filaments. However, in which form is actin present in the nucleus is still not sufficiently understood. After actin overexpression, we observed formation of actin filaments in the nucleus. These filaments resemble cytoplasmic F-actin and recruit cofilin and Arp3 actin binding proteins. The formation of actin filaments in the nucleus results in an increased transcription in S-phase, decreased cell proliferation and aberrant mitosis.

ABSTRACT (CZECH)

Fosfoinositidy jsou negativně nabité fosfolipidy. Jejich inositolová hlavička může být fosforylována na třech pozicích, a tak mohou tvořit sedm různě fosforylovaných forem. Cytoplasmatické fosfoinositidy regulují dynamiku buněčných membrán a cytoskeletu, transport membránových váčků, funkci iontových kanálů a transportérů a produkci druhých poslů. Jaderné fosfoinositidy ovlivňují postranskripční úpravy pre-mRNA, DNA transkripci a remodelování chromatinu. Jejich jaderné funkce jsou nicméně nedostatečně prozkoumány. Tato práce se zaměřuje na jaderný fosfatidylinositol 4-fosfát (PI(4)P) a fosfatidylinositol 4,5-bisfosfát (PI(4,5)P2), jejich lokalizaci a interakce s proteiny regulujícími transkripci.

PI(4)P je součástí jaderné membrány, nachází se v jaderných speckles a v nukleoplasmě. Většina jaderného PI(4)P je navázána na chromatin a kolokalizuje s H3K4me2 histonovou značkou. PI(4,5)P2 lokalizuje do jadérka a jaderných speckles. Přibližně 30 % jaderného PI(4,5)P2 tvoří malé ostrůvky v nukleoplasmě. Nitro těchto ostrůvků je bohaté na uhlík a je pravděpodobně tvořeno lipidy. Ostrůvky jsou obklopeny proteiny a nukleovými kyselinami. Aktivní forma RNA polymerázy II lokalizuje k PI(4,5)P2 ostrůvkům a v blízkosti ostrůvků dochází k aktivní transkripci. Jaderný myosin 1 (NM1) váže PI(4,5)P2. Tato interakce je zásadní pro vazbu NM1 na transkripční komplex a probíhající transkripci. Předpokládáme proto, že PI(4,5)P2 ostrůvky zprostředkovávají časově-prostorovou koordinaci tvorby aktivních transckripčních komplexů.

Lyzín-specifická histon demetyláza 1 (LSD1) interaguje s PI(4)P i PI(4,5)P2. Interakce s PI(4)P inhibuje, zatímco interakce s PI(4,5)P2 stimuluje LSD1 demetylační aktivitu a ovlivňuje tak hladinu H3K4me2 *in vitro*. Tímto způsobem by PI(4)P a PI(4,5)P2 mohly regulovat transkripční aktivitu na epigenetické úrovni i *in vivo*.

Dalším PI(4,5)P2 vazebným proteinem, který jsme studovali, je aktin. Aktin existuje v cytoplasmě ve formě monomerů, které mohou polymerizovat a vytvářet vlákna. Zatím není dostatečně objasněno, v jaké formě se aktin vyskytuje v buněčném jádře. Po exogenní overexpresi aktinu jsme pozorovali tvorbu jaderných aktinových vláken. Tato vlákna připomínala svými vlastnostmi cytoplasmatická aktinová vlákna. Aktin vazebné proteiny cofilin a Arp3 lokalizovaly k těmto jaderným vláknům. Následkem tvorby jaderných aktinových vláken byla zvýšená transkripce během S fáze buněčného cyklu, snížená buněčná proliferace a aberantní mitóza.

1. INTRODUCTION

Phosphatidylinositol (PI) is a negatively charged glycerol-based phospholipid. As an amphipathic molecule, PI is formed by hydrophobic acyl tail and hydrophilic inositol head. The inositol head can be phosphorylated at three different positions generating 7 phosphorylated species – phosphoinositides (PIs) – phosphatidylinositol 3-phosphate (PI(3)P), phosphatidylinositol 4-phosphate (PI(4)P), phosphatidylinositol 5-phosphate (PI(5)P), phosphatidylinositol 3,4-bisphosphate (PI(3,4)P2), phosphatidylinositol 3,5-bisphosphate (PI(3,5)P2), phosphatidylinositol 4,5-bisphosphate (PI(4,5)P2) and phosphatidylinositol 3,4,5-trisphosphate (PI(3,4,5)P3; Fig. 1). Their metabolism is very dynamic, regulated by numerous PIs kinases, phosphatases and phospholipases. Although PIs represent only about 2 % of cellular phospholipids, they are very important signalling molecules (reviewed in Viaud et al. 2015; Tan et al. 2015).

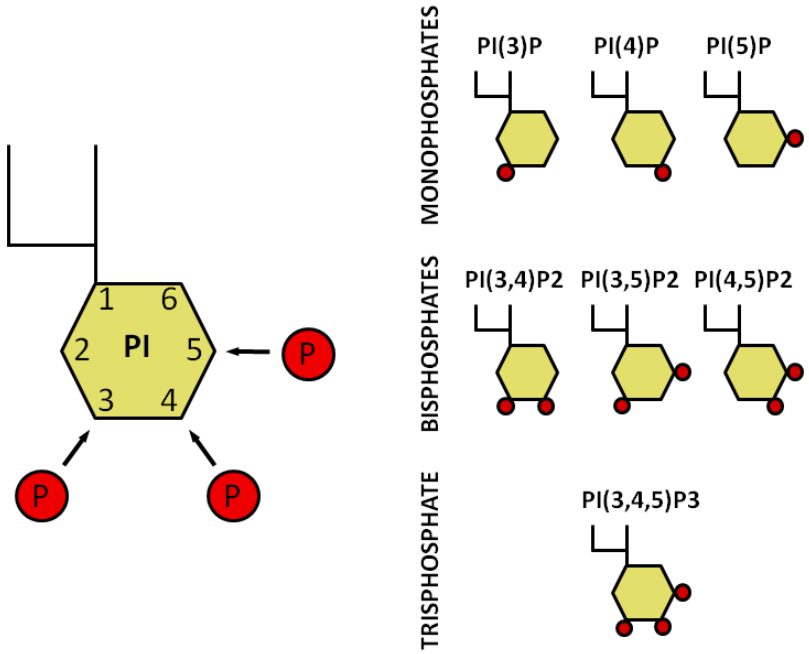

Fig. 1 Schematic representation of PI and seven differently phosphorylated PIs. PI can be phosphorylated at 3', 4' and 5' positions yielding three phosphatidylinositol monophosphates (PI(3)P, PI(4)P, PI(5)P), three phosphatidylinositol bisphosphates (PI(3,4)P2, PI(3,5)P2, PI(4,5)P2) and one phosphatidylinositol trisphosphate (PI(3,4,5)P3). Red circles depict sites of inositol ring phosphorylation.

1.1 Phosphoinositides in the cytoplasm

As phospholipids, cytoplasmic PIs are components of cellular membranes. Their localization can be visualized by specific PIs-binding protein domains coupled to GFP and can also be concluded from the localization of their metabolizing enzymes. There are many PIs metabolizing enzymes, which differ in their specificity, activity and localization. Therefore, several pools of particular PIs are produced in different membranes and organelles (Fig. 2). PIs then recruit their binding partners to these sites, which results in unique functions of individual PIs within the cell (reviewed in Balla and Várnai 2009; Balla 2013)

.

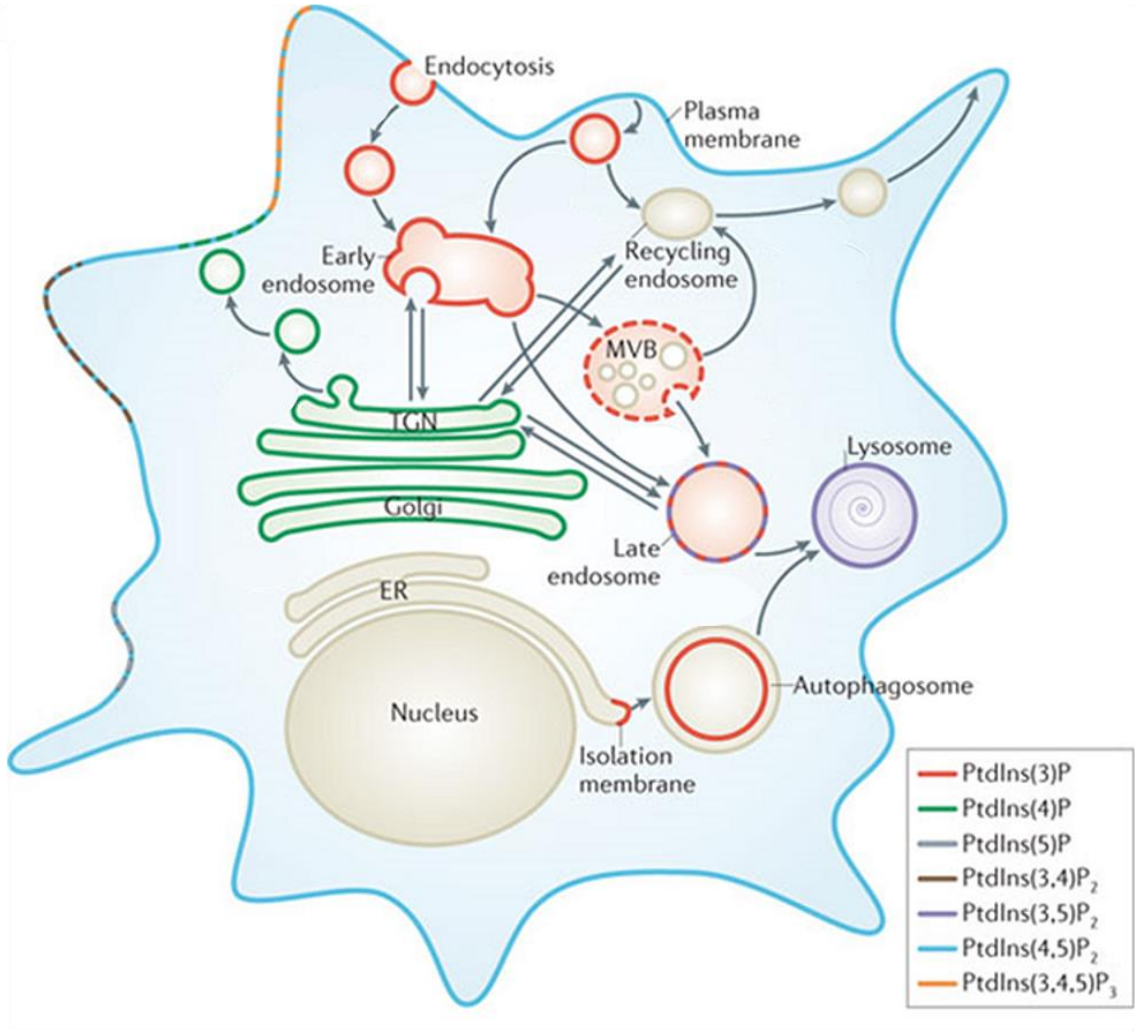

Fig. 2. PIs distribution in the cellular membranes. MBV- multivesicular body; TGN – trans-Golgi network; ER – endoplasmic reticulum. Figure is taken from (Jean and Kiger 2012) and modified.

1.1.1 PI(3)P

PI(3)P is predominantly present in endosomes (Ivetac et al. 2005; Slessareva et al. 2006) but localizes also to the plasma membrane (Ivetac et al. 2005), smooth endoplasmic reticulum and the Golgi apparatus (Sarkes and Rameh 2010). It can be produced also in autophagosome (Kihara 2001). PI(3)P binds to Fab1/YOTB/Vac1/EEA1 (FYVE) domain (Gaullier et al. 1998; Patki et al. 1998) and phox homology (PX) domain protein modules (Xu et al. 2001; Ellson et al. 2001; Kanai et al. 2001; Cheever et al. 2001) and tethers proteins containing these domains to PI(3)P enriched membranes. PI(3)P regulates vesicular trafficking from early endosomes to recycling endosomes and to the lysosomes (Xu et al. 2001), as well as autophagosome formation, exocytosis or cytokinesis (reviewed in Schink et al. 2013). PI(3)P interacts with nicotinamide adenine dinucleotide phosphate-oxidase (NADPH) through a p40-PX domain, targets NADPH oxidase to endosomes and stimulates formation of reactive oxygen species (ROS) in neutrophils (Ellson et al. 2001; Ellson et al. 2006).

Moreover, PI(3)P in endosomes can regulate transcription in a response to transforming growth factor- β (TGF-β). After TGF-β stimuli, FYVE domain of Smad anchor for receptor activation (SARA) targets SARA to early endosomes. SARA then triggers a formation of Smad2 and Smad3 transcriptional complex and Smad-dependent transcription (Tsukazaki et al. 1998; Itoh et al. 2002).

1.1.2 PI(4)P

PI(4)P is together with PI(4,5)P2 the most abundant PIs species. PI(4)P is mostly present in the Golgi apparatus, the plasma membrane and endosomes (reviewed in (Viaud et al. 2015) and regulates vesicular transport between these compartments (Mills et al. 2003; Wang et al. 2003; Godi et al. 2004). PI(4)P promotes formation of secretory vesicles in the Golgi apparatus and regulates their association with the plasma membrane (Mizuno-Yamasaki et al. 2010) in growth factor-dependent manner (Blagoveshchenskaya et al. 2008). Moreover, PI(4)P recruits lipid transfer proteins to the Golgi apparatus and thus enables import of ceramide and synthesis of sphingomyelin in the Golgi apparatus (Tóth et al. 2006; Yamaji et al. 2008).

Interestingly, PI(4)P itself can be transported between the endoplasmic reticulum and trans-Golgi membranes. Oxysterol-binding protein 4 (Osh4p) transports sterol from the endoplasmic reticulum to trans-Golgi. In Golgi, sterol is released and PI(4)P is loaded and retrogradely transported to endoplasmic reticulum. In the endoplasmic reticulum, PI(4)P is released and the Osh4p transport cycle can be repeated (de Saint-Jean et al. 2011). PI(4)P restores the level of sterol also at the plasma membrane (Beh and Rine 2004) probably by the same mechanism.

1.1.3 PI(5)P

Cellular level of PI(5)P is more than 50 times lower than the level of PI(4)P. The majority of PI(5)P localizes to the plasma membrane but it is present also in the smooth endoplasmic reticulum and the Golgi apparatus (Sarkes and Rameh 2010). PI(5)P is a key regulator of endosome to lysosome trafficking (reviewed in Viaud et al. 2014). Particularly interesting is the production of PI(5)P after an infection by bacterium *Shigella flexneri*. Bacteria injects ipgD, a phosphatase dephosphorylating PI(4,5)P2 to PI(5)P, into the host cell (Niebuhr 2002). Subsequently, the upregulation of PI(5)P in early endosomes of the host cell impairs the endosomes-lysosomes trafficking and protects bacteria from degradation (Ramel et al. 2011).

Although the basal level of PI(5)P is low, it is upregulated in response to various stimuli, such as insulin (Sbrissa et al. 2004; Sarkes and Rameh 2010), thrombin (Morris et al. 2000), specific oncogenes (Dupuis-Coronas et al. 2011), H_2O_2 treatment (Wilcox and Hinchliffe 2008; Sarkes and Rameh 2010; Jones et al. 2013), T-cell receptor activation (Guittard et al. 2009; Guittard et al. 2010), or bacterial infection (Niebuhr et al. 2002; Mason et al. 2007).

1.1.4 PI(3,4)P2

PI(3,4)P2 localizes mostly to the plasma membrane, where it regulates endocytosis (Posor et al. 2013; Boucrot et al. 2015), recruits lamellopodin to the plasma membrane and stimulates formation of lamellipodia (Krause et al. 2004; Boucrot et al. 2015) or podosomes (Oikawa et al. 2008). It negatively regulates insulin signalling through its interaction with tandem pleckstrin homology (PH) domain containing protein 1 and 2 (TAPP1 and TAPP2) and downregulation of protein kinase B (Akt) signalling (Wullschleger et al. 2011).

1.1.5 PI(3,5)P2

PI(3,5)P2 is mainly synthesized from PI(3)P by FYVE finger-containing phosphoinositide kinase (PIKfyve) and localizes to endosomes and lysosomes (reviewed in McCartney et al. 2014). It is involved in the regulation of retrograde endosome to trans-Golgi trafficking as well as fission or fusion of late endosomes (Rutherford et al. 2006; Zhang et al. 2007; de Lartigue et al. 2009). Downregulation of PI(3,5)P2 causes vacuolation of neurons and thus leads to neurodegeneration in mice (Zhang et al. 2007). The levels of PI(3,5)P2 increase upon UV radiation (Jones et al. 1999) and under an osmotic shock both in yeast (Dove et al. 1997; Duex et al. 2006) and mammalian cells (Dove et al. 1997).

Interestingly, lysosomal PI(3,5)P2 is implicated in the regulation of DNA transcription in *S. cerevisiae*. PI(3,5)P2 interacts with the general transcription factor Tup1. PI(3,5)P2 further mediates assembly of a Tup1 transcriptional coactivator complex and facilitates Tup1 switch from corepressor to coactivator function. Moreover, Cti6, which is required for Tup1 activation, also binds PI(3,5)P2. The nuclear localization of Cti6 and Cti6-Tup1 association with target promoters is PI(3,5)P2 dependent (Han and Emr 2011).

1.1.7 PI(4,5)P2

PI(4,5)P2 is one of the most abundant cellular PIs. It is predominantly present in the inner leaflet of the plasma membrane but localize also to other cellular membranes, such as the Golgi apparatus, endosomes and endoplasmatic reticulum. PI(4,5)P2 is recognized by several protein binding modules, such as PH, epsin N-terminal homology (ENTH), 4.1/ezrin/radixin/moesin (FERM) or Tubby domains. PI(4,5)P2 regulates actin dynamics, epithelial cell polarity and morphology, cell migration, endocytosis and exocytosis, phagocytosis, function of distinct ion channels and transporters. PI(4,5)P2 has also a very important signalling role, as it can be cleaved by phospholipases C to generate inositol 1,4,5-trisphosphate (Ins(1,4,5)P3) and diacylglycerol (DAG), second messengers.

Moreover, PI(4,5)P2 regulates β-catenin transcriptional activity. β-catenin interacts with phosphatidylinositol 4-phosphate 5-kinase I γ (PIP5KIγ). The activity of PIPKIγ and thus the production of PI(4,5)P2 promotes transclocation of β-catenin to the nucleus and activation of its target genes (reviewed in Sun et al. 2013; Viaud et al. 2015).

1.1.8 PI(3,4,5)P3

PI(3,4,5)P3 localizes mainly to the inner leaflet of the plasma membrane. It is present in a small amount in quiescent cells and it is produced in response to the activation of receptor tyrosine kinases or G-protein coupled receptors. PI(3,4,5)P3 is recognized by many PH domain-containing proteins and therefore it is a very important molecule involved in the formation of intracellular signalling complexes. It regulates the cell proliferation and survival, glucose homeostasis, cell polarization and motility (reviewed in Salamon and Backer 2013; Viaud et al. 2015).

1.2 Phosphoinositides in the nucleus

Beside their cytoplasmic functions, PIs play an important role also in the cell nucleus (reviewed in Shah et al. 2013). It is still unclear whether or how PIs are transported from the sites of their synthesis to the nucleus. However, two isoforms of PI transfer proteins (PIPTs) are able to translocate to the nucleus (De Vries et al. 1996). As many PIs metabolizing enzymes also localize to the nucleus (Fig. 3), it is plausible that PI is transported to the nucleus, where it is further metabolized. Indeed, several studies have confirmed an active intranuclear PIs metabolism. Smith and Wells (1983) showed that after an incubation of isolated nuclear membranes with [γ^{32}P]-ATP the radioactive phosphate is incorporated into PI(4,5)P2 and PI(4)P (Smith and Wells 1983). Cocco et al. (1987) showed that even nuclei deprived of the nuclear membrane can incorporate the radioactive phosphate into phosphatidylinositol monophosphates and PI(4,5)P2. They also observed that the intranuclear synthesis of PI(4,5)P2 is stimulated during cell differentiation (Cocco et al. 1987). In agreement, Deleris at al. (2006) demonstrated that PI(3,4,5)P3 and PI(3,4)P2 can be dephosphorylated in vascular smooth muscle cells nuclei regardless of the nuclear membrane (Déléris et al. 2003). In addition, we have shown that nuclear PI(4,5)P2 is synthesized co-transcriptionally at RNA polymerase I promoters (RNA Pol I; Yildirim et al. 2013). These results point towards the existence of an intranuclear PIs cycle, which is independent on cytoplasmic PIs metabolism (Fig. 3).

1.3 Metabolism of nuclear PIs

1.3.1 Nuclear PIs kinases

Nuclear PI can be phosphorylated at 3' position by class II phosphatidylinositol 3-kinases PI3KC2α (Didichenko and Thelen 2001) and PI3KC2β (Sindić et al. 2001) and at 4' by phosphatidylinositol 4-kinases PI4Kα and PI4Kβ (de Graaf et al. 2002; Strahl et al. 2005; Kakuk et al. 2006; Kakuk et al. 2008) generating PI(3)P and PI(4)P, respectively. PI3KC2α and PI3KC2β can further phosphorylate PI(4)P to PI(3,4)P2 (Didichenko and Thelen 2001; Sindić et al. 2001). PI4Kα is targeted to the nucleolus (Kakuk et al. 2006; Kakuk et al. 2008) while PI4Kβ (Szivak et al. 2006) and PI3KC2α (Didichenko and Thelen 2001) localize to the nuclear speckles. Moreover, PI4Kβ accumulates in the nuclear speckles after inhibition of RNA polymerase II (RNA Pol II; Szivak et al. 2006).

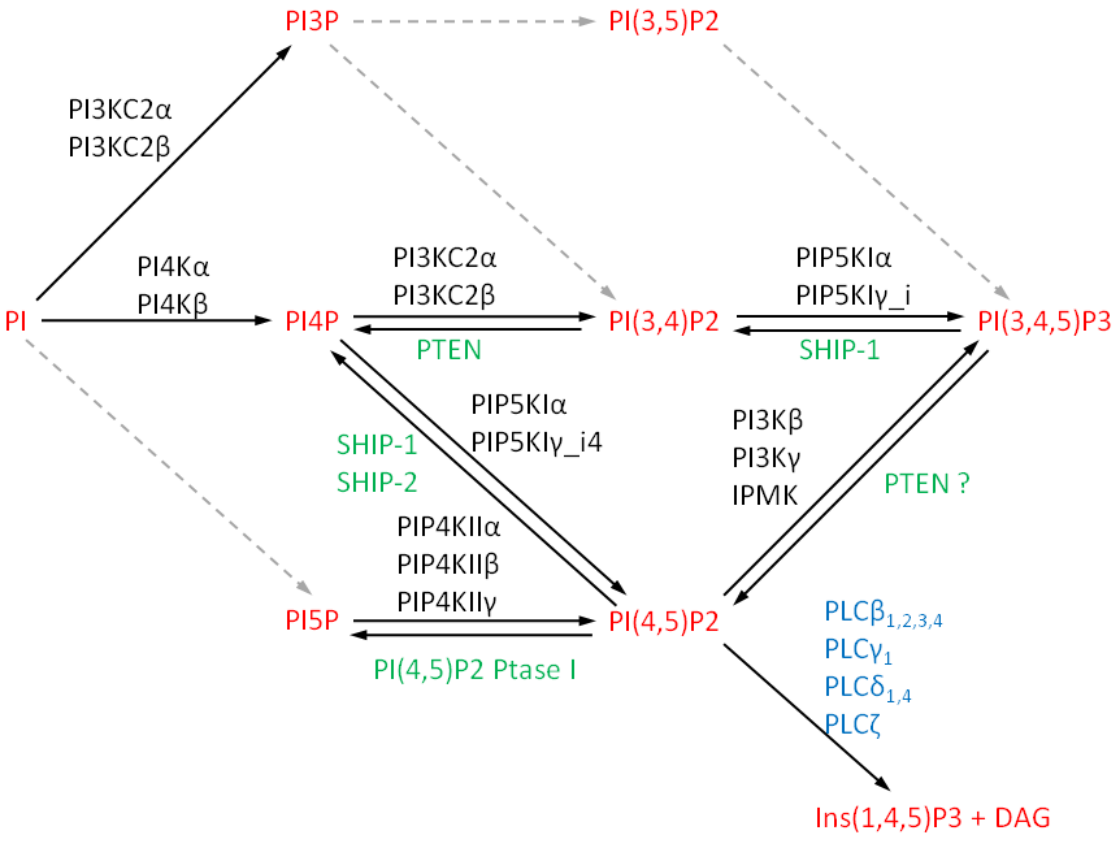

Fig. 3 PIs metabolism in the nucleus. Enzymes involved in PIs metabolism that localize to the nucleus are depicted. PIs kinases (black), phosphatases (green), and phospholipases (blue) form a metabolic network that most likely facilitates a formation of different PIs species (red) in the nucleus. Pathways catalysed by enzymes confirmed to be present in the nucleus (solid black arrows) and also possible pathways without known nuclear enzyme (dashed grey

arrows) are illustrated. A specific case is phosphatase and tensin homolog (PTEN), which localizes to the nucleus but has been shown to be unable to dephosphorylate nuclear PI(3,4,5)P3 (Lindsay 2006).

The major precursor for nuclear PI(4,5)P2 is PI(4)P (Vann et al. 1997). PI(4)P is phosphorylated at 5' position by type I phosphatidylinositol 4-phosphate 5-kinases PIP5KIα and PIP5Kγ_i4. Both, PIP5KIα and PIP5Kγ_i4 localize to nuclear speckles (Boronenkov et al. 1998; Mellman et al. 2008; Schill and Anderson 2009).

Yet, PI(4,5)P2 can be formed also from PI(5)P. PI(5)P is phosphorylated at 4' position by type II phosphatidylinositol 5-phosphate 4-kinases PIP4KIIα, PIP4KIIβ (Boronenkov et al. 1998; Richardson et al. 2007; Wang et al. 2010; Clarke and Irvine 2012), and PIP4KIIγ (Clarke et al. 2009; Clarke and Irvine 2012). PIP4KIIβ kinase is inhibited upon cellular stress as UV irradiation, oxidative stress or etoposide treatment (Jones et al. 2006).

PI(3,4,5)P3 can be formed from PI(3,4)P2 by nuclear type I phosphatidylinositol 4-phosphate 5-kinases. Alternatively, PI(3,4,5)P3 can be synthesized from PI(4,5)P2 by class I phosphatidylinositol 3-kinases PI3Kβ and PI3Kγ (Neri et al. 1994; Zini et al. 1996; Metjian et al. 1999; Bacqueville et al. 2001) and inositol multiphosphate kinase (IPMK) (Nalaskowski et al. 2002; Resnick et al. 2005; Maag et al. 2011). The activity of class I PI3K increases during the granulocytic differentiation (Bertagnolo et al. 1999) or after growth factors stimulation (Tanaka et al. 1999; Ahn et al. 2004).

1.3.2. Nuclear PIs phosphatases

Four different PIs phosphatases localize to the nucleus. Two Src-homology 2-containing inositol 5-phosphatases (SHIP-1, SHIP-2) hydrolyse phosphate group at 5' position of PI(3,4,5)P3 and PI(4,5)P2 and generate PI(3,4)P2 and PI(4)P, respectively (Damen et al. 1996; Lioubin et al. 1996). Both SHIP phosphatases localize to the nucleus (Déléris et al. 2003; Elong Edimo et al. 2011; Nalaskowski et al. 2012; Ehm et al. 2015). Moreover, SHIP-2 localizes to the nuclear speckles (Déléris et al. 2003; Elong Edimo et al. 2011) and when it is phosphorylated at S132, it acts only on PI(4,5)P2 generating PI(4)P (Elong Edimo et al. 2011).

Phosphatidylinositol (4,5)-bisphosphate 4-phosphatase (PI(4,5)P2 4-Ptase I) dephosphorylates PI(4,5)P2 at 4' position and generates PI(5)P (Ungewickell et al. 2005). PI(4,5)P2 4-Ptase I translocates to the nucleus in a response to DNA damage (Zou et al.

2007). Moreover, phosphatase and tensin homolog phosphatase (PTEN) localizes to the nucleus (Lachyankar et al. 2000; Gimm et al. 2000; Déléris et al. 2003). PTEN acts at 3' position of PI(3,4,5)P3 and PI(3,4)P2 (reviewed in Vanhaesebroeck et al. 2001) however it has been shown that nuclear PTEN dephosphorylate mostly PI(3,4)P2 generating PI(4)P (Déléris et al. 2003; Lindsay et al. 2006).

1.3.3 Nuclear PIs-specific phospholipases

Phosphoinositide-specific phospholipase C (PI-PLC) cleaves PI(4,5)P2 and generates second messengers - Ins(1,4,5)P3 and DAG. Eight isoforms of PI-PLC were detected within the nucleus.

The most studied PI-PLCβ_1 contains the nuclear localization signal (NLS) in its C-terminus (Kim et al. 1996) and localizes in the nuclear speckles (Zini et al. 1993; Tabellini et al. 2003). Also other subtypes of PI-PLCβ (PI-PLCβ_2, β_3 and β_4) and other isozymes such as PI-PLCγ_1, PI-PLCδ_1, PI-PLCδ_4 and PI-PLCζ have been confirmed to localize to the nucleus (Bertagnolo et al. 1995; Liu et al. 1996; Kim et al. 1996; Bertagnolo et al. 1997; Yamaga et al. 1999; Yoda et al. 2004; Larman et al. 2004; Klein et al. 2008; Cooney et al. 2010; Fiume et al. 2012).

1.4 Functions of nuclear PIs

Approximately 15 % of cellular PIs reside in the nucleus (York and Majerus 1994). Recent high-throughput studies identified more than 120 nuclear PIs-interacting proteins involved in different nuclear functions including DNA repair, chromatin remodelling and rRNA or mRNA processing (Lewis et al. 2011; Jungmichel et al. 2014). In the following section, data about nuclear PIs and their roles in these processes will be summarized.

1.4.1 Pre-rRNA and pre-mRNA processing

We have recently shown that PI(4,5)P2 binds to nucleolar protein fibrillarin (Yildirim et al. 2013). Fibrillarin functions in pre-rRNA processing, modification, and ribosomal assembly (Tollervey et al. 1993). PI(4,5)P2 binds to fibrillarin in the transcriptionally active regions of the nucleolus, alters its conformation and modulates the binding of fibrillarin to pre-rRNA (Yildirim et al. 2013).

Depletion of PI(4,5)P2 from HeLa nuclear extract by anti-PI(4,5)P2 antibody inhibits pre-mRNA splicing *in vitro*. However, addition of PI(4,5)P2 itself into depleted extract does not restore splicing reaction indicating that not only PI(4,5)P2 but also its binding partners are necessary to restore splicing activity. Indeed, the same antibody against PI(4,5)P2 immunoprecipitates both small nuclear RNAs and the active form of RNA Pol II (Osborne et al. 2001). These results indicate that PI(4,5)P2 interacts with nuclear proteins and small nuclear RNAs and forms RNA-protein-lipid complexes which are directly involved in pre-mRNA splicing. However, the exact molecular mechanism behind this phenomenon remains unknown.

PI(4,5)P2 acts also as a regulatory molecule in mRNA polyadenylation. PI(4,5)P2 synthesized by PIP5KIα stimulates processivity of a non-canonical Speckles targeted PIP5KIα regulated poly(A) polymerase (Star-PAP) resulting in a longer poly(A) tail of targeted mRNAs and their stabilization. PIP5KIα and Star-PAP enzymes interact directly in nuclear speckles, and their knock-down downregulates polyadenylation of mRNA coding proteins involved mostly in detoxification and oxidative stress response (Mellman et al. 2008).

Once mRNA is maturated, it is exported to the cytoplasm upon an association with RNA-interacting protein complexes (Nojima et al. 2007; Fuke and Ohno 2008). PI(4,5)P2 and PI(3,4,5)P3 directly interact with the N-terminal part of export factor Aly/REF. The disruption of phosphoinositide binding displaces Aly from nuclear speckles and mRNA export is attenuated (Okada et al. 2008). Recently, Wickramasinghe et al. (2013) showed that the PI3K activity of IPMK and nuclear PI(3,4,5)P3 formation is essential for Aly binding to target mRNA. The downregulation of IPMK activity inhibits the export of mRNA coding proteins implicated in DNA repair and homologous recombination (Wickramasinghe et al. 2013).

1.4.2 DNA damage response and apoptosis

Nuclear PI(3,4,5)P3 is an important molecule in the cell differentiation and anti-apoptotic signalling (Bertagnolo et al. 1999; Ahn et al. 2004; Ahn et al. 2005). The activity of class I PI3K is increased upon induction of granulocytic differentiation (Bertagnolo et al. 1999) and also after growth factors stimulation of various cell lines (Tanaka et al. 1999) or isolated nuclei (Ahn et al. 2004). PI(3,4,5)P3 binds directly to nuclephosmin (B23) in the nucleus, their interaction is induced by nerve growth factor (NGF) treatment (Ahn et al. 2005). Moreover, Akt, a PI(3,4,5)P3 effector protein, translocates to the nucleus after NGF

stimulation in PI3K dependent manner (Borgatti et al. 2003; Xuan Nguyen et al. 2006). In the nucleus, Akt interacts directly with B23 and protects B23 from degradation (Lee et al. 2008). The PI(3,4,5)P3-B23 complex then mediates anti-apoptotic signalization, inhibits caspase-activated DNAse and therefore protects DNA against fragmentation (Ahn et al. 2005). The action of both SHIP-2 and phosphatase and tensin homolog (PTEN) phosphatases (Ahn et al. 2004; Ahn et al. 2005) as well as overexpression of B23 PI(3,4,5)P3-binding mutant (Ahn et al. 2005) can inhibit NGF induced anti-apoptotic actions. Because it was reported that PTEN does not dephosphorylate PI(3,4,5)P3 in the nucleus (Déléris et al. 2003; Lindsay et al. 2006), it is unclear whether PTEN can antagonize NGF pathway through the decrease of PI(3,4,5)P3 level or through a different mechanism.

Besides its role in the stabilization of particular mRNAs, Star-PAP-PIP5KIα complex takes part in DNA damage response and apoptosis. Via PIP5KIα, Star-PAP interacts with PKCδ (Li et al. 2012), which is a key regulator of apoptosis (reviewed in Brodie and Blumberg 2003). Following DNA damage, PI(4,5)P2 generated by PIP5KIα stimulates PKCδ activity. PKCδ then phosphorylates Star-PAP, leading to Star-PAP activation and stabilization of a pro-apoptotic protein Bcl2-interacting killer (BIK) mRNA (Li et al. 2012).

PI(5)P is an important player in DNA damage response through its interaction with inhibitor of growth protein 2 (ING2; Gozani et al. 2003). Following DNA damage, ING2 expression is induced. ING2 then stimulates acetylation of the cellular tumour antigen p53 leading to enhancement of p53-dependent transcription, G1-phase cycle arrest, and apoptosis (Nagashima et al. 2001). PI(5)P binds to ING2 through the plant homeodomain (PHD) finger domain (Gozani et al. 2003) and stabilizes it at the promoters of target genes (Bua et al. 2013). The ING2 mutant, which is unable to bind PI(5)P, fails to regulate p53 acetylation and apoptosis (Bua et al. 2013). Therefore, Jones et al. (2006) studied the alteration of PI(5)P levels in response to cellular stress induced by UV irradiation, oxidative stress, and etoposide treatment in murine erythroleukaemia cells. They showed that the PIP4KIIβ kinase, which phosphorylates PI(5)P to PI(4,5)P2, is inhibited upon cellular stress resulting in accumulation of PI(5)P within the nucleus (Jones et al. 2006). Similarly, PI(4,5)P2 4-Ptase I, which dephosphorylates PI(4,5)P2 to PI(5)P, translocates into the nucleus upon DNA damage (Zou et al. 2007). Elevated PI(5)P levels result in increased ING2 association with chromatin (Jones et al. 2006) and induction of apoptosis through ING2-p53 pathway (Zou et al. 2007).

1.4.3 Chromatin remodeling and modifications

The accessibility of DNA is crucial for gene expression regulation. There are data demonstrating that PI(4,5)P2 plays an important role in DNA topological change and chromatin remodelling, since it interacts with proteins involved in these processes (Yu et al. 1998; Zhao et al. 1998; Rando et al. 2002; Lewis et al. 2011; Toska et al. 2012).

Histone acetylation reduces a positive charge of histones and loosens their association with negatively charged DNA. As a result, DNA is more accessible for transcription factors that can facilitate DNA transcription (Lee et al. 1993; Garcia-Ramirez et al. 1995). A recent study showed that chromatin acetylation is repressed by a process which requires a myristoylation of transcriptional co-repressor brain acid soluble protein 1 (BASP1) and PI(4,5)P2. Myristoylation of BASP1 is essential for its function as a transcriptional co-repressor. It was shown that nuclear PI(4,5)P2 interacts with BASP1 through its myristoyl moiety and facilitates BASP1 interaction with histone deacetylase 1 (HDAC1). BASP1-PI(4,5)P2-HDAC1 complex is then recruited to the promoter of target genes, where HDAC1 deacetylates histones and reduces promoter accessibility for RNA Pol II transcription machinery (Toska et al. 2012). Moreover, DNA topoisomerase IIα associates with RNA pol II transcription machinery and relaxes the superhelical tension of DNA during transcription (Mondal and Parvin 2001). PI(4,5)P2 interacts directly with DNA topoisomerase IIα and inhibits its activity *in vitro* (Lewis et al. 2011).

On the contrary, PI(4,5)P2 may stimulate RNA Pol II through a direct interaction with histones H1 and H3 (Yu et al. 1998). *In vitro*, RNA Pol II transcription is inhibited by H1 (Croston et al. 1991; Levine et al. 1993; Johnson et al. 1995). This inhibition can be partially restored by addition of PI(4,5)P2. Another mechanism of PI(4,5)P2 action in chromatin remodelling is through its direct interaction with SWI/SNF-like BAF chromatin remodelling complex (Rando et al. 2002). PI(4,5)P2 binds BAF complex, targets it to the chromatin, and facilitates changes in chromatin structure during T-lymphocyte activation (Zhao et al. 1998).

Gelato et al. (2014) described the regulation of ubiquitin-like PHD and really interesting new gene (RING) finger domain- containing protein 1 (UHRF1) by PI(5)P (Gelato et al. 2014). UHRF1 is a multidomain protein that binds unmodified histone H3 and recruits histone methyltransferases to methylate H3K9 and establish transcription repressive marks. Moreover, UHRF1 is able to bind H3K9me3 modification and in a complex with histone

methyltransferases maintains heterochromatin state (reviewed in (Bronner et al. 2013). PI(5)P binds directly to the polybasic region in the C-terminal part of UHRF1, changes the conformation of UHRF1, and allosterically regulates its histone binding specificity. When not bound to PI(5)P, UHRF1 recognizes unmodified histone H3 tail, while PI(5)P-UHRF1 complex binds histone H3K9me3 (Gelato et al. 2014). Therefore, PI(5)P levels could regulate UHFR1 association with chromatin and heterochromatic state of the genome.

1.4.4 DNA transcription

Recent findings show that PI(4,5)P2 and PI(3,4,5)P3 can interact with steroidogenic factor 1 (SF-1; Blind et al. 2012; Blind et al. 2014). As a transcription factor, SF-1 regulates transcription of genes involved a lipid and steroid metabolism, cytoskeleton dynamics, cell cycle, or apoptosis (reviewed in Lalli et al. 2013). PI(4,5)P2 or PI(3,4,5)P3 bind to SF-1 sterol binding pocket through their acyl chains (Blind et al. 2012; Blind et al. 2014) and stabilize the tertiary structure of SF-1. SF-1 in a complex with PI(3,4,5)P3 displays significantly higher affinity for a coactivator peptide than in a complex with PI(4,5)P2 (Blind et al. 2014). Therefore, the action of IMPK kinase or PTEN phosphatase can regulate SF-1 activity and SF-1 target genes expression (Blind et al. 2012).

Furthermore, PI(4,5)P2 plays a role in gene regulation through the interaction with RNA Pol II and RNA Pol I transcription machinery (Osborne et al. 2001; Toska et al. 2012; Sobol et al. 2013; Yildirim et al. 2013). PI(4,5)P2 forms a complex with the active form of RNA Pol II (Osborne et al. 2001; Toska et al. 2012). Yet, there is no evidence of a direct interaction between PI(4,5)P2 and RNA Pol II.

In comparison to RNA Pol II, the mode of PI(4,5)P2 action in RNA Pol I transcription is more understood. The upstream binding factor (UBF) and the promoter selectivity factor 1 form a complex, which is recruited to the rDNA promoter and facilitates the initiation of RNA Pol I transcription (Bell et al. 1988). Recently, we have shown that PI(4,5)P2 binds to UBF and enhances the binding of UBF to the rDNA promoter. Moreover, the depletion of PI(4,5)P2 from HeLa nuclear extract decreases the level of RNA Pol I transcription *in vitro*. The decrease can be partially restored by addition of PI(4,5)P2 into the transcription reaction (Yildirim et al. 2013). These data suggest that PI(4,5)P2-UBF interaction might be required for association of the transcription initiation complex with rDNA and activation of RNA Pol I transcription.

2. AIMS

PIs and PIs-interacting proteins are important cellular regulators. Although it becomes apparent that PIs have important roles also in the cell nucleus, still only a little is known about their nuclear localization and functions. Therefore we addressed these questions:

1) **Which PIs localize to the cell nucleus?**
2) **In which subnuclear domains are they localized?**
3) **What are the binding partners of PIs in the nucleus?**

Actin is a well-known PI(4,5)P2 interacting protein. In the cytoplasm, monomeric actin can polymerize and form filaments. The state of actin in the nucleus (monomeric, filamentous, alternative polymeric) is unclear. We will address these questions:

4) **Can actin form filaments in the nucleus? Does the filament formation affect nuclear functions?**
5) **Is the localization of actin in the nucleus regulated by PI(4,5)P2?**

3. RESEARCH PAPERS

Tools for visualization of phosphoinositides in the cell nucleus

Kalasova I, Fáberová V, Kalendová A, Yildirim S, Uličná L, Venit T and Hozák P

Histochem Cell Biol. 2016 Feb 4 [Epub ahead of print]. doi: 10.1007/s00418-016-1409-8.

IF: 3.054 (2014)

I. K. designed and performed experiments (DNA cloning, DNA mutagenesis, fluorescence microscopy, protein expression and purification) and wrote the manuscript.

Nuclear phosphatidylinositol 4,5-bisphosphate islets contribute to efficient DNA transcription

Sobol M, Kalendová A, Yildirim S, Philimonenko V, Marášek P, Kalasová I, Pastorek, Hozák P

Manuscript.

I.K. performed experiments (pull-down assay and western blotting).

Chromatin associated PI(4)P regulates lysine-specific histone demethylase 1

Kalasova I, Kalendová A, Fáberová V, Marášek P, Uličná L, Vacík T and Hozák P

Manuscript.

I.K. designed and performed most of the experiments (DNA cloning, DNA mutagenesis, protein expression and purification, cellular fractionations, pull-down assays, fluorescence microscopy, western blotting, demethylation assays, qPCR) and wrote the manuscript.

Nuclear actin filaments recruit cofilin and Arp3 and their formation is connected with a mitotic block

Kalendová A, Kalasová I, Yamazaki S, Uličná L, Harata M and Hozák P

Histochem Cell Biol. 2014 Aug;142(2):139-52. doi: 10.1007/s00418-014-1243-9. Epub 2014 Jul 8.

IF: 3.054 (2014)

I. K. performed experiments (fluorescence microscopy)

3.1 Tools for visualization of phosphoinositides in the cell nucleus

Kalasova I, Fáberová V, Kalendová A, Yildirim S, Uličná L, Venit T and Hozák P

Histochem Cell Biol. 2016 Feb 4 [Epub ahead of print]. doi: 10.1007/s00418-016-1409-8.

IF: 3.054 (2014)

I. K. designed and performed experiments (DNA cloning, DNA mutagenesis, fluorescence microscopy, protein expression and purification) and wrote the manuscript.

Histochem Cell Biol
DOI 10.1007/s00418-016-1409-8

ORIGINAL PAPER

Tools for visualization of phosphoinositides in the cell nucleus

Ilona Kalasova[1,2] · Veronika Fáberová[1] · Alžběta Kalendová[1] · Sukriye Yildirim[1] · Lívia Uličná[1] · Tomáš Venit[1] · Pavel Hozák[1]

Accepted: 14 January 2016

Abstract Phosphoinositides (PIs) are glycerol-based phospholipids containing hydrophilic inositol ring. The inositol ring is mono-, bis-, or tris-phosphorylated yielding seven PIs members. Ample evidence shows that PIs localize both to the cytoplasm and to the nucleus. However, tools for direct visualization of nuclear PIs are limited and many studies thus employ indirect approaches, such as staining of their metabolic enzymes. Since localization and mobility of PIs differ from their metabolic enzymes, these approaches may result in incomplete data. In this paper, we tested commercially available PIs antibodies by light microscopy on fixed cells, tested their specificity using protein–lipid overlay assay and blocking assay, and compared their staining patterns. Additionally, we prepared recombinant PIs-binding domains and tested them on both fixed and live cells by light microscopy. The results provide a useful overview of usability of the tools tested and stress that the selection of adequate tools is critical. Knowing the localization of individual PIs in various functional compartments should enable us to better understand the roles of PIs in the cell nucleus.

Keywords Nucleus · Phosphoinositides · PI(4,5)P2 · PI(4)P

✉ Pavel Hozák
hozak@img.cas.cz

[1] Department of Biology of the Cell Nucleus, Institute of Molecular Genetics of the Academy of Sciences of the Czech Republic, v.v.i., Vídeňská 1083, 142 20 Prague, Czech Republic

[2] Faculty of Science, Charles University in Prague, Albertov 6, 128 43 Prague, Czech Republic

Introduction

Phosphoinositides (PIs) are glycerol-based phospholipids. As amphipathic molecules, they consist of hydrophobic tail and hydrophilic head. Their head is formed by the inositol ring that can be phosphorylated at three different positions yielding seven mono-, bis-, or tris-phosphorylated PIs species. PIs are important signalling molecules involved in membrane and cytoskeletal dynamics, modulation of ion channels and transporters, or generation of second messengers (reviewed in Balla 2013; Tan et al. 2015). These functions are related to PIs present in the cytoplasm and the plasma membrane. Approximately 15 % of cellular PIs are nuclear (York and Majerus 1994). It is, however, not well understood whether nuclear PIs originate in the cytoplasm or whether they are synthesized in the nucleus de novo. Many PIs metabolizing enzymes—kinases, phosphatases, and phospholipases (reviewed in Keune et al. 2011; Martelli et al. 2011; Shah et al. 2013)—as well as phosphatidylinositol (PI) transfer proteins (De Vries et al. 1996) localize to the nucleus. Besides, several in vitro studies reported intranuclear synthesis of PIs (Smith and Wells 1983; Cocco et al. 1987; Yildirim et al. 2013). These data suggest that PIs are in the nucleus metabolized independently of the cytoplasm and do not require the presence of membranes. However, spatiotemporal visualization of such events in the nucleus is still missing. Since a large fraction of PIs does not associate with nuclear membrane (Vann et al. 1997), it is currently unclear where the synthesis and metabolism of nuclear PIs occur. Several studies suggested that PIs are retained in the nucleus in the form of protein–lipid complexes, where proteins shield the hydrophobic tails of PIs (Blind et al. 2014; Sablin et al. 2015) and thus could prevent their extraction by detergents. Using various approaches, more than 300 nuclear PIs-interacting

Published online: 04 February 2016

Table 1 Summary of PIs-binding domains used for overexpression in U2OS cells

Domain	Specificity	Protein	Size (kDa)	Mutant
EEA1-FYVE	PI(3)P	Early endosome antigen 1	~18	RRHH126-129AANN
OSH1-PH	PI(4)P	Oxysterol-binding protein homolog 1	~15	KR37,39EE
Akt-PH	PI(3,4)P2, PI(3,4,5)P3	Protein kinase B	~21	KR14,15AA
Tubby	PI(4,5)P2	Tubby-like protein	~31	KR300,302AA
PLCδ1-PH	PI(4,5)P2	Phosphoinositide phospholipase C δ1	~20	R40A
Grp1-PH	PI(3,4,5)P3	General receptor for phosphoinositides 1	~15	K273A

Domains were mutated according to Yagisawa et al. (1998), Levine and Munro (2001), Santagata et al. (2001), Lee et al. (2005), Guillou et al. (2007), Jo et al. (2012)

proteins were identified. These proteins are involved in essential nuclear processes, and therefore, nuclear PIs are probably important regulators of these events (Lewis et al. 2011; Jungmichel et al. 2014). And indeed, nuclear phosphatidylinositol 4,5-bisphosphate (PI(4,5)P2) modulates protein functions and thus plays a role in chromatin remodelling (Zhao et al. 1998), transcription by RNA polymerase I and II (Osborne et al. 2001; Toska et al. 2012; Yildirim et al. 2013), or pre-mRNA processing (Osborne et al. 2001; Mellman et al. 2008). Nuclear phosphatidylinositol 3,4,5-trisphosphate (PI(3,4,5)P3) was linked to mRNA export (Okada et al. 2008; Wickramasinghe et al. 2013) and anti-apoptotic signalling (Ahn et al. 2004, 2005), while nuclear phosphatidylinositol 5-phosphate (PI(5)P) is implicated in DNA damage response (Gozani et al. 2003; Jones et al. 2006; Zou et al. 2007). Despite the fact that there are no data on functions of other nuclear PIs, their presence in the nucleus has been confirmed (Vann et al. 1997; Gillooly et al. 2000; Yokogawa et al. 2000; Clarke et al. 2001; Višnjić et al. 2003; Watt et al. 2004).

To better understand functions of individuals PIs, it is important to have information about their localization within the nucleus. So far, two fundamental approaches of PIs visualization have been employed. First, commercially available antibodies against PI(4,5)P2 (Mazzotti et al. 1995; Boronenkov et al. 1998; Osborne et al. 2001) and phosphatidylinositol 3,4-bisphosphate (PI(3,4)P2; Yokogawa et al. 2000) have been used. Second, PIs-binding domains from PLCδ1 (Watt et al. 2002; Hammond et al. 2009; Yildirim et al. 2013), Tapp1 (Watt et al. 2004), Hrs (Gillooly et al. 2000), and Grp1 (Lindsay et al. 2006) proteins specifically recognizing PI(4,5)P2, PI(3,4)P2, phosphatidylinositol 3-phosphate (PI(3)P), and PI(3,4,5)P3, respectively, were generated. The use of anti-PI(4,5)P2 and PLCδ1-PH domain provided similar results and made it possible to address functions of PI(4,5)P2 as well as its localization in the nucleus, nuclear speckles, and heterochromatin regions (Mazzotti et al. 1995; Boronenkov et al. 1998; Osborne et al. 2001; Watt et al. 2002; Hammond et al. 2009; Yildirim et al. 2013). Similarly, both antibodies and domains demonstrated localization of PI(3,4)P2 in the nuclear membrane. FYVE domain of tyrosine kinase Hrs detected PI(3)P signal in nucleoli of BHK cells (Gillooly et al. 2000). PH domain of Grp1 showed an increased level of nuclear PI(3,4,5)P3 after stimulation of Swiss 3T3 cells with PDGF (Lindsay et al. 2006).

In this paper, we explored localization of nuclear PI(4,5)P2, PI(3,4)P2, and phosphatidylinositol 4-phosphate (PI(4)P) in greater detail. First, we tested commercial antibodies against PI(4,5)P2, PI(3,4)P2, and PI(4)P. Since tools for visualization of nuclear PIs in live cells are missing, we next inspected nuclear patterns of different PIs-binding protein domains (Table 1) after overexpression in U2OS cells. Given that most domains did not specifically label nuclear PIs in live cells, we purified eGFP-fused PLCδ1-PH, OSH1-PH, and Tubby domains and used them in analogy to antibodies for labelling in fixed cells. Using these approaches, we identified anti-PI4P antibody, OSH1-PH, EEA1-FYVE, and PLCδ1-PH, and Tubby domains as a potential tools for visualization of PI(4)P, PI(3)P, and PI(4,5)P2 in live or fixed cells.

Materials and methods

Cell cultures and transfections

U2OS were cultured in D-MEM supplemented with 10 % FBS in 5 % CO_2/air, 37 °C, and humidified atmosphere. Cells were transfected with Lipofectamine (Life Technologies) according to manufacturer's instructions.

Constructs used in this study

For overexpression in U2OS cells, PLCδ1-PH, EEA1-FYVE, Grp1-PH, OSH1-PH, Akt-PH, and Tubby domains in pEGFP (Clontech, kind gifts from Dr Tamas Balla, National Institutes of Health, Bethesda, MD) were used. PLCδ1-PH with nuclear localization signal (NLS) was

prepared by insertion of SV40 NLS into PLCδ1-PH pEGFP-N1 by BsrGI and AFlII restriction sites. Mutant domains (PLCδ1-PH R40A, EEA1-FYVE RRHH123-129AANN, Grp1-PH K273A, OSH1-PH KR37,39EE, Akt-PH KR14,15AA, Tubby domain KR330,332AA) were prepared by site-directed mutagenesis by Q5® Site-Directed Mutagenesis Kit (New England Biolabs, E0552S) according to the manufacturer's instructions. For expression in *E. Coli*, eGFP fusions of wild-type as well as mutant forms of PLCδ1-PH, OSH1-PH domains were amplified by PCR and ligated to pET-15b (Merck Millipore). Tubby domain in pET-23a (Merck Millipore, a kind gift from Dr Tamas Balla, National Institutes of Health, Bethesda, MD) was used, and mutant Tubby domain was prepared as described above.

Antibodies

Following primary antibodies were used: anti-PI(4)P (Echelon, Z-P004; 10 μg/ml), anti-PI(3,4)P2 (Echelon, Z-P034b; 20 μg/ml), anti-PI(4,5)P2 (Echelon, Z-A045; 4.9 μg/ml).

For immunofluorescence, secondary antibodies were used: goat anti-mouse IgG conjugated with Alexa Fluor 555 and goat anti-mouse IgM conjugated with Alexa Fluor 555 all purchased from Life Sciences. For protein–lipid overlay assay, the following secondary antibodies were used: donkey anti-mouse IgG IRDye®680RD and goat anti-mouse IgM IRDye®680RD (LI-COR Biosciences).

Expression and purification of recombinant proteins

Recombinant PLCδ1-PH, OSH1-PH, and Tubby domains were expressed in *E. coli* BL21-Gold(DE3). Bacteria transformed with PLCδ1-PH and Tubby domains were grown up to OD(600) = 0.6. The expression of PLCδ1-PH was induced with 0.6 mM IPTG for 4 h at 37 °C. The expression of Tubby domain was induced with 0.3 mM IPTG for 8 h at 18 °C. Bacteria transformed with OSH1-PH domain were grown up to OD(600) = 0.4. The expression of OSH1-PH was induced with 0.1 mM IPTG for 16 h at 25 °C. Cells were lysed in lysis buffer (10 mM Tris, pH 7.4, 150 mM NaCl, 0.5 % Triton X-100, AEBSF) and sonicated. The purification was carried on HIS-Select Nickel Affinity Gel (Sigma, P6611). The beads were equilibrated with lysis buffer and incubated with protein lysates for 1 h at 4 °C. Then the beads were washed three times (10 m M Tris, pH 7.4, 150 mM NaCl, AEBSF). Bound proteins were eluted (10 mM Tris, pH 8, 150 mM NaCl, 250 mM imidazole, pH 8, 20 % glycerol, AEBSF). Subsequently, imidazole was removed by dialysis (10 mM Tris, pH 8, 150 mM NaCl, 20 % glycerol, AEBSF). Purified PIs-binding domains were used for immunofluorescence (1 μg/μl).

Indirect immunofluorescence and confocal fluorescence microscopy

Cells seeded on glass coverslips were washed with PBS, fixed with 3 % paraformaldehyde in PBS, and permeabilized with 0.1 % Triton X-100 in PBS for 20 min. Coverslips were blocked with 5 % normal goat serum (Invitrogen) in PBS for 30 min. Coverslips were incubated with primary antibodies diluted in PBS for 1 h at room temperature (RT) and then washed with PBS or with purified domains diluted in PBS with 0.05 % Tween 20 (PBS-T) for 1 h at RT and then washed with PBS-T. In case of antibodies, coverslips were incubated with corresponding secondary antibodies diluted in PBS-T for 1 h at RT. After final washes in PBS-T, coverslips were mounted in ProLong Gold anti-fade reagent with DAPI (Life Technologies). Images were acquired using confocal microscope Leica TCS SP8 with 63× (NA 1.4) immersion oil objective lens with 405 and 561 laser excitations, Leica advanced fluorescence software (LAS AF).

Antibody blocking assay

Antibodies were incubated with phosphatidylinositol diC8 (P-0008), PI(3)P diC8 (P-3008), PI(4)P diC8 (P-4008), PI(5)P diC8 (P-5008), PI(3,4)P2 diC8 (P-3408), phosphatidylinositol 3,5-bisphosphate diC8 (P-3508), PI(4,5)P2 diC8 (P-4508), PI(3,4,5)P3 diC8 (P-3908), all purchased from Echelon Biosciences Inc. Antibodies were incubated with PIs in molar ratio 1:1000. Concentrations of antibodies were as described above. Concentrations of PIs were 5, 10, and 130 nM to block anti-PI(4,5)P2, anti-PI(4)P, and anti-PI(3,4)P2 antibody, respectively. Incubations were performed in 1 % BSA, PBS for 30 min. Pre-blocked antibodies were used for immunostaining.

Protein–lipid overlay assay

PIP Strips (P-6001, Echelon Biosciences Inc.) were blocked with 3 % BSA in PBS-T for 1 h at RT and then incubated with antibodies (1 ug/ml) in 3 % BSA, PBS-T for 1 h at RT. Membranes were washed three times with PBS-T for 1 h at RT. Membranes were incubated with goat/donkey anti-mouse IgG or anti-mouse IgM secondary antibodies conjugated to IRDye. The signal was detected by Odyssey Infrared Imaging System (LI-COR Biosciences).

Results

Antibodies show nuclear localization of PI(4,5)P2, PI(3,4)P2, and PI(4)P

To describe the localization of particular nuclear PIs, we used antibodies against PI(4,5)P2, PI(3,4)P2, and PI(4)P, which are all commercially available (Echelon).

As it has been reported before, the antibody against PI(4,5)P2 detects nuclear PI(4,5)P2 in nuclear speckles and nucleoplasmic foci. Moreover, weak nucleolar PI(4,5)P2 pool can be also detected (Osborne et al. 2001; Yildirim et al. 2013; Fig. 1a, inset). To test the specificity of PI(4,5)P2 antibody, we used protein–lipid overlay assay, where the antibody is incubated with different phospholipids spotted on a nitrocellulose membrane. Protein–lipid overlay assay shows that PI(4,5)P2 antibody detects not only PI(4,5)P2 but also PI(3,4,5)P3 (Fig. 2a). Therefore, we used lipid blocking assay to further investigate the antibody specificity. In this approach, the antibody was preincubated with an excess amount of each PI (1:1000) and then used for immunofluorescence (Fig. 2b). Although preincubation with PI(3,4,5)P3 decreased the detected signal to 15 % of the original value, preincubation with PI(4,5)P2 abolished the signal completely (Fig. 2c). The results of protein–lipid overlay assay suggest that PI(4,5)P2 antibody has higher affinity to PI(3,4,5)P3 (Fig. 2a). However, the lipid blocking assay shows that PI(4,5)P2 antibody detects mostly PI(4,5)P2 in fixed cells, as shown in Fig. 2c. As the total amount of cellular PI(3,4,5)P3 is more than 20-fold lower than the amount of cellular PI(4,5)P2 (Stephens et al. 1993; Nasuhoglu et al. 2002), we believe that the antibody predominantly but not exclusively recognizes PI(4,5)P2 in the cells.

The antibody against PI(3,4)P2 shows nuclear pattern similar to PI(4,5)P2 with nuclear speckles and smaller nucleoplasmic foci (Fig. 1b). The antibody recognizes mainly PI(3,4)P2 on protein–lipid overlay assay, but binds also to PI(4,5)P2 and PI(3,4,5)P3 (Fig. 2d). Lipid blocking assay shows that the fluorescence signal is not abolished after preincubation of anti-PI(3,4)P2 antibody with PI(3,4)P2; however, the signal decreases after preincubations with PI(3)P, PI(4)P, PI(5)P, PI(3,4)P2, PI(3,5)P2, and PI(3,4,5)P3 (Fig. 2e). Our results therefore suggest that although the PI(3,4)P2 antibody can be used to detect PI(3,4)P2 spotted on a membrane, it is not suitable for immunofluorescence studies under experimental conditions we tested.

The antibody against PI(4)P detects nuclear PI(4)P signal, which resembles the signal of PI(4,5)P2 in nuclear speckles and small foci in nucleoplasm and nucleoli (Fig. 1c). The antibody detects specifically PI(4)P on protein–lipid overlay assay with a weak signal coming from PI(4,5)P2 and PI(3)P (Fig. 2f). Moreover, the lipid blocking assay shows that the fluorescence signal diminishes only after preincubation with PI(4)P (Fig. 2g). Therefore, we concluded that the PI(4)P antibody can be used for PI(4)P detection by immunofluorescence in fixed cells.

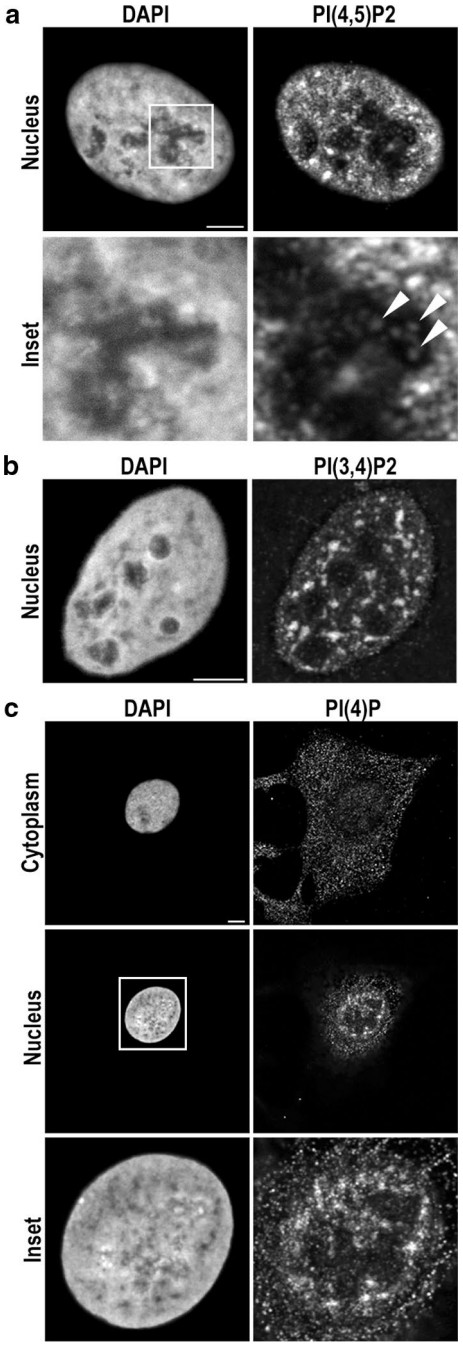

Fig. 1 Antibodies detect nuclear PI(4,5)P2, PI(3,4)P2, and PI(4)P. Anti-PI(4,5)P2 detects PI(4,5)P2 in the nucleoplasm and nuclear speckles (**a**) and weak foci in nucleoli (*inset*, *arrowheads*). Anti-PI(3,4)P2 antibody detects nuclear pattern similar to anti-PI(4,5)P2 antibody (**b**) Anti-PI(4)P antibody detects both cytoplasmic and nuclear signal (**c**, optical sections focused on the cytoplasm and on the nucleus). In the nucleus, anti-PI(4)P antibody gives similar pattern to anti-PI(4,5)P2 antibody (*inset*). *Scale bars* 5 μm

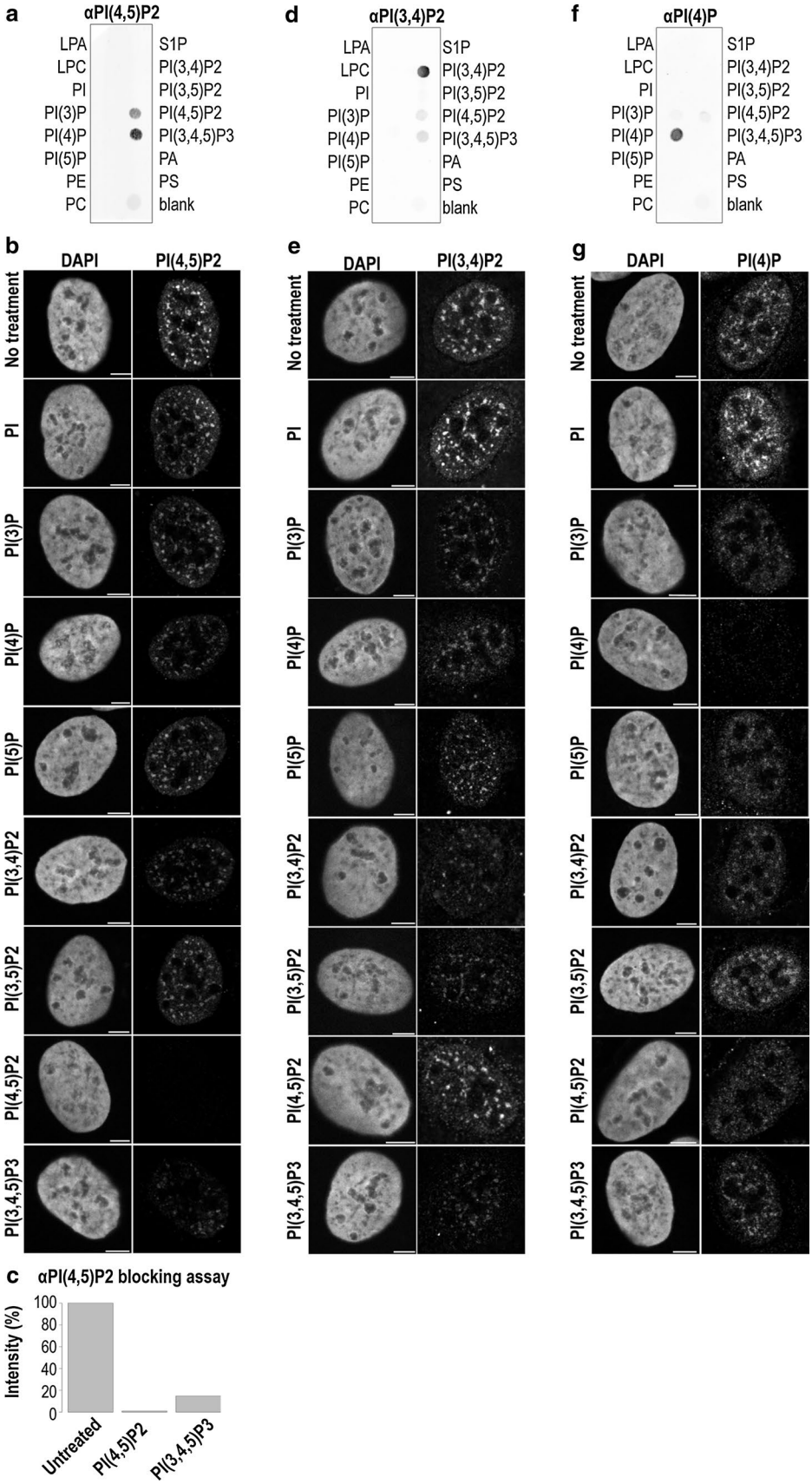

Fig. 2 Antibody against PI(4,5)P2 binds to PI(4,5)P2 and PI(3,4,5)P3 on protein–lipid overlay assay (**a**). On immunofluorescence, the antibody is blocked by preincubation with PI(4,5)P2 and PI(3,4,5)P3 (**b**). The *graph* shows signal intensities from images of the cell without treatment and after pre-blocking with PI(4,5)P2 and PI(3,4,5)P3. The blocking is only partial (up to 85 %) after preincubation with PI(3,4,5)P3, while preincubation with PI(4,5)P2 blocks signal completely (**c**). The antibody against PI(3,4)P2 detects mostly PI(3,4)P2 and weakly also PI(4,5)P2 and PI(3,4,5)P3 on protein–lipid overlay (**d**). The immunofluorescence signal from anti-PI(3,4)P2 antibody is decreased after preincubation of the antibody with PI(3)P, PI(4)P, PI(5)P, PI(3,4)P2, PI(3,5)P2, and PI(3,4,5)P3 (**e**). Anti-PI(4)P antibody detects PI(4)P and very weakly binds to PI(3)P and PI(4,5)P2 on protein–lipid overlay assay (**f**). Immunofluorescence signal of anti-PI(4)P antibody is completely abolished after preincubation with PI(4)P only (**g**). LPA, lysophosphatidic acid, LPC, lysophosphocholine, PtdIns, phosphatidylinositol, PE, phosphatidylethanolamine, S1P, sphingosine-1-phosphate, PA, phosphatidic acid, PS, phosphatidylserine, *Scale bars* 5 µm

Overexpressed PIs-binding domains show nuclear staining in U2OS cells

In addition to commercially available antibodies, we tested several PIs-binding domains (Table 1). These protein modules have been used before for PIs detection in cellular membranes (reviewed in Balla and Várnai 2009). We transfected PLCδ1-PH, EEA1-FYVE, Akt-PH, Grp1-PH, OSH1-PH, and Tubby domains coupled to eGFP into U2OS cells and inspected their nuclear patterns. As a control, we prepared mutant form of each domain, which prevents binding of the domain to the respective PIs. As published before, PLCδ1-PH binds PI(4,5)P2 in the plasma membrane (Stauffer et al. 1998; Varnai and Balla 1998; Kavran et al. 1998). Indeed, overexpressed PLCδ1-PH localizes mainly to the plasma membrane and is diffused throughout the cytoplasm (Fig. 3a), while mutant PLCδ1-PH loses the plasma membrane localization (Fig. 3b). Both wild-type and mutant PLCδ1-PH show diffused nuclear signal. The nuclear signal is enriched in mutant probably due to relocalization of the domain from the plasma membrane. To target PLCδ1-PH to the nucleus, we cloned NLS sequence downstream of GFP. Even though this construct was efficiently imported into the nucleus, we did not observe any difference between localization patterns of wild-type and mutant domains (Fig. 3c, d). Since the overexpressed PLCδ1-PH does not seem to be a suitable tool for nuclear PI(4,5)P2 detection, we tested also another PI(4,5)P2 binding domain, a Tubby domain (Santagata et al. 2001; Quinn et al. 2008; Szentpetery et al. 2009). Similarly to PLCδ1-PH, wild-type Tubby domain localizes to the plasma membrane (Fig. 3e). Moreover, we detected signal in the nucleus and small foci in nucleoli. Mutant Tubby domain loses the plasma membrane localization and relocalizes to the nucleus, where the pattern resembles the signal of wild-type Tubby domain (Fig. 3f). In conclusion, both PLCδ1-PH and Tubby fail to specifically recognize nuclear PI(4,5)P2.

EEA1-FYVE has been previously used for visualization of PI(3)P in endosomes (Burd and Emr 1998; Gaullier et al. 1998). We observed the same pattern, which is lost after mutation in EEA1-FYVE confirming its specificity (Fig. 3g, h). Both wild-type and mutant EEA1-FYVE enter nucleus, where they show the same diffused nuclear signal. In addition, wild-type also recognizes foci in nucleoli, which are absent in mutant (Fig. 3h, inset). This suggests that EEA1-FYVE domain recognizes nucleolar specific pool of PI(3)P.

Akt-PH binds PI(3,4,5)P3 and PI(3,4)P2 (Kavran et al. 1998; Watton and Downward 1999; Rowland et al. 2012). After overexpression, Akt-PH localizes to the plasma membrane and intracellular membranes (Fig. 3i), while mutant Akt-PH is diffused throughout the cytoplasm (Fig. 3j). Both wild-type and mutant Akt-PH localize to the nucleus, where they display a similar pattern suggesting their inability to recognize nuclear PI(3,4,5)P3 or PI(3,4)P2. An alternative tool for visualization of PI(3,4,5)P3 is Grp1-PH domain (Venkateswarlu et al. 1998; Kavran et al. 1998; Gray et al. 1999; Manna et al. 2007). Using Grp1-PH, we detected only a weak signal in the cytoplasm (Fig. 3k, l). It is therefore possible that Akt-PH detects mostly PI(3,4)P2 in the plasma membrane. Both, wild-type and mutant Grp1-PH domains localized mostly to the nucleus, where they display a similar pattern suggesting the inability of Grp1 to detect nuclear PI(3,4,5)P3 specifically (Fig. 3k, l).

It has been reported that overexpressed OSH1-PH binds to PI(4)P present in the plasma membrane and Golgi apparatus (Roy and Levine 2004; Yu et al. 2004; Balla et al. 2008). In agreement with this, we show OSH1-PH localization to the plasma membrane and other cellular membranes (Fig. 3m), while mutant OSH1-PH is diffused throughout the cytoplasm (Fig. 3n). Both wild-type and mutant OSH1-PH localize to the nucleus, where they display a similar pattern.

Taken together, our results are consistent with previously published data and show that overexpressed PIs-binding domains localize to the nucleus. Careful comparison with mutant domains, however, revealed that in the nucleus, these domains do not specifically interact with PIs. Among

Fig. 3 Comparison of PIs-binding domains after overexpression in U2OS cells. Images are taken at optical sections focused on the plasma membrane (*Cytopl.*) and on the nucleus (*Nucleus*). Wild-type PLCδ1-PH (**a**) but not mutant PLCδ1-PH (**b**) is accumulated at the plasma membrane. Both domains are diffused throughout the cytoplasm and the nucleus (**a**, **b** *inset*). With NLS, both wild-type PLCδ1-PH (**c**) and mutant PLCδ1-PH (**d**) are accumulated in the nucleus and display the same nuclear pattern (**c**, **d** *inset*). Wild-type Tubby domain localizes to the plasma membrane and weakly also to the nucleus (**e**), where it forms small foci in the nucleoli (*inset, arrowheads*). Mutant Tubby domain is absent from the plasma membrane and accumulates in the nucleus (**f**), where it displays pattern similar to the wild-type domain (*inset, arrowheads*). Wild-type EEA1-FYVE localizes to endosomes and also to the nucleus (**g**), where it localizes to the nucleoplasm and forms foci in the nucleoli (*inset, arrowheads*). Mutant EEA1-FYVE is diffused throughout the cytoplasm and the nucleus (**h**), whereas nucleoli foci are absent (*inset*). Wild-type Akt-PH localizes to the plasma membrane and other cellular membranes (**i**) and to the nucleus (*inset*). While mutant Akt-PH is absent from the membranes (**j**), it displays similar nuclear pattern as the wild-type domain (*inset*). Both wild-type Grp1-PH (**k**) and mutant Grp1-PH (**l**) are almost absent from the cytoplasm and are accumulated in the nucleus, where they display similar pattern (**k**, **l** *inset*). Wild-type OSH1-PH localizes to the plasma membrane and other cellular membranes, probably Golgi apparatus (**m**), while the mutant OSH1-PH is diffused throughout the cytoplasm (**n**). Both wild-type and mutant OSH1-PH domains localize to the nucleus (**m**, **n** *inset*). *Scale bars* 5 μm

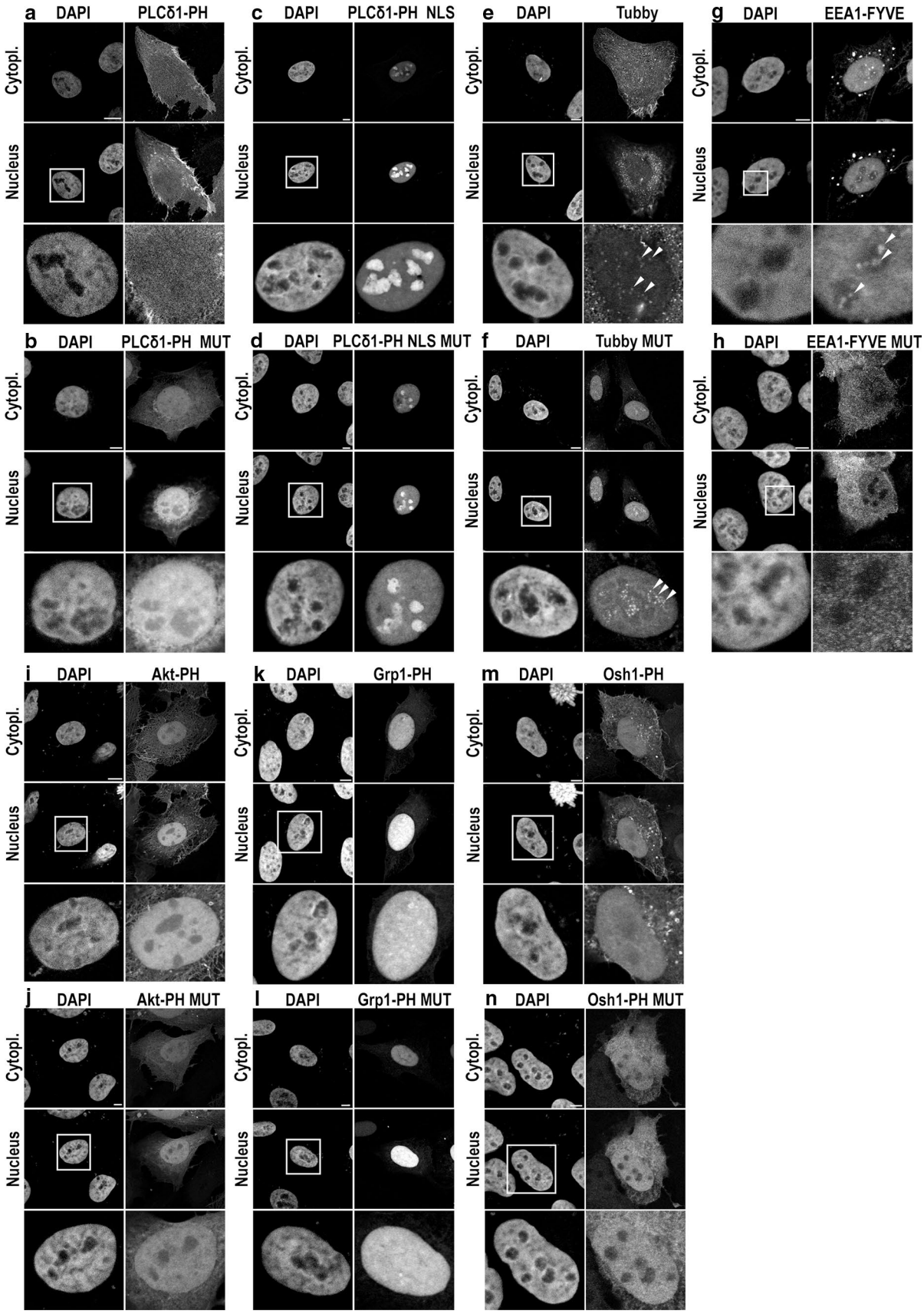
a DAPI PLCδ1-PH
c DAPI PLCδ1-PH NLS
e DAPI Tubby
g DAPI EEA1-FYVE
b DAPI PLCδ1-PH MUT
d DAPI PLCδ1-PH NLS MUT
f DAPI Tubby MUT
h DAPI EEA1-FYVE MUT
i DAPI Akt-PH
k DAPI Grp1-PH
m DAPI Osh1-PH
j DAPI Akt-PH MUT
l DAPI Grp1-PH MUT
n DAPI Osh1-PH MUT
Cytopl.
Nucleus

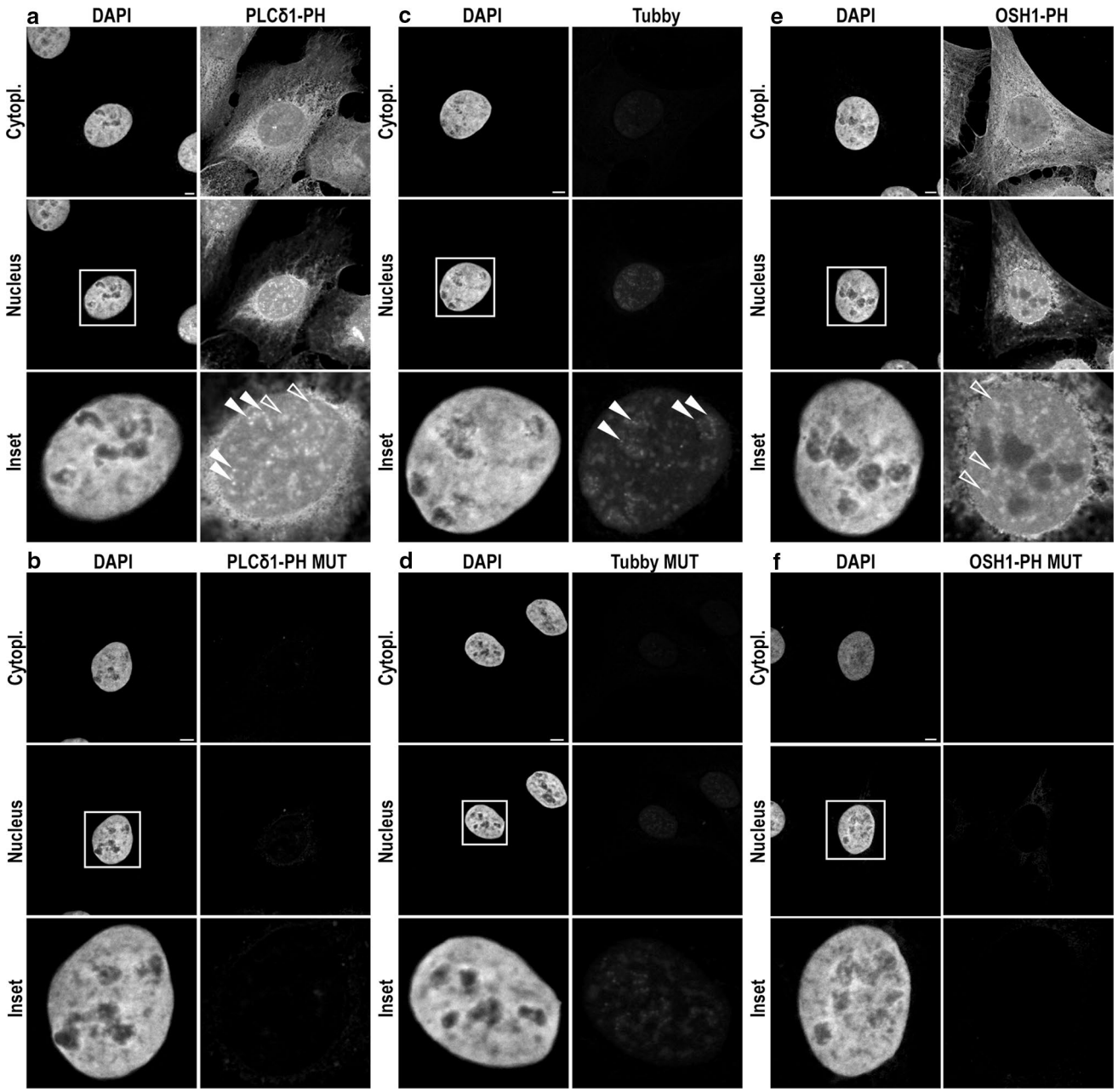

Fig. 4 Purified PLCδ1-PH, Tubby, and OSH1-PH domains recognize nuclear PIs. The images are taken at optical sections focused on the plasma membrane (*Cytopl.*) and on the nucleus (*Nucleus*). Purified PLCδ1-PH detects PI(4,5)P2 in intracellular membranes and in a lesser extent also in the plasma membrane (**a**). Moreover, wild-type PLCδ1-PH detects nuclear PI(4,5)P2 in the nucleus (**a** *inset*), where it accumulates in nucleoli (*arrowheads*) and nuclear speckles (*empty arrowheads*). The signal is completely abolished when mutant PLCδ1-PH is used (**b**). Wild-type Tubby domain detects PI(4,5)P2 only in the nucleus (**c**), where it localizes to nucleolar foci (*inset, arrowheads*). Mutant Tubby shows very weak nuclear signal (**d**). Wild-type OSH1-PH detects PI(4)P in the plasma membrane and other cellular membranes (**e**). Moreover, it has strong nuclear signal with larger bright foci, probably nuclear speckles (*inset, empty arrowheads*). Mutant OSH1-PH detects very weak cytoplasmic signal (**f**), while nuclear signal is completely abolished (*inset*). *Scale bars* 5 μm

the domains tested, the only exception was the EEA1-FYVE. It displays nucleolar localization, which is lost after mutation of PIs-binding site. Therefore, we believe that overexpressed EEA1-FYVE can be used for imaging of PI(3)P in nucleoli.

Purified PIs-binding domains conjugated with eGFP show nuclear pattern

Since overexpressed PIs-binding domains do not follow PIs to the nucleus, we looked for an alternative approach.

Fused with GST, PIs-binding domains have been successfully used for imaging of nuclear PIs in fixed cells (Gilloloy et al. 2000; Watt et al. 2002, 2004; Lindsay et al. 2006; Yildirim et al. 2013). In this system, the purified domain was incubated with fixed and permeabilized cells and subsequently detected by anti-GST antibody. To omit the use of an additional antibody, we fused PLCd1-PH, OSH1-PH, and Tubby domains with eGFP, cloned them into bacterial expression vector, and purified them from bacteria. The purified domains were tested for specificity in protein–lipid overlay assay and then used in an analogy to antibodies for immunofluorescence staining (Fig. 4). Mutant domains which are not able to bind PIs were used as negative controls.

It has been reported that GST tagged PLCδ1-PH recognizes PI(4,5)P2 in nuclear speckles and nucleoli (Watt et al. 2002; Hammond et al. 2009; Yildirim et al. 2013). Therefore, we selected PI(4,5)P2 binding domains—PLCδ1-PH and Tubby—to test their eGFP fusions on immunofluorescence. In addition, we purified eGFP tagged OSH1-PH that recognizes PI(4)P, whose nuclear signal is unknown. Since antibodies against both PI(4,5)P2 and PI(4)P are available and specific, we were able to compare results obtained by immunofluorescence.

Purified PLCδ1-PH detects PI(4,5)P2 foci in nucleoli and nuclear speckles (Fig. 4a). The signal is diminished in mutant PLCδ1-PH (Fig. 4b). In comparison with overexpressed wild-type PLCδ1-PH (Fig. 3a), purified PLCδ1-PH stains the plasma membrane to a lesser extent but detects signal from other cellular membranes. On the other hand, the nuclear pattern of purified PLCδ1-PH resembles PI(4,5)P2 labelling obtained by anti-PI(4,5)P2 antibody. In contrast, purified Tubby domain shows PI(4,5)P2 signal only in nucleoli of U2OS cells (Fig. 4c). We still detected a weak signal from mutant Tubby domain (Fig. 4d); however, the signal from wild-type domain was stronger, and therefore, we believe that it is specific. Similarly to PLCδ1-PH, Tubby is also absent from the plasma membrane. These results suggest that purified PLCδ1-PH is specific and detects similar pool of PI(4,5)P2 as anti-PI(4,5)P2 antibody. Tubby domain probably specifically recognizes nucleolar PI(4,5)P2 only.

Purified wild-type OSH1-PH detects PI(4)P in the plasma membrane and other cellular membranes, in the nucleoplasm and larger nuclear foci, and probably in nuclear speckles (Fig. 4e). The signal is lost when the cells are incubated with mutant OSH1-PH (Fig. 4f). The nuclear pattern of purified OSH1-PH resembles anti-PI(4)P labelling. We conclude that purified OSH1-PH can be used for visualization of PI(4)P in the nucleus. Importantly, we noted that nuclear patterns of all domains used for staining on fixed cells are similar to antibody-based labelling; however, they differ significantly from the patterns of overexpressed domains.

Table 2 Summary and specificity of tools used for PIs detection in the cytoplasm and in the nucleus

Tools	Target	Suitable for detection in	
		Cytoplasm	Nucleus
Antibodies			
αPI(4,5)P2	PI(4,5)P2	−	+++
αPI(3,4)P2	PI(3,4)P2	−	−
αPI(4)P	PI(4)P	−	+++
Overexpressed domains			
EEA1-FYVE	PI(3)P	+++	+ (nucleoli)
OSH1-PH	PI(4)P	+++	−
Akt-PH	PI(3,4)P2, PI(3,4,5)P3	+++	−
Tubby	PI(4,5)P2	+++	−
PLCδ1-PH	PI(4,5)P2	+++	−
PLCδ1-PH NLS	PI(4,5)P2	−	−
Grp1-PH	PI(3,4,5)P3	−	−
Purified domains			
Tubby	PI(4,5)P2	−	+ (nucleoli)
PLCδ1-PH	PI(4,5)P2	+	+++
OSH1-PH	PI(4)P	+	+++

Based on our results, antibodies and domains were rated as unsuitable (−), good (+), or very good (+++)

Discussion

Nuclear PIs have been identified as important regulators of various nuclear functions (reviewed in Shah et al. 2013). To better understand their role in the nucleus, tools for nuclear PIs visualization both in vivo and in vitro are needed. Here we performed a screen in which we aimed to identify an approach to track nuclear PIs in space and time. We compared labelling patterns of antibodies and protein domains that can be used for detection of nuclear PIs (summarized in Table 2). We showed that PI(4,5)P2 antibody recognizes PI(4,5)P2 and PI(3,4,5)P3 on protein–lipid overlay. However, according to the results of the blocking assay, the antibody is blocked by PI(3,4,5)P3 only partially while the incubation with PI(4,5)P2 abolishes the antibody signal completely (Fig. 2a–c). Because the cellular level of PI(3,4,5)P3 is more than 20-fold smaller in comparison with PI(4,5)P2 (Stephens et al. 1993; Nasuhoglu et al. 2002), we believe that the signal detected by anti-PI(4,5)P2 antibody comes from the nuclear PI(4,5)P2. Although antibody against PI(3,4)P2, the second antibody we tested, is specific on protein–lipid overlay assay, we show that it is not suitable for immunofluorescence

under our experimental conditions since it can be partially blocked by preincubation with most PIs tested (Fig. 2a, b). We suspect that these discrepancies are caused by high concentration of PIs spotted on the membrane, which do not resemble well enough the physiological conditions. On the other hand, the antibody against PI(4)P, the third antibody we tested, recognizes mainly PI(4)P as shown on both protein–lipid overlay and blocking assay (Fig. 2a, b). Using this antibody, we demonstrated for the first time that PI(4)P can be detected in the cell nucleus and that its pattern resembles the localization of PI(4,5)P2 in nuclear speckles. This antibody also detects small foci in the nucleoplasm and nucleoli (Fig. 1c). These results are in agreement with published data, which repeatedly reported localization of PI(4)P metabolizing enzymes in nuclear speckles (Boronenkov et al. 1998; Szivak et al. 2006; Mellman et al. 2008; Schill and Anderson 2009; Elong Edimo et al. 2011) and nucleoli (Kakuk et al. 2008). Regarding the nucleolar PI(4)P signal, we have shown previously that nucleolar PI(4,5)P2 forms foci in fibrillar centres and in the dense fibrillar component where it regulates rDNA synthesis and processing (Sobol et al. 2013; Yildirim et al. 2013). It is possible that the nucleolar PI(4)P serves as a precursor for PI(4,5)P2 in these compartments.

To track PIs in live cells, we overexpressed PIs-binding domains fused with eGFP in U2OS cells (Table 1; Fig. 3). We confirm that these domains are suitable for PIs monitoring in the plasma membrane and other cellular membranes. The localization of overexpressed PIs-binding domains in the nucleus has been described earlier, and it was considered as a consequence of overexpression. Since the domains are relatively small, they could diffuse passively through the nuclear pore (reviewed in Hammond and Balla 2015). We decided to inspect carefully the nuclear signal of several overexpressed domains. Mostly, we observed similar nuclear patter of wild-type and mutant domains. However, we show that wild-type but not mutant EEA1-FYVE domain localizes to foci in nucleoli. Therefore, the overexpressed EEA-1 FYVE domain can be used for visualization of PI(3)P in nucleoli.

Since most of the overexpressed PIs-binding domains were not suitable for PIs detection in the nucleus, we prepared purified PLCδ1-PH, Tubby, and OSH1-PH domains fused with eGFP. In contrast to the results obtained after overexpression, purified PLCδ1-PH and Tubby domains specifically detect PI(4,5)P2 in nucleoli. Moreover, PLCδ1-PH shows PI(4,5)P2 localization also in nuclear speckles. OSH1-PH detects nuclear PI(4)P in the nucleoplasm and concentrated in bigger nucleoplasmic foci, probably nuclear speckles. It is known that the concentration and type of detergent used for permeabilization affect the detection of PIs in the cell (Mazzotti et al. 1995; Hammond et al. 2009). Therefore, we think that different conditions used for PIs detection are the reason for diversities between overexpressed and purified domains staining. After overexpression, PIs-binding domains are targeted to the site of their ligand, where they are fixed, and therefore, stronger signal from cellular membranes can be detected. In case of purified PIs-binding domains and antibodies, cell membranes are first permeabilized, and then, PIs detection tools are applied. We believe that these differences in sample preparation result in reduction in the PIs signal from cellular membranes while the signal from the nucleus, where PIs form complexes with nuclear proteins, is more prominent. Therefore, purified domains are more suitable tools for nuclear PIs detection.

We also report differences in the nuclear signal detected by purified domains and antibodies in fixed cells. We show that anti-PI(4,5)P2 detects signal mostly in nuclear speckles and the nucleoplasm while purified PLCδ1-PH detects strong signal also in nucleolar foci. Tubby domain detects PI(4,5)P2 predominantly in nucleoli (Figs. 1a, 4). We believe that domains and antibodies recognize different pools of nuclear PIs with different affinities. It might be caused by different mechanism of PIs recognition. Moreover, anti-PI(4,5)P2 is IgM isotype and is therefore more than tenfold larger than both purified domains. Therefore, the antibody might not be able to access the nucleolar pool of PI(4,5)P2.

Here we identified some useful tools for PIs detection in the nucleus (Table 2). Unfortunately, the tools which would enable the visualization of nuclear PIs in vivo are still missing. One possibility is the use of labelled PIs. However, their use is problematic since they can be modified or cleaved in the cell. The future goal is thus to engineer such modifications of PIs which would enable their delivery to the nucleus and subsequently study their involvement in endogenous pathways, while preventing their cleavage.

Acknowledgments P. H., I. K., V. F., and L. U. were supported by the Grant agency of the Czech Republic (15-08738S, P305/11/2232, 16-03403S), P. H. and L. U. were supported by Human Frontier Science Program (RGP0017/2013), I. K., A. K., and L. U. were supported by the Grant Agency of the Charles University (606112), and I. K., V. F., A. K., and L. U. were supported by the Charles University in Prague. This publication is supported by the project "BIOCEV—Biotechnology and Biomedicine Centre of the Academy of Sciences and Charles University" (CZ.1.05/1.1.00/02.0109), from the European Regional Development Fund. This research was performed with support of the Institute of Molecular Genetics, Academy of Sciences of the Czech Republic (RVO: 68378050). We are very grateful to Dr. Tamas Balla (National Institutes of Health, Bethesda) for providing us the PLCδ1-PH, EEA1-FYVE, Grp1-PH, OSH1-PH, Akt-PH, and Tubby domains constructs. We would like to thank Iva Jelínková and Pavel Kříž for excellent technical assistance.

Compliance with ethical standards

Conflict of interest The authors have no conflict of interest to declare.

References

Ahn J-Y, Rong R, Liu X, Ye K (2004) PIKE/nuclear PI 3-kinase signaling mediates the antiapoptotic actions of NGF in the nucleus. EMBO J 23:3995–4006. doi:10.1038/sj.emboj.7600392

Ahn JY, Liu X, Cheng D et al (2005) Nucleophosmin/B23, a nuclear PI(3,4,5)P3 receptor, mediates the antiapoptotic actions of NGF by inhibiting CAD. Mol Cell 18:435–445. doi:10.1016/j.molcel.2005.04.010

Balla T (2013) Phosphoinositides: tiny lipids with giant impact on cell regulation. Physiol Rev 93:1019–1137. doi:10.1152/physrev.00028.2012

Balla T, Várnai P (2009) Visualization of cellular phosphoinositide pools with GFP-fused protein-domains. Curr Protoc Cell Biol 24(4). doi: 10.1002/0471143030.cb2404s42

Balla A, Kim YJ, Varnai P et al (2008) Maintenance of hormone-sensitive phosphoinositide pools in the plasma membrane requires phosphatidylinositol 4-kinase IIIalpha. Mol Biol Cell 19:711–721. doi:10.1091/mbc.E07-07-0713

Blind RD, Sablin EP, Kuchenbecker KM et al (2014) The signaling phospholipid PIP3 creates a new interaction surface on the nuclear receptor SF-1. Proc Natl Acad Sci USA 111:15054–15059. doi:10.1073/pnas.1416740111

Boronenkov IV, Loijens JC, Umeda M, Anderson RA (1998) Phosphoinositide signaling pathways in nuclei are associated with nuclear speckles containing pre-mRNA processing factors. Mol Biol Cell 9:3547–3560

Burd CG, Emr SD (1998) Phosphatidylinositol(3)-phosphate signaling mediated by specific binding to RING FYVE domains. Mol Cell 2:157–162. doi:10.1016/S1097-2765(00)80125-2

Clarke JH, Letcher AJ, D'santos CS et al (2001) Inositol lipids are regulated during cell cycle progression in the nuclei of murine erythroleukaemia cells. Biochem J 357:905–910. doi:10.1042/0264-6021:3570905

Cocco L, Gilmour RS, Ognibene A et al (1987) Synthesis of polyphosphoinositides in nuclei of friend cells. Evidence for polyphosphoinositide metabolism inside the nucleus which changes with cell differentiation. Biochem J 248:765–770

De Vries KJ, Westerman J, Bastiaens PI et al (1996) Fluorescently labeled phosphatidylinositol transfer protein isoforms (alpha and beta), microinjected into fetal bovine heart endothelial cells, are targeted to distinct intracellular sites. Exp Cell Res 227:33–39. doi:10.1006/excr.1996.0246

Elong Edimo W, Derua R, Janssens V et al (2011) Evidence of SHIP2 Ser132 phosphorylation, its nuclear localization and stability. Biochem J 439:391–401. doi:10.1042/BJ20110173

Gaullier JM, Simonsen A, D'Arrigo A et al (1998) FYVE fingers bind PtdIns(3)P. Nature 394:432–433. doi:10.1038/28767

Gillooly DJ, Morrow IC, Lindsay M et al (2000) Localization of phosphatidylinositol 3-phosphate in yeast and mammalian cells. EMBO J 19:4577–4588. doi:10.1093/emboj/19.17.4577

Gozani O, Karuman P, Jones DR et al (2003) The PHD finger of the chromatin-associated protein ING2 functions as a nuclear phosphoinositide receptor. Cell 114:99–111. doi:10.1016/S0092-8674(03)00480-X

Gray A, Van Der Kaay J, Downes CP (1999) The pleckstrin homology domains of protein kinase B and GRP1 (general receptor for phosphoinositides-1) are sensitive and selective probes for the cellular detection of phosphatidylinositol 3,4-bisphosphate and/or phosphatidylinositol 3,4,5-trisphosphate. Biochem J 344(Pt 3):929–936

Guillou H, Lécureuil C, Anderson KE et al (2007) Use of the GRP1 PH domain as a tool to measure the relative levels of PtdIns(3,4,5)P3 through a protein-lipid overlay approach. J Lipid Res 48:726–732. doi:10.1194/jlr.D600038-JLR200

Hammond GRV, Schiavo G, Irvine RF (2009) Immunocytochemical techniques reveal multiple, distinct cellular pools of PtdIns4 *P* and PtdIns(4,5) *P* $_2$. Biochem J 422:23–35. doi:10.1042/BJ20090428

Hammond GRV, Balla T (2015) Polyphosphoinositide binding domains: key to inositol lipid biology. Biochim Biophys Acta 1851:746–758. doi:10.1016/j.bbalip.2015.02.013

Jo H, Mondal S, Tan D et al (2012) Small molecule-induced cytosolic activation of protein kinase Akt rescues ischemia-elicited neuronal death. Proc Natl Acad Sci USA 109:10581–10586. doi:10.1073/pnas.1202810109

Jones DR, Bultsma Y, Keune W-J et al (2006) Nuclear PtdIns5P as a transducer of stress signaling: an in vivo role for PIP4Kbeta. Mol Cell 23:685–695. doi:10.1016/j.molcel.2006.07.014

Jungmichel S, Sylvestersen KB, Choudhary C et al (2014) Specificity and commonality of the phosphoinositide-binding proteome analyzed by quantitative mass spectrometry. Cell Rep 6:578–591. doi:10.1016/j.celrep.2013.12.038

Kakuk A, Friedländer E, Vereb G et al (2008) Nuclear and nucleolar localization signals and their targeting function in phosphatidylinositol 4-kinase PI4K230. Exp Cell Res 314:2376–2388. doi:10.1016/j.yexcr.2008.05.006

Kavran JM, Klein DE, Lee A et al (1998) Specificity and promiscuity in phosphoinositide binding by pleckstrin homology domains. J Biol Chem 273:30497–30508. doi:10.1074/jbc.273.46.30497

Keune Wj, Bultsma Y Y, Sommer L et al (2011) Phosphoinositide signalling in the nucleus. Adv Enzyme Regul 51:91–99. doi:10.1016/j.advenzreg.2010.09.009

Lee SA, Eyeson R, Cheever ML et al (2005) Targeting of the FYVE domain to endosomal membranes is regulated by a histidine switch. Proc Natl Acad Sci USA 102:13052–13057. doi:10.1073/pnas.0503900102

Levine TP, Munro S (2001) Dual targeting of Osh1p, a yeast homologue of oxysterol-binding protein, to both the Golgi and the nucleus-vacuole junction. Mol Biol Cell 12:1633–1644

Lewis AE, Sommer L, Arntzen MO et al (2011) Identification of nuclear phosphatidylinositol 4,5-bisphosphate-interacting proteins by neomycin extraction. Mol Cell Proteomics 10:M110.003376. doi:10.1074/mcp.M110.003376

Lindsay Y, McCoull D, Davidson L et al (2006) Localization of agonist-sensitive PtdIns(3,4,5)P3 reveals a nuclear pool that is insensitive to PTEN expression. J Cell Sci 119:5160–5168. doi:10.1242/jcs.000133

Manna D, Albanese A, Park WS, Cho W (2007) Mechanistic basis of differential cellular responses of phosphatidylinositol 3,4-bisphosphate- and phosphatidylinositol 3,4,5-trisphosphate-binding pleckstrin homology domains. J Biol Chem 282:32093–32105. doi:10.1074/jbc.M703517200

Martelli AM, Ognibene A, Buontempo F et al (2011) Nuclear phosphoinositides and their roles in cell biology and disease. Crit Rev Biochem Mol Biol 46:436–457. doi:10.3109/10409238.2011.609530

Mazzotti G, Zini N, Rizzi E et al (1995) Immunocytochemical detection of phosphatidylinositol 4,5-bisphosphate localization sites within the nucleus. J Histochem Cytochem 43:181–191. doi:10.1177/43.2.7822774

Mellman DL, Gonzales ML, Song C et al (2008) A PtdIns4,5P2-regulated nuclear poly(A) polymerase controls expression of select mRNAs. Nature 451:1013–1017. doi:10.1038/nature06666

Nasuhoglu C, Feng S, Mao J et al (2002) Nonradioactive analysis of phosphatidylinositides and other anionic phospholipids by anion-exchange high-performance liquid chromatography with suppressed conductivity detection. Anal Biochem 301:243–254. doi:10.1006/abio.2001.5489

Okada M, Jang S-W, Ye K (2008) Akt phosphorylation and nuclear phosphoinositide association mediate mRNA export and

cell proliferation activities by ALY. Proc Natl Acad Sci USA 105:8649–8654. doi:10.1073/pnas.0802533105

Osborne SL, Thomas CL, Gschmeissner S, Schiavo G (2001) Nuclear PtdIns(4,5)P2 assembles in a mitotically regulated particle involved in pre-mRNA splicing. J Cell Sci 114:2501–2511

Quinn KV, Behe P, Tinker A (2008) Monitoring changes in membrane phosphatidylinositol 4,5-bisphosphate in living cells using a domain from the transcription factor tubby. J Physiol 586:2855–2871. doi:10.1113/jphysiol.2008.153791

Rowland MM, Gong D, Bostic HE et al (2012) Microarray analysis of Akt PH domain binding employing synthetic biotinylated analogs of all seven phosphoinositide headgroup isomers. Chem Phys Lipids 165:207–215. doi:10.1016/j.chemphyslip.2011.12.001

Roy A, Levine TP (2004) Multiple pools of phosphatidylinositol 4-phosphate detected using the pleckstrin homology domain of Osh2p. J Biol Chem 279:44683–44689. doi:10.1074/jbc.M401583200

Sablin EP, Blind RD, Uthayaruban R et al (2015) Structure of liver receptor homolog-1 (NR5A2) with PIP3 hormone bound in the ligand binding pocket. J Struct Biol 192:342–348. doi:10.1016/j.jsb.2015.09.012

Santagata S, Boggon TJ, Baird CL et al (2001) G-protein signaling through tubby proteins. Science 292:2041–2050. doi:10.1126/science.1061233

Schill NJ, Anderson RA (2009) Two novel phosphatidylinositol-4-phosphate 5-kinase type Igamma splice variants expressed in human cells display distinctive cellular targeting. Biochem J 422:473–482. doi:10.1042/BJ20090638

Shah ZH, Jones DR, Sommer L et al (2013) Nuclear phosphoinositides and their impact on nuclear functions. FEBS J 280:6295–6310. doi:10.1111/febs.12543

Smith CD, Wells WW (1983) Phosphorylation of rat liver nuclear envelopes. I. Characterization of in vitro protein phosphorylation. J Biol Chem 258:9360–9367

Sobol M, Yildirim S, Philimonenko VV et al (2013) UBF complexes with phosphatidylinositol 4,5-bisphosphate in nucleolar organizer regions regardless of ongoing RNA polymerase I activity. Nucleus 4:478–486. doi:10.4161/nucl.27154

Stauffer TP, Ahn S, Meyer T (1998) Receptor-induced transient reduction in plasma membrane PtdIns(4,5)P2 concentration monitored in living cells. Curr Biol 8:343–346. doi:10.1016/S0960-9822(98)70135-6

Stephens LR, Jackson TR, Hawkins PT (1993) Agonist-stimulated synthesis of phosphatidylinositol(3,4,5)-trisphosphate. Biochim Biophys Acta Mol Cell Res 1179:27–75. doi:10.1016/0167-4889(93)90072-W

Szentpetery Z, Balla A, Kim YJ et al (2009) Live cell imaging with protein domains capable of recognizing phosphatidylinositol 4,5-bisphosphate; a comparative study. BMC Cell Biol 10:67. doi:10.1186/1471-2121-10-67

Szivak I, Lamb N, Heilmeyer LMG (2006) Subcellular localization and structural function of endogenous phosphorylated phosphatidylinositol 4-kinase (PI4K92). J Biol Chem 281:16740–16749. doi:10.1074/jbc.M511645200

Tan X, Thapa N, Choi S, Anderson RA (2015) Emerging roles of PtdIns(4,5)P2 - beyond the plasma membrane. J Cell Sci 128:4047–4056. doi:10.1242/jcs.175208

Toska E, Campbell HA, Shandilya J et al (2012) Repression of transcription by WT1-BASP1 requires the myristoylation of BASP1 and the PIP2-dependent recruitment of histone deacetylase. Cell Rep 2:462–469. doi:10.1016/j.celrep.2012.08.005

Vann LR, Wooding FB, Irvine RF, Divecha N (1997) Metabolism and possible compartmentalization of inositol lipids in isolated rat-liver nuclei. Biochem J 327(Pt 2):569–576

Varnai P, Balla T (1998) Visualization of phosphoinositides that bind Pleckstrin homology domains: calcium- and agonist-induced dynamic changes and relationship to myo-[3H]inositol-labeled phosphoinositide pools. J Cell Biol 143:501–510. doi:10.1083/jcb.143.2.501

Venkateswarlu K, Gunn-Moore F, Oatey PB et al (1998) Nerve growth factor- and epidermal growth factor-stimulated translocation of the ADP-ribosylation factor-exchange factor GRP1 to the plasma membrane of PC12 cells requires activation of phosphatidylinositol 3-kinase and the GRP1 pleckstrin homology domain. Biochem J 335(Pt 1):139–146

Višnjić D, Ćurić J, Crljen V et al (2003) Nuclear phosphoinositide 3-kinase C2β activation during G2/M phase of the cell cycle in HL-60 cells. Biochim Biophys Acta Mol Cell Biol Lipids 1631:61–71. doi:10.1016/S1388-1981(02)00356-6

Watt SA, Kular G, Fleming IN et al (2002) Subcellular localization of phosphatidylinositol 4,5-bisphosphate using the pleckstrin homology domain of phospholipase C delta1. Biochem J 363:657–666. doi:10.1074/jbc.M301418200

Watt SA, Kimber WA, Fleming IN et al (2004) Detection of novel intracellular agonist responsive pools of phosphatidylinositol 3,4-bisphosphate using the TAPP1 pleckstrin homology domain in immunoelectron microscopy. Biochem J 377:653–663. doi:10.1042/BJ20031397

Watton SJ, Downward J (1999) Akt/PKB localisation and 3′ phosphoinositide generation at sites of epithelial cell–matrix and cell–cell interaction. Curr Biol 9:433–436. doi:10.1016/S0960-9822(99)80192-4

Wickramasinghe V, Savill J, Chavali S et al (2013) Human inositol polyphosphate multikinase regulates transcript-selective nuclear mRNA export to preserve genome integrity. Mol Cell 51:737–750. doi:10.1016/j.molcel.2013.08.031

Yagisawa H, Sakuma K, Paterson HF et al (1998) Replacements of single basic amino acids in the pleckstrin homology domain of phospholipase C-δ1 alter the ligand binding, phospholipase activity, and interaction with the plasma membrane. J Biol Chem 273:417–424. doi:10.1074/jbc.273.1.417

Yildirim S, Castano E, Sobol M et al (2013) Involvement of phosphatidylinositol 4,5-bisphosphate in RNA polymerase I transcription. J Cell Sci 126:2730–2739. doi:10.1242/jcs.123661

Yokogawa T, Nagata S, Nishio Y et al (2000) Evidence that 3′-phosphorylated polyphosphoinositides are generated at the nuclear surface: use of immunostaining technique with monoclonal antibodies specific for PI 3,4-P2. FEBS Lett 473:222–226. doi:10.1016/S0014-5793(00)01535-0

York JD, Majerus PW (1994) Nuclear phosphatidylinositols decrease during S-phase of the cell cycle in HeLa cells [published erratum appears in J Biol Chem 1994 Dec 9;269(49):31322]. J Biol Chem 269:7847–7850

Yu JW, Mendrola JM, Audhya A et al (2004) Genome-wide analysis of membrane targeting by *S. cerevisiae* pleckstrin homology domains. Mol Cell 13:677–688. doi:10.1016/S1097-2765(04)00083-8

Zhao K, Wang W, Rando OJ et al (1998) Rapid and phosphoinositol-dependent binding of the SWI/SNF-like BAF complex to chromatin after T lymphocyte receptor signaling. Cell 95:625–636. doi:10.1016/S0092-8674(00)81633-5

Zou J, Marjanovic J, Kisseleva MV et al (2007) Type I phosphatidylinositol-4,5-bisphosphate 4-phosphatase regulates stress-induced apoptosis. Proc Natl Acad Sci USA 104:16834–16839. doi:10.1073/pnas.0708189104

3.2 Nuclear phosphatidylinositol 4,5-bisphosphate islets contribute to efficient DNA transcription

Sobol M, Kalendová A, Yildirim S, Philimonenko V, Marášek P, Kalasová I, Pastorek L, Hozák P

Manuscript.

I. K. performed experiments (pull-down assay and western blotting).

Nuclear phosphatidylinositol 4,5-bisphosphate islets contribute to efficient DNA transcription

Margarita Sobol, Alžběta Kalendová, Sukriye Yildirim, Vlada Philimonenko, Pavel Marášek, Ilona Kalasová, Lukáš Pastorek, Pavel Hozák

Institute of Molecular Genetics ASCR v.v.i., Department of Biology of the Cell Nucleus, Vídeňská 1083, 142 20, Prague 4, Czech Republic

Corresponding Author: Pavel Hozák, hozak@img.cas.cz

Tel: +420 241 062 219

Fax: +420 241 062 289

Abstract

Phosphatidylinositol 4,5-bisphosphate (PIP2) is a major phosphoinositide of plasma membrane. In addition, it is present in nucleoplasm, where it seems to be a universal regulator involved in chromatin remodelling, transcription, and splicing. Since its role in RNA polymerase II transcription is still little understood, we studied PIP2 association with Pol II transcription complexes and its overall nuclear distribution. Based on the fact that NM1 is known as interacting partner of PIP2 in cytoplasm, we studied the interactions of PIP2 with NM1 and the importance of this complex for Pol II transcription. Here we demonstrate the involvement of nucleoplasmic PIP2 in Pol II transcription through PIP2 islets. These previously undescribed nucleoplasmic 40-100 nm structures are decorated by PIP2 molecules and composed mainly of lipids, while the periphery of PIP2 islets is covered by chromatin, nascent RNA transcripts, and proteins engaged in Pol II transcription, including NM1. Using DNase and RNase digestion, we demonstrated that PIP2 islets are chromatin-independent but RNA-associated structures. We showed that either the disruption of PIP2 islets or NM1 depletion decrease Pol II transcription. We suggest that PIP2 islets provide a platform for the proper arrangement of the RNA polymerase II transcription complexes.

Key words: nucleus, PIP2, Pol II transcription, chromatin

Introduction

Phosphoinositides are amphipathic lipids containing hydrophilic inositol head group and hydrophobic fatty acid tails. Phosphatidylinositol 4,5-bisphosphate (PIP2) is a phosphoinositide (PI) phosphorylated at 4C and 5C hydroxyl groups of the inositol ring (Tanaka et al. 2003; Balla 2013). PIP2 predominantly localizes to plasma membrane, where it participates in signalling (Balla 2013). In addition to the cytoplasm, PIP2 exists also in the nucleus together with the enzymes and substrates involved in its metabolism. In striking contrast to the cytoplasm, nuclear PIP2 is localized exclusively in the nuclear interior and is absent in the nuclear membrane (Cocco et al. 1987; Payrastre et al. 1992; Vann et al. 1997). Under extraction with high detergent concentrations, nearly half of the PIP2 amount is retained in the nucleus. This suggests that PIP2 is a part of the discrete intranuclear structures, where it interacts with the various proteins (Vann et al. 1997; Gonzales and Anderson 2006; Layerenza et al. 2013). Upon binding to a protein, PIP2 causes its conformational changes and/or affects its binding properties, which finally lead to a modulation of protein activity. In this manner, PIP2 participates in a regulation of a variety of nuclear processes like chromatin remodelling, cell proliferation, cell cycle progression, DNA transcription, and mRNA processing (Cocco et al. 1987; Divecha et al. 1991; Yu et al. 1998; Zhao et al. 1998; Anderson et al. 1999; Osborne et al. 2001; Rando et al. 2002; Jones and Divecha 2004; Mellman et al. 2008; Toska et al. 2012; Geeraerts et al. 2013). It was shown that PIP2 promotes the binding of chromatin-remodelling SWI/SNF-like BAF complex to chromatin, which leads to T-lymphocyte activation (Zhao et al. 1998; Rando et al. 2002). Recently, we have found that the organization of nucleolus during cell cycle and transcription of genes coding ribosomal RNA (rRNA) require PIP2 (Sobol et al. 2013; Yildirim et al. 2013). We showed that PIP2 interacts with RNA polymerase I (Pol I), upstream binding factor (UBF), and fibrillarin. In such a way, PIP2 triggers conformational changes of these proteins, thus affecting their binding to DNA and RNA, respectively. Remarkably, PIP2 is required not only during rRNA synthesis and processing, but also serves as a scaffold which retains the components of Pol I pre-initiation complex such as UBF, PAF53, and RPA116 even during mitosis (Sobol et al. 2013; Yildirim et al. 2013). Even though PIP2 is a scaffold and an activator of Pol I transcription machinery, the effects of PIP2 on RNA polymerase II (Pol II) transcription are diverse. With various *in vivo* and *in vitro* biochemical approaches, Yu et al. (1998) identified PIP2 as a transcription activator. PIP2 binding to histone H1 results in a dissociation of H1 from DNA thus promoting transcription in a *Drosophila* embryo

transcription system (Yu et al. 1998). On the contrary, it was demonstrated that PIP2 facilitates the recruitment of the transcriptional co-factor BASP1 and histone deacetylase 1 (HDAC1) to the promoter, thus eliciting transcriptional repression (Toska et al. 2012). These data indicate that nuclear PIP2 might have diverse effects depending on its interactions with particular proteins or complexes.

With a set of biochemical approaches, Osborne et al. (2001) showed the association of PIP2 with hyperphosphorylated Pol II and snRNAs, suggesting the involvement of PIP2 in Pol II transcription and mRNA splicing. However, the particular binding partners of PIP2 participating in Pol II transcription are not clear. To associate with hydrophilic part of PIP2, many proteins contain specific motifs enriched in basic amino acids, such as pleckstrin homology (PH) domain (Watt et al. 2002; Mortier et al. 2005; Geeraerts et al. 2013). Nevertheless, some proteins are able to interact with hydrophilic and even hydrophobic parts of PIP2 through yet unknown moieties (Harlan et al. 1994; Ferguson et al. 1995; Lemmon et al. 1995; Wang et al. 2001; Zimmermann et al. 2002; Mortier et al. 2005; Gonzales and Anderson 2006; Irvine 2006; Sugi et al. 2008). Therefore we searched for nuclear PIP2-interacting proteins containing known PIP2-binding motifs. One of such possible candidates is NM1, which possesses PH domain in the C-terminus and binds PIP2 in cytoplasm (Hokanson et al. 2006; Hokanson and Ostap 2006). Previously, it has been shown that NM1 facilitates chromatin remodelling (Cavellan et al. 2006; Percipalle et al. 2006) as well as DNA transcription and RNA processing (Fomproix and Percipalle 2004; Philimonenko et al. 2004; Cisterna et al. 2006; Hofmann et al. 2006; Venit et al. 2013). The role of NM1 in rRNA biogenesis was revealed in detail (Ye et al. 2008; Sarshad et al. 2013). The amount of nascent pre-rRNA transcripts is reduced upon RNAi-mediated knockdown of NM1 gene (Sarshad et al. 2013). Overexpression of NM1 mutant lacking C-terminal domain decreases Pol I level at the rDNA promoter and transcribed region as shown by chromatin immunoprecipitation (ChIP) assay, suggesting a role for PIP2-binding motif in transcription (Ye et al. 2008). C-terminus of NM1 is responsible as well for binding to rDNA and histone acetyl transferase PCAF (HAT PCAF) as revealed using NM1 C-terminal deletion mutant (Sarshad et al. 2013). In contrast, the involvement of NM1 in Pol II transcription as well as its interaction with nuclear PIP2 are not described in detail.

Therefore, we investigated the association of PIP2 with Pol II transcription complexes and its distribution throughout the nucleus. Furthermore, we also studied the interactions of PIP2 with NM1 and the importance of NM1-PIP2 complex for Pol II transcription.

In this study, we show the involvement of nucleoplasmic PIP2 in Pol II transcription through PIP2 islets. These previously uncharacterized nucleoplasmic 40-100 nm structures are decorated by PIP2 molecules and composed mainly of lipids, while the periphery of PIP2 islets is enclosed by chromatin, nascent RNA transcripts, and proteins engaged in Pol II transcription, including NM1. Most importantly, disruption of PIP2 islets integrity causes a substantial decrease of Pol II transcription level. Altogether, our results allow us to suggest that PIP2 islets serve as a platform which facilitates the proper arrangement of the different complexes involved in Pol II transcription.

Results

Nucleoplasmic PIP2 appears as small roundish structures, which colocalize with nascent RNA and proteins involved in Pol II transcription

Previously published data showed that PIP2 is pulled-down with Pol II (Osborne et al. 2001) and binds to Pol I transcription machinery (Sobol et al. 2013; Yildirim et al. 2013). These findings prompted us to study the particular proteins associated with nucleoplasmic PIP2, which are the core subunits of Pol II. Using super-resolution structured illumination microscopy (SIM), we analyzed the colocalization between PIP2 and the components of Pol II transcription machinery, including BrUTP-labeled nascent RNA. We found that nucleoplasmic PIP2 forms small foci and colocalizes with nascent BrRNA transcripts, C-terminal domain of Pol II, and TATA-box binding protein (TBP) of the Pol II general transcription factor TFIID (Figure 1a, b). The extent of colocalization between PIP2 and BrRNA was expressed by the high values of Manders' (MCC) and Pearson's (PCC) colocalization coefficients (Figure 1c). Another protein involved in Pol II transcription activation through the recruitment of chromatin remodeling proteins and histone modification enzymes is NM1 (Hofmann et al. 2006; Almuzzaini et al. 2015). Transmission electron microscopy (TEM) showed more accurately that these PIP2 foci are roundish structures of 40-100 nm in size and revealed presence of NM1 at the periphery of these structures (Figure 1d). Based on their roundish shape and size, we refer to them as PIP2 islets. We show that the colocalization between PIP2 molecules and NM1 is significant at the distances of 25 – 75 nm (**p value ≤ 0.01).

In conclusion, nucleoplasmic PIP2 appears as small roundish 40-100 nm structures - PIP2 islets, which colocalize with some of the various components of Pol II transcription machinery and might participate in transcription.

NM1 associates with PIP2 islets and is anchored in nucleoplasm by PIP2

We detected NM1 on the surface of PIP2 islets. Based on the fact that NM1 contains PH domain which mediates its interaction with cytoplasmic PIP2 (Hokanson et al. 2006; Hokanson and Ostap 2006), we studied whether NM1-PIP2 interaction occurs also in the nucleus. First, we pulled-down NM1 from the HeLa nuclear extract using PIP2-coupled agarose beads (Figure 2a). To see if this interaction is direct, we prepared a recombinant wild-type NM1 as well as NM1 mutated in the PH domain - NM1(K908A), and verified their PIP2 binding ability using PIP2 spotted on nitrocellulose membrane. Unlike to wild-type NM1, NM1(K908A) showed no reaction with PIP2 (Figure 2b), so the mutation in the PH domain prevents binding of NM1 to PIP2 and this interaction is direct. Furthermore, NM1(K908A) with abolished binding to PIP2 demonstrated the increased mobility measured by fluorescence recovery after photobleaching (FRAP) technique as compared to wild-type NM1 (Figure 2c), so PIP2 seems to anchor NM1 into the nuclear complexes. To confirm the association of NM1 with PIP2, we employed nucleus-targeted inositol 5-phosphatase or PH domain of phospholipase C isoform δ1 (PLCδPH) for hydrolyzing or blocking nuclear PIP2, respectively. Indeed, both treatments led to an increase in NM1 mobility monitored by FRAP (Figure 2c) upon disabling the interaction between NM1 and PIP2. To demonstrate that NM1 is anchored to PIP2 islets, we performed a flotation of extracted HeLa nuclei on a sucrose density gradient in the presence of a weak non-ionic detergent Brij 98. Both NM1 and PIP2 were present in the light fraction 1, which contains detergent-insoluble complexes composed of lipids and proteins, such as PIP2 islets (Figure 2d). NM1 and PIP2 were also present in the heavy fraction 10, which corresponds to complexes efficiently solubilized by detergent (Figure 2d). Hence we conclude that NM1 is anchored in nucleoplasm to PIP2 islets.

PIP2-NM1 interaction and integrity of PIP2 islets are important for Pol II-dependent transcription

It is known that NM1 associates with Pol II (Hofmann et al. 2006; Venit et al. 2013), however the details of this interaction are not clear. When we used NM1(K908A), we observed the loss of association with Pol II, as tested by immunoprecipitation (Figure 3a). Therefore we also studied the effect of this NM1 mutation on Pol II transcription. We pulse-labelled nascent transcripts with fluorouridine (FU) *in vivo* and quantified the signal intensity by indirect immunofluorescence microscopy. The depletion of NM1 by shRNA-mediated knock-down (Figure 3b) significantly reduced Pol II transcription by ~25% (Figure 3c). The

overexpression of NM1 rescued Pol II transcription close to its original level. In contrast, the overexpression of NM1(K908A) did not rescue Pol II transcription, which remained at the knocked-down level. Thus we suggest that NM1 requires PIP2 in order to associate with Pol II and to participate in transcription.

Since NM1 and the components of Pol II transcription machinery colocalized with PIP2 islets, we investigated whether the integrity of PIP2 islets is important for DNA transcription on their periphery. To disintegrate PIP2 islets, we treated the cells with PLC (Supplementary Figure 1). Upon PIP2 hydrolysis, we quantified the level of transcription using indirect immunofluorescence microscopy of FU-labelled nascent RNA. For this and all following colocalization analyses, we considered only regions occupied by PIP2 islets, which we referred to as PIP2 islets area. In experiments using fluorescent microscopy, PIP2 islets area was identified based on the absence of labeling by a speckle-specific marker Son. We showed that reducing of PIP2 level to 38.2±2.9% (***p value $\leq$ 0.001) resulted in a decrease of transcription level to 42.4±0.1% (**p value $\leq$ 0.01) in the area of PIP2 islets (Figure 3d). Mutated PLC(R40A) with abolished binding to PIP2 as well as inactivated by heating PLC or irrelevant protein BSA did not substantially affect the level of transcription by Pol II. Interestingly, Pol II transcription level was directly proportional to the level of PIP2 in the PIP2 islets under both control and experimental conditions. In other words, cells with high level of PIP2 exhibited high level of Pol II transcription, while cells with low level of PIP2 displayed low level of Pol II transcription. Altogether our results indicate that Pol II transcription is strictly dependent on the presence of intact PIP2 islets. In support, TEM clearly demonstrated that nascent BrRNA transcripts colocalize with the periphery of PIP2 islets (Figure 3e). The colocalization between PIP2 molecules and nascent BrRNA transcripts was significant at 25 - 75 nm; **p value $\leq$ 0.01 (Figure 3f). Furthermore, the analysis of the relative colocalization of BrRNA and PIP2 molecules showed that almost half of nascent RNA transcripts is colocalized with PIP2 islets; ***p value $\leq$ 0.001 (Figure 3g). On the other hand, only a minor part of PIP2 islets – 8.8±0.3% is colocalized with BrRNA. In accordance, the inhibition of Pol II transcription did not significantly alter either the pattern or the quantity of PIP2 islets per μm^2 as compared to the control (Figure 3h, i).

In conclusion, Pol II transcription is dependent on PIP2 islets and predominantly takes place on their surface, while PIP2 islets seem to be independent of ongoing transcription. Moreover, PIP2 islets mediate the interaction of NM1 with Pol II transcription complex. Therefore, we suggest that PIP2 islets serve as a standard platform which facilitates the spatial-temporal arrangement of the various complexes involved in Pol II transcription.

PIP2 islets are DNA-independent but RNA-associated structures

Here we demonstrated the relationship between PIP2 islets and Pol II transcription. To further disclose the interrelation between PIP2 islets and chromatin, we studied pattern of PIP2 islets upon hypertony-triggered chromatin condensation (Figure 4). As shown by SIM, PIP2 islets overlapped with histone H1 under isotonic conditions (Figure 4a). This observation is supported by MCC and PCC measured for PIP2 islets area (Figure 4d, e). Under hypertonic conditions (final salt concentration 300 mM, 15 min), PIP2 islets minimally overlapped and did not significantly colocalize with histone H1 as represented by MCC and PCC, which decreased four- and five-fold, respectively (Figure 4b, d, e). After 3 min of recovery under isotonic conditions, chromatin decondensed and PIP2 islets colocalized with histone H1 (Figure 4c). This was documented by MCC and PCC, which regained their initial values (Figure 4d, e). These observations suggest that PIP2 islets do not alter their pattern, when chromatin dynamically changes its state. To confirm this, we calculated the relative volumes of PIP2 islets and chromatin in the nucleus (Figure 4f). We revealed that hypertonic conditions resulted in a significant decrease in the relative volume of chromatin (41.9±0.9% vs 27.1±0.7%). After the recovery, the relative volume of chromatin was restored to the initial value (40.6±0.9%). In contrast, the relative volume of PIP2 islets did not significantly change under hypertonic conditions as compared to the control. Therefore we conclude that PIP2 islets do not follow the chromatin rearrangements.

To further test if PIP2 islets are chromatin-independent structures, we studied the pattern of PIP2 islets upon DNase treatment. In accordance with the previous observations, PIP2 islets were arranged in a similar pattern in both control and DNase-treated cells (Figure 5a, b). Since we demonstrated that PIP2 islets colocalize with nascent RNA transcripts (Figure 1a-c, 3e, f), we also studied the effect of RNase on the arrangement of PIP2 islets. Surprisingly, the treatment of cells with RNase caused disappearance of PIP2 islets labeling (Figure 5c). These results encouraged us to assess the overall association of RNA molecules with PIP2 islets. We simultaneously labeled PIP2 and total RNA with anti-PIP2 antibody and RNase conjugated to gold nanoparticles - RNase-gold complex (Supplementary Figure 2a, b). TEM revealed that RNA molecules are located on the surface of PIP2 islets (Figure 5d). For TEM colocalization analyses, PIP2 islets area was distinguished from nuclear speckles and nucleoli based on the ultrastructure and the pattern of PIP2 labeling. The colocalization of RNA and PIP2 molecules was significant (**p value ≤ 0.01) at the distance of 25 – 75 nm. Moreover, the analysis of their relative colocalization showed that 73.2±7.5% of PIP2 in the area of PIP2

islets is colocalized with RNA molecules and *vice versa*, 21.8±4.2% of RNA molecules is colocalized with PIP2 islets (***p value ≤ 0.001).

These data altogether clearly demonstrated that RNA is an essential part of PIP2 islets. Furthermore, RNA does not form the core of PIP2 islets, but associates with their surface.

Morphology, composition and distribution of PIP2 islets

We showed that nucleoplasmic PIP2 is involved in Pol II transcription through PIP2 islets. Previously, PIP2 was detected predominantly in nuclear speckles (Osborne et al. 2001; Mortier et al. 2005) as well as in nucleoli (Sobol et al. 2013; Yildirim et al. 2013). That is why we decided to map thoroughly nuclear PIP2 localization by anti-PIP2 antibody. Using SIM, we acquired z-stacks, reconstructed the nuclei in three-dimensional space and calculated the distribution of PIP2 labeling in the nuclear volume by the procedure described in Materials and Methods section (Figure 6a). We used Son as a speckle-specific marker as well as histone H1 and DAPI as the markers of nucleoplasm. We revealed that 68.4±4.4% of nuclear PIP2 localizes to speckles, while nucleolar PIP2 constitutes 3.4±1.1%. The remaining 28.2±4.9% was dispersed throughout nucleoplasm. To visualize this pool of PIP2 more accurately, we inspected the nucleoplasmic PIP2 labeling by TEM (Figure 6b). We showed that these 28.2±4.9% of nucleoplasmic PIP2 pool were indeed located in PIP2 islets, which can be clearly discriminated from the nuclear speckles by size (40-100 nm) and roundish shape. PIP2 islets occupy up to 10.6±4.0 μm^3 per nucleus, which is 1.9±0.2% of the total nuclear volume. Even though PIP2 is a known component of plasma membrane, ultrastructural analysis showed that PIP2 islets are excluded from the nuclear envelope.

To uncover the composition of PIP2 islets, we mapped the presence of nitrogen, phosphorus, and carbon, which are the basic components of proteins, chromatin, and lipids. To achieve this, we performed electron energy loss spectroscopy (EELS) on ultrathin sections of U2OS cells immunolabeled with anti-PIP2 antibody (Figure 6c). We showed that PIP2 islets are enclosed by phosphorus- and nitrogen-containing shield, while the inner space of PIP2 islets lacks them both (Figure 6d-f). On the contrary, the interior of PIP2 islets is mainly composed of carbon-rich compounds (Figure 6g). These data indicate that nucleic acids and proteins surround PIP2 islets, which is in agreement with the results shown in Figures 1, 3, 4, and 5, while lipids form the inner space of PIP2 islets.

Since PIP2 islets are surrounded by nucleic acids and proteins, we performed a colocalization of PIP2 islets with histones H3K4me2 and H3K9me2, the hallmarks of active chromatin and heterochromatin, respectively. Using immunolabelling followed by SIM we

showed that PIP2 islets partially overlap with both histone marks with no preference for either type of chromatin (Figure 6h, i).

We can summarize that nuclear PIP2 islets are globular structures of 40-100 nm in size with lipidic interior decorated by PIP2 molecules on their surface, surrounded by proteins and nucleic acids.

Discussion

The presence of PIP2 in a cell nucleus was shown in the early studies (Mazzotti et al. 1995; Osborne et al. 2001; Watt et al. 2002), but it was attributed mainly to the nuclear speckles. Later, the involvement of PIP2 in rDNA transcription and nucleolar organization was shown (Sobol et al. 2013; Yildirim et al. 2013). Besides, PIP2 was demonstrated to participate in chromatin remodelling and Pol II transcription (Yu et al. 1998; Zhao et al. 1998; Osborne et al. 2001; Rando et al. 2002; Toska et al. 2012), which occur in nucleoplasm outside nuclear speckles. This motivated us to study nucleoplasmic pool of PIP2 in greater detail.

We found that nearly 30% of total nuclear PIP2 is located outside nuclear speckles and nucleoli. Using SIM and TEM, we revealed that this nucleoplasmic PIP2 forms 40-100 nm roundish structures, which we termed PIP2 islets. Recently, nuclear lipid droplets (nLDs) were described in rat and human liver hepatocytes (Layerenza et al. 2013). nLDs are 530-800 nm in diameter and are composed of a hydrophobic lipid core surrounded by a hydrophilic outer monolayer. Among the inner part of nLDs, triacylglycerols and cholesteryl esters were found, while polar lipids, cholesterol, and proteins form their surface. PIP2 islets are organized in a similar way with a carbon-rich interior and phosphorus- and nitrogen-rich exterior. We suggest that the inner core of PIP2 islets is hence composed of lipids while PIP2 molecules form outer layer with hydrophilic heads facing outwards. PIP2 islets are surrounded by nucleic acids and proteins. This observation is further reinforced by our pull-down experiments, where we identified various phospholipids as PIP2-binding partners in the nucleus (data not shown).

Up to now, the only known nuclear subcompartments containing PIP2 have been the nucleoplasmic vesicles found in the bovine adrenal chromaffin cells by Yoo et al. (2014). Even though similar to PIP2 islets in size (50 nm), these vesicles are enclosed by a membrane. nLDs and vesicles serve as storage nuclear domains for lipids and calcium, respectively. PIP2 islets might be the storage sites for PIP2 as well, however our results indicate their involvement in RNA synthesis. Indeed, PIP2 islets colocalize with nascent RNA transcripts as

well as Pol II transcription machinery proteins, Pol II CTD and TFIID TBP. During the initiation phase of Pol II transcription, TFIID recognizes DNA promoter thus recruiting Pol II (Bieniossek et al. 2013). Phosphorylations of Poll II CTD at Ser5 and Ser2 are required for transcription initiation and elongation, respectively (Heidemann et al. 2013). RNA is being synthesized predominantly during elongation phase and remains attached until termination. Since these molecules are engaged in different phases of Pol II transcription, PIP2 islets serve as a scaffold for the arrangement of various functional subunits of Pol II transcription machinery. In agreement, PIP2 hydrolysis results in a significant decrease of transcription level in the PIP2 islets area. On the other hand, inhibition of Pol II transcription does not disturb PIP2 islets. Hence, PIP2 islets are stable nuclear structures independent of ongoing transcription.

Next, we asked how the transcription complexes are associated with PIP2 islets surface. Our results document, that neither DNase treatment nor hypertony-triggered chromatin condensation affect PIP2 islets. Therefore, they are chromatin-independent structures and DNA template does not mediate the interaction between PIP2 islets and Pol II transcription machinery. On the contrary, RNase treatment disrupts PIP2 islets. We found that majority of PIP2 islets colocalizes with RNA detected by RNase-gold. Since RNase-gold complex recognizes total RNA, we can't identify the type of this RNA. Our results show that PIP2 islets however colocalize with nascent RNA transcripts, which thus contribute to the pool of RNA recognized by RNase-gold. However, nascent RNA does not seem to link the transcription complexes with PIP2 islets, because it is synthesized after the association of Pol II transcription machinery with PIP2 islets surface. That is why we hypothesize that other types of RNA and/or proteins mediate the interaction of PIP2 islets with the transcription complexes. It is unlikely, that RNA itself serves as a mediator, because negative charges of PIP2 hydrophilic heads exposed to the surface of the islets would repulse negatively charged RNA. Therefore, PIP2 islets and RNA molecules should have some positively charged interface, presumably basic protein domains.

Here we show that PIP2 islets interact with NM1. It is known that C-terminal part of NM1 containing PIP2-binding site is essential for NM1 to promote chromatin remodelling and Pol II transcription (Hofmann et al. 2006; Almuzzaini et al. 2015). We revealed that K908A mutation in NM1 causes loss of interaction with Pol II. Furthermore, NM1(K908A) is incapable to rescue drop in transcription caused by knock-down of endogenous NM1. Therefore we speculate that the interaction between NM1 and Pol II complex occurs via PIP2 on the surface of PIP2 islets. In such a way, NM1 recruits chromatin remodelling complexes

to PIP2 islets, where they create open chromatin structure thus promoting transcription. In the absence of NM1-PIP2 islets association, Pol II complexes remain attached to the surface of PIP2 islets, but transcription cannot occur due to the lack of chromatin remodellers. Additionally, due to its basic nature, NM1 is able to create interface in between negatively charged PIP2 and RNA.

Here we describe that PIP2 islets are required for Pol II transcription. Similarly, few studies demonstrated the contribution of other lipid-based structures in transcription. Scassellati et al. (2010) showed that sphingomyelin and nascent RNA are both located in the transcriptionally active chromatin regions. Yoo et al. (2014) suggested that nucleoplasmic vesicles containing PIP2 might be engaged in transcription via calcium-regulated chromatin remodelling. nLDs might indirectly participate in transcription via nuclear lipids metabolism (Layerenza et al. 2013). All these nuclear structures have been found in specialized cell types: sphingomyelin in rat and mouse liver cells, T24 human bladder carcinoma cells, and V79 Chinese hamster cells (Scassellati et al. 2010); nLDs in rat and human liver hepatocytes (Layerenza et al. 2013); nucleoplasmic vesicles in bovine adrenal chromaffin cells (Yoo et al. 2014). Nuclear granules have been described only under stress conditions (Jolly et al. 2004). Noteworthy, we have found PIP2 islets not only in cancer cells (HeLa, U2OS), but also in primary fibroblasts and mesenchymal stem cells (data not shown). This indicates that PIP2 islets are common structures essential for nuclear processes regardless of a cell type.

Altogether, we suggest that PIP2 islets serve as a platform, which facilitates the spatial-temporal arrangement of various complexes involved in Pol II transcription. These findings point towards existence of previously undefined nuclear structures. Future experiments are needed to clarify the contribution of such structures in nuclear functions and architecture.

Materials and methods

Cell cultures and transfections

Human cervical carcinoma (HeLa, ATCC No. CCL2) cells, osteosarcoma (U2OS, ATCC No. HTB96), and H1299 (ATCC No. CRL5803) cells were grown in D-MEM with 10% fetal bovine serum (FBS) at 37 ^{o}C in 5% CO_2 humidified atmosphere. Suspension HeLa were kept in S-MEM supplemented with 5% FBS at 37 °C in 5% CO2 humidified atmosphere. Transfections were carried out using Lipofectamine 2000 (Invitrogen) according to the manufacturer's protocol. Stable cell lines were prepared by lentiviral transduction using packaging plasmids psPAX and pMD2.G (Addgene, Didier Trono lab).

Constructs

NM1-EGFP and NM1(K908A)-EGFP: NM1 cDNA was ligated into pEGFP-N3 vector (Clontech) using HindIII and KpnI (Dzijak et al. 2012). K908A mutant was obtained by site-directed mutagenesis. NLS-mRFP-FKBP-Inositol-5-phosphatase: SV40 NLS sequence was prepared by PCR from pEYFP-Nuc (Clontech). The NLS was then cloned using NheI and AgeI to the N-terminus of mRFP-FKBP-Inositol-5-phosphatase, which was a kind gift of Dr. Tamas Balla (Varnai et al. 2006). PLCPH-mCherry-NLS: SV40 NLS was released from pEYFP-Nuc (Clontech) vector by cutting at BsrGI and AflII restriction sites, and inserted in the C-terminus of PLCPH-GFP vector, which was a kind gift from Dr. Tamas Balla (Varnai and Balla 1998). PLCPH-GFP-NLS was then cloned to XbaI and AfeI restriction sites of pPSG-IBA-103 vector (Iba BioTagnology). For FRAP experiments, mCherry was exchanged with GFP using AgeI and BsrGI restriction sites. R40A mutant was prepared by site-directed mutagenesis. NM1-Flag and NM1(K908A)-Flag: cDNAs of NM1 and NM1(K908A) were C-terminally fused with Flag tag and cloned into lentiviral expression vector pCDH-CMV-MCS-EF1-Neo (Systems Bio) using EcorI and BamHI. Flag-HDL: cDNA fragment of NM1 (corresponding to amino acids 712 to 1044) was amplified by PCR, fused with N-terminal Flag tag and ligated into pCDNA3.1 (Invitrogen) using SacI and XmaI. HIS-tagged phospholipase C isotype δ1 (PLC) and PIP2-binding mutant R40A in pRSETA were both generous gift from Dr. Hitoshi Yagisawa and Dr. Klim King (Cheng et al. 1995). NM1 shRNA: NM1 shRNA targeting the sequence 5'-gcccgtccagtatttcaac-3' (Open Biosystems No TRCN0000122925 AAO75-C-8) was ligated into pLKO.1 (Addgene, Stewart et al RNA 2003 Apr;9).

Expression and purification of recombinant proteins

NM1-Flag and NM1(K908A)-Flag were stably expressed in H1299 cell line. Cells were washed with PBS and extracted with lysis buffer (50 mM HEPES pH 8, 300 mM NaCl, 4 mM $MgCl_2$, 1% Triton X-100). The extract was sonicated, filtered through 0.45 μm filter, and incubated 2 h with pre-equilibrated anti-Flag-M2 agarose beads (Sigma-Aldrich). The beads were then washed three times with lysis buffer, and bound proteins were eluted five times with 100 μg/ml Flag peptide in elution buffer (10 mM Tris pH 8, 100 mM NaCl, 0.5% EDTA, 20% glycerol).

HIS-tagged PLC and PLC(R40A) were expressed in *E. coli* strain BL21-Gold (Agilent Technologies) and purified over Ni-NTA column as described previously (Cheng et al. 1995).

FRAP

Transiently transfected U2OS cells were photobleached in nucleoplasm with a 488-nm laser for 20 msec. GFP fluorescence intensities were monitored every 0.175 sec on an Olympus microscope (IX71) with a 60x 1.42 NA objective. Approximately 15 cells were analyzed for each condition. All images were corrected for overall photobleaching and analyzed by DeltaVision software SoftWoRx 5.5 (Applied Precision). Two-dimensional diffusion of the fluorescent molecules is calculated according to a previously published model (Axelrod et al. 1976).

Immunofluorescent labeling for super-resolution microscopy

Cells grown on high performance cover glasses 18x18 mm² with restricted thickness-related tolerance D=0.17 mm +/- 0.005 mm and refractive index = 1.5255 +/- 0.0015 were fixed with 3% formaldehyde and permeabilized with 0.1% Triton X-100. Unspecific targets were blocked with 0.25% bovine serum albumin (BSA) and 0.25% gelatine. All solutions were diluted in PBS. Then, cells were incubated with primary antibodies diluted in PBS, secondary antibodies diluted in PBS or PBST, stained with DAPI and mounted in Mowiol. Importantly for super-resolution microscopy technique, five extensive washes for 5 or 10 min in PBS or PBST were done in between all steps.

Super-resolution structured illumination microscopy (SIM)

Images were acquired using microscope ECLIPSE Ti-E equipped with Andor iXon3 897 EMCCD camera by objective CFI SR Apochromat TIRF 100x/1.49 oil (Nikon, Tokyo, Japan). Software NIS-Elements AR 4.20.01 and NIS Elements AR 4.30 was used for capturing and analysis of the images. In each experiment, the images of all samples were acquired and reconstructed with the same parameters to ensure their comparability. To assess the distribution of PIP2 in the nucleus, z-stack was acquired, reconstructed, and analysed with 3D Object Measurement tool. We defined the nucleus with DAPI and histone H1, and the nucleoli as the regions, where both markers were absent. Nuclear speckles were distinguished from PIP2 islets based on the co-labeling with a speckle-specific marker, Son. All markers were visualized with different secondary antibodies than PIP2. The respective volumes of nuclear speckles, PIP2 islets, and nucleolar PIP2 were calculated. To determine the proper threshold, MATLAB 7.7.0 (R2008b) software was used. Firstly, the maximum intensity value for each pixel in the projection image was computed as maximum value of the overlapping voxels in z-stack (PIP2 channel). Secondly, the upper quartile was applied to filter out 75%

non-significant pixel intensities of the projection image. The zero intensity values were assigned to all these pixels, which have intensity value lower than given upper quartile, so they are considered as a black background or noise. Consequently, the projection image in PIP2 channel includes 25% of the intensity values of the original projection image. The image was color-coded in red. Simultaneously, the same method was applied to z-stack in Son, H1, and DAPI channels. The ninth decile was chosen to sort out non-significant intensity values in projection image in Son channel. The zero values were assigned to all pixels with intensity values less than the 90th percentile. In the next step, we combined the projection images (PIP2 channel and Son channel). All overlapping pixels with non-zero values in both channels were classified as nuclear speckles in PIP2 channel and color-coded in yellow. Then, we used the information of the maximum projection images of H1 and DAPI channels to distinguish the nucleoli in PIP2 channel and classified pixels were color-coded in blue. The data on the volumes were exported and the percentage distribution of PIP2 in the nucleus was calculated and presented as a diagram using Microsoft Excel software. Similarly, the volumes of chromatin and PIP2 islets were analysed with 3D Object Measurement tool, exported to Microsoft Excel and related to the nuclear volume. The colocalization analysis was done using software ImageJ/plugin JACoP (n=10 cells). Quantitative results given in graphs are presented as mean ± standard deviation. The statistical significance was determined using the F-test two-sample for variances followed by the t-test: two-sample assuming (un-)equal variances.

Transmission electron microscopy (TEM)

HeLa cells and yeast cells were either fixed in 3% formaldehyde with 0.1% glutaraldehyde and embedded into LR White resin or Lowicryl K4M resin by a standard protocol (Wright 2000; Sobol et al. 2010). Alternatively, HeLa cells were high-pressure frozen, freeze-substituted and embedded into LR White resin or Lowicryl K4M resin according to a previously published procedure (Sobol et al. 2011). Ultrathin sections (70 nm) were immunolabeled by a conventional protocol (Stradalova et al. 2008) and examined with a transmission electron microscope (TEM) Morgagni 268 at 80 kV and Tecnai G2 20 LaB6 at 200 kV (FEI, Eindhoven, The Netherlands). The images were captured with a camera Mega View III CCD and Gatan Model 894 UltraScan 1000. Multiple sections of at least three independent immunogold labeling experiments were analyzed (n=100 cells). To facilitate the visualization of 6 nm gold nanoparticles in images, Adobe Photoshop CS3 Version 10.0 was used to identify the geometrical centers of the small nanoparticles and then cover co-

centrically with red dots. To evaluate computationally the spatial distribution and quantitative mutual dependence of the nanoparticles in electron microscopy images, we developed and used the quantitative objective approach (Pastorek et al., in preparation), based on the previously published one describing pair cross-correlation function (PCCF) (Philimonenko et al. 2000). In this study, we used new developed plugin (Pastorek et al., in preparation) on the ImageJ software platform. Quantitative results given in graphs are presented as mean ± standard deviation. The statistical significance was determined using the F-test two-sample for variances followed by the t-test: two-sample assuming (un-)equal variances.

PIP strip

Membranes spotted with PIs (PIP strips; Echelon) were blocked with 3% BSA in PBST for 1 h at 4 °C. Recombinant NM1-Flag and NM1(K908A)-Flag were diluted to 2 µg/ml with 3% BSA in PBST and incubated with PIP strips for 4 h at 4 °C. After five washes with PBST, bound proteins were detected by western blotting with anti-Flag antibody.

Electron energy loss spectroscopy (EELS) and elemental mapping

Elemental mapping was performed on ultrathin sections of U2OS cells embedded in LR White resin. The 80-nm sections were immunolabeled with anti-PIP2 antibody and secondary antibody conjugated with 12 nm gold particles according to conventional protocol (Stradalova et al. 2008). Contrasting by uranyl acetate was omitted. EELS mapping of specific elements distribution was performed using a Tecnai G2 20 LaB6 TEM at 200 kV equipped with Gatan 863 Tridiem Imaging Filter. Two pre-edge and one post-edge energy filtered images were collected at 100 eV, 120 eV, and 152 eV ($L_{II,\ III}$ edge) for phosphorus; at 353 eV, 383 eV, and 416 eV (K edge) for nitrogen; at 484 eV, 514 eV, and 532 eV (K edge) for oxygen; at 130 eV, 150 eV, and 165 eV ($L_{II,\ III}$ edge) for sulphur; at 252 eV, 272 eV, and 294 eV (K edge) for carbon. Drift correction was performed using an automated statistically determined spatial drift (SDSD) correction script for Digital Micrograph (Schaffer et al. 2004), and elemental maps were calculated by three-windows method using Digital Micrograph. The images were processed using Digital Micrograph and Adobe Photoshop CS3 Version 10.0.

Hypertony-induced chromatin condensation

U2OS cells grown under standard conditions were subjected to D-MEM adjusted with NaCl to the final salt concentration of 300 mM for 15 min. After this period, cells were let to recover under standard conditions in isotonic D-MEM for 3 min. For SIM, cells were fixed

with 4% formaldehyde diluted in either PBS adjusted with NaCl to the final 300 mM salt concentration (hypertonic samples) or in PBS (isotonic condition, initial and recovery). Then, cells were permeabilized with 0.1% Triton X-100 in PBS. Unspecific targets were blocked with 2% BSA in PBS. Then, cells were processed for SIM as described above.

DNase and RNase treatments

U2OS cells were gently fixed with 1% formaldehyde for 5 min on ice and then treated with either RNase A (1 mg/ml) or DNase I (250 U/ml) diluted in buffer (130 mM KCl, 10 mM Na_2HPO4, 1 mM $MgCl_2$, 1 mM DTT, 1 mM Na_2ATP, 0.1 mM PMSF; pH 7.4) for 30 min at 32 ^oC. Subsequently, cells were fixed, permeabilized, and further processed for SIM as described above.

BrUTP labeling of nascent transcripts for SIM and TEM

HeLa cells were washed in PB buffer on ice (100 mM CH_3COOK, 30 mM KCl, 10 mM Na_2HPO4, 1 mM $MgCl_2$, 1 mM DTT, 0.2 mM PMSF, 10 U/ml human placental RNase inhibitor (HPRI), 1 mM Na_2ATP; pH 7.2) and permeabilized with 0.5 mg/ml saponin for 5 min on ice. Transcription reactions were started by incubation with 100 µM BrUTP, 100 µM CTP, 100 µM GTP, and 300 µM $MgCl_2$ in PB. To inhibit Pol II transcription, cells were pre-incubated with 100 µg/ml α-amanitin for 5 min. After 15 min at 35 ^oC, reactions were stopped by rinsing in ice-cold PB. Cells were either fixed with 4% formaldehyde for 40 min on ice, additionally permeabilized with 0.5% Triton X-100 for 20 min, and further processed for SIM as described above or processed for TEM (Sobol et al. 2010).

Ultrastructural detection of RNA molecules using RNase-gold

RNase A (Thermo Fisher Scientific, Waltham, Massachusetts, USA) was conjugated with 10 nm gold nanoparticles (BBI Solutions, Cardiff, UK) as published previously (Bendayan 1981; Bendayan and Puvion 1984; Cheniclet and Bendayan 1990). HeLa cells were embedded into Lowicryl K4M resin and the ultrathin sections (70 nm) were sequentially double labeled. First, the anti-PIP2 antibody followed by the secondary antibody conjugated with 6 nm gold nanoparticles was applied. Next, sections were incubated with RNase-gold conjugates (0.08 µg/ml). The activity of RNase-gold complex was checked using *in vitro* reaction with RNA (0.5 µg of RNA for 18 ng of RNase-gold). The incubation was carried out for 15 min on ice. To control the labeling specificity, RNase-gold complex (3.2 ng) was pre-blocked with RNA (5.2 µg – 20.0 µg), and these mixtures were used for labeling.

Quantification of transcription using 5-FU labeling of transcripts

U2OS cells grown on the coverslips were slightly permeabilized with 0.05% Triton-X-100 on ice for 5 min and then treated with recombinant PLC (84 µg/ml in the buffer consisting of 50 mM HEPES pH7.4, 100 mM KCl) and 0.04 µg/ml actinomycin D (AMD) as an inhibitor of Pol I transcription for 1 h at RT. After 30 min of treatment, 5-fluorouridine (FU) was added to the final 2 mM and the cells were incubated for 30 min. Then the cells were washed, fixed, permeabilized and FU incorporated into the nascent RNA transcripts was detected with anti-BrdU antibody as described (Boisvert et al. 2000; Casafont et al. 2006; So et al. 2010; Kalendova et al. 2014). As the controls, buffer only or mutated PLC(R40A), or BSA, or inactivated by heating PLC were used. Images were acquired using IX81 high-throughput wide-field microscope with objective UPLSAPO 40x/0.90 oil (Olympus Corporation, Tokyo, Japan). SCAN-R automated image and data analysis software was used for capturing and analysing the images. Images were captured as 1 µm z-stacks with 200 nm z-step. For the analysis, DAPI channel was used to determine the nuclear area and Son channel was used to determine the nuclear speckles area. Total intensity of fluorescence was calculated from maximal projection image for each z-stack in PIP2 channel and FU channel separately. 1500 treated cells were analyzed. Fluorescence intensity in each channel and the area of PIP2 islets were calculated as a result of the subtraction of the corresponding parameter for the nuclear speckles from this parameter for the whole nucleus. Results are presented as the intensity of fluorescence per unit area (mean ± standard deviation). The statistical significance was determined using the F-test two-sample for variances followed by the t-test: two-sample assuming (un-)equal variances.

H1299 cells were treated for 1 h with 0.04 µg/ml AMD. After 30 min of treatment, cells were incubated for 30 min with 2 mM FU under standard conditions. After this time period, cells were washed, fixed, and permeabilized. FU incorporated into nascent transcripts was detected using anti-BrdU antibody and fluorescence intensity was measured and quantified as described above.

Nuclear extract fractionation and dot blot analysis

HeLa nuclear extracts were fractionated by discontinuous sucrose gradient ultracentrifugation method, adapted from (Marmor and Julius 2001). Nuclei from suspension HeLa cells were prepared as described previously (Trinkle-Mulcahy et al. 2008). Clean nuclei were extracted by TKM buffer (50 mM Tris pH 7.4, 25 mM KCl, 5 mM $MgCl_2$, 1 mM

EDTA, 0.5% Brij 98, EDTA-free protease inhibitor), sonicated 3x10 sec on ice, and centrifuged for 5 min at 16 000 g. 250 µl of nuclear extract was mixed with the same amount of 80% sucrose in TKM buffer and placed at the bottom of the tube. Samples were sequentially overlaid with 4.3 ml of 36% and 0.2 ml of 5% sucrose solution to a total volume of 5 ml. The mixture was subjected to equilibrium density gradient centrifugation at 50000 rpm for 18 h at 4 C in a MLS50 rotor (Beckman Coulter, Fullerton, CA). 200 µl from each of the collected fractions were spotted on a nitrocellulose membrane and probed for PIP2. To identify the protein composition, 20 µl of each fraction was resolved by SDS-PAGE, transferred onto a nitrocellulose membrane and immunoprobed with the respective antibody.

Pull-down assay and co-immunoprecipitation

Nuclei from suspension HeLa cells were prepared as described previously (Trinkle-Mulcahy et al. 2008). Pure nuclei were extracted using RIPA buffer (50 mM Tris pH 8, 150 mM NaCl, 0.5% NP-40, complete protease inhibitors (Roche)), sonicated and spun at 16000 g for 15 min. Clear lysate was incubated with pre-equilibrated PI(4,5)P2-coated agarose beads (Echelon Biosciences) for 2 h at 4 °C. Beads were then washed three times with RIPA. Bound proteins were eluted by boiling in Laemmli buffer, separated by SDS-PAGE, and detected by subsequent immunoblotting.

H1299 stable cell lines were lysed in lysis buffer (20 mM HEPES pH 8, 150 mM NaCl, 0.5 % Triton X-100, complete protease inhibitors, PhosStop phosphatase inhibitors (both Roche)). Lysate was sonicated and cleared by centrifugation at 16000 g for 15 min. Clear lysate was incubated with pre-equilibrated anti-Flag-M2 agarose beads (Sigma-Aldrich) for 2 h. After three washes with lysis buffer, bound proteins were processed as described above.

Antibodies

Primary antibodies: anti-PIP2 mouse monoclonal IgM antibody (Echelon Biosciences Inc., clone 2C11, Z-A045, 5-10 µg/ml for SIM and STED, 10 µg/ml for TEM); anti-PIP2 mouse monoclonal IgM antibody (Abcam, clone 2C11, 2 µg/ml for dot blot); anti-H3K9me2 rabbit polyclonal IgG antibody (Merck Millipore, 17-648, 1:300 for SIM and STED); anti-H3K4me2 rabbit polyclonal IgG antibody (Merck Millipore, 07-030, 1:300 for SIM and STED); anti-bromodeoxyuridine mouse IgG1 antibody (Roche, clone BMC9318, 11170376001, 4 µg/ml for SIM, 20 µg/ml for TEM); anti-bromodeoxyuridine (Sigma-Aldrich, clone BU-33, B8434, 8.8 µg/ml for SCAN-R); anti-histone H1 mouse monoclonal

IgG2a antibody (Abcam, clone AE-4, ab71594, 10 µg/ml for SIM); anti-Son rabbit polyclonal IgG antibody (Abcam, ab121759, 1 µg/ml for SIM); anti-RNA Pol II CTD rabbit polyclonal IgG antibody (Abcam, ab26721, 6 µg/ml for SIM); anti-RNA Pol II CTD S2 rabbit polyclonal IgG antibody (Abcam, ab24758, 4 µg/ml for western blot); anti-TFIID (TBP) rabbit polyclonal IgG antibody (Santa Cruz, sc-204, 2 µg/ml for SIM); anti-His mouse monoclonal IgG2a antibody (Sigma, H1029, 0.4 µg/ml for western blot); anti-NM1 antibody (Sigma-Aldrich, M3567, 1 µg/ml for western blot), anti-flag antibody (Stratagene, clone M2, 200471, 0.4 µg/ml for western blot and 20 µg/ml for TEM).

Secondary antibodies: goat anti-mouse IgM (µ-chain specific) antibody conjugated with Alexa Fluor 555 (Invitrogen, A21426, 5 µg/ml for SIM and SCAN-R); goat anti-mouse IgG (Fcγ fragment specific) antibody conjugated with DyLight 488 (Jackson, 115-485-008, 1:100 for SIM and SCAN-R); goat anti-rabbit IgG (H+L) antibody conjugated with Alexa Fluor 647 (Invitrogen, A21245, 5 µg/ml for SIM and SCAN-R); donkey anti-rabbit IgG (H+L) antibody conjugated with Alexa Fluor 488 (Invitrogen, A-21206, 5 µg/ml for SIM); donkey anti-human IgG (H+L) antibody conjugated with Cy5 (Jackson, 709-175-149, 1:50 for SIM); goat anti-rabbit IgG (H+L) antibody conjugated with TMR (Invitrogen, T-2769, 5 µg/ml for STED); goat anti-mouse IgG (H+L) antibody conjugated with Alexa Fluor 532 (Invitrogen, A-11002, 5 µg/ml for STED); IRDye 680 donkey anti-mouse IgG (H+L) antibody (LI-COR Biosciences; 926-68072, 1:20000 for western blotting); IRDye 800 donkey anti-rabbit IgG (H+L) antibody (LI-COR Biosciences; 925-32213, 1:20000 for western blotting); goat anti-mouse IgM (µ-chain specific) antibody coupled with 12 nm colloidal gold particles (Jackson ImmunoResearch Laboratories Inc., 115-205-075, for TEM); goat anti-mouse IgM (µ-chain specific) antibody coupled with 6nm colloidal gold particles (Jackson ImmunoResearch Laboratories Inc., 115-195-075, for TEM); goat anti-mouse IgG (Fcγ fragment specific) antibody coupled with 6 nm colloidal gold particles (Jackson ImmunoResearch Laboratories Inc., 115-195-071, for TEM); all gold-conjugated secondary antibodies were diluted 1:30.

References

Almuzzaini B, Sarshad AA, Farrants AK, Percipalle P. 2015. Nuclear myosin 1 contributes to a chromatin landscape compatible with RNA polymerase II transcription activation. *BMC Biol* **13**: 35.

Anderson RA, Boronenkov IV, Doughman SD, Kunz J, Loijens JC. 1999. Phosphatidylinositol phosphate kinases, a multifaceted family of signaling enzymes. *The Journal of biological chemistry* **274**: 9907-9910.

Balla T. 2013. Phosphoinositides: tiny lipids with giant impact on cell regulation. *Physiological reviews* **93**: 1019-1137.

Bieniossek C, Papai G, Schaffitzel C, Garzoni F, Chaillet M, Scheer E, Papadopoulos P, Tora L, Schultz P, Berger I. 2013. The architecture of human general transcription factor TFIID core complex. *Nature* **493**: 699-702.

Cavellan E, Asp P, Percipalle P, Farrants AK. 2006. The WSTF-SNF2h chromatin remodeling complex interacts with several nuclear proteins in transcription. *The Journal of biological chemistry* **281**: 16264-16271.

Cisterna B, Necchi D, Prosperi E, Biggiogera M. 2006. Small ribosomal subunits associate with nuclear myosin and actin in transit to the nuclear pores. *FASEB J* **20**: 1901-1903.

Cocco L, Gilmour RS, Ognibene A, Letcher AJ, Manzoli FA, Irvine RF. 1987. Synthesis of polyphosphoinositides in nuclei of Friend cells. Evidence for polyphosphoinositide metabolism inside the nucleus which changes with cell differentiation. *The Biochemical journal* **248**: 765-770.

Divecha N, Banfic H, Irvine RF. 1991. The polyphosphoinositide cycle exists in the nuclei of Swiss 3T3 cells under the control of a receptor (for IGF-I) in the plasma membrane, and stimulation of the cycle increases nuclear diacylglycerol and apparently induces translocation of protein kinase C to the nucleus. *The EMBO journal* **10**: 3207-3214.

Ferguson KM, Lemmon MA, Schlessinger J, Sigler PB. 1995. Structure of the high affinity complex of inositol trisphosphate with a phospholipase C pleckstrin homology domain. *Cell* **83**: 1037-1046.

Fomproix N, Percipalle P. 2004. An actin-myosin complex on actively transcribing genes. *Exp Cell Res* **294**: 140-148.

Geeraerts A, Hsiu-Fang F, Zimmermann P, Engelborghs Y. 2013. The characterization of the nuclear dynamics of syntenin-2, a PIP2 binding PDZ protein. *Cytometry A* **83**: 866-875.

Gonzales ML, Anderson RA. 2006. Nuclear phosphoinositide kinases and inositol phospholipids. *J Cell Biochem* **97**: 252-260.

Harlan JE, Hajduk PJ, Yoon HS, Fesik SW. 1994. Pleckstrin homology domains bind to phosphatidylinositol-4,5-bisphosphate. *Nature* **371**: 168-170.

Heidemann M, Hintermair C, Voss K, Eick D. 2013. Dynamic phosphorylation patterns of RNA polymerase II CTD during transcription. *Biochimica et biophysica acta* **1829**: 55-62.

Hofmann WA, Vargas GM, Ramchandran R, Stojiljkovic L, Goodrich JA, de Lanerolle P. 2006. Nuclear myosin I is necessary for the formation of the first phosphodiester bond during transcription initiation by RNA polymerase II. *J Cell Biochem* **99**: 1001-1009.

Hokanson DE, Laakso JM, Lin T, Sept D, Ostap EM. 2006. Myo1c binds phosphoinositides through a putative pleckstrin homology domain. *Molecular biology of the cell* **17**: 4856-4865.

Hokanson DE, Ostap EM. 2006. Myo1c binds tightly and specifically to phosphatidylinositol 4,5-bisphosphate and inositol 1,4,5-trisphosphate. *Proc Natl Acad Sci U S A* **103**: 3118-3123.

Irvine RF. 2006. Nuclear inositide signalling -- expansion, structures and clarification. *Biochimica et biophysica acta* **1761**: 505-508.

Jolly C, Metz A, Govin J, Vigneron M, Turner BM, Khochbin S, Vourc'h C. 2004. Stress-induced transcription of satellite III repeats. *The Journal of cell biology* **164**: 25-33.

Jones DR, Divecha N. 2004. Linking lipids to chromatin. *Curr Opin Genet Dev* **14**: 196-202.

Layerenza JP, Gonzalez P, Garcia de Bravo MM, Polo MP, Sisti MS, Ves-Losada A. 2013. Nuclear lipid droplets: a novel nuclear domain. *Biochimica et biophysica acta* **1831**: 327-340.

Lemmon MA, Ferguson KM, O'Brien R, Sigler PB, Schlessinger J. 1995. Specific and high-affinity binding of inositol phosphates to an isolated pleckstrin homology domain. *Proc Natl Acad Sci U S A* **92**: 10472-10476.

Mazzotti G, Zini N, Rizzi E, Rizzoli R, Galanzi A, Ognibene A, Santi S, Matteucci A, Martelli AM, Maraldi NM. 1995. Immunocytochemical detection of phosphatidylinositol 4,5-bisphosphate localization sites within the nucleus. *J Histochem Cytochem* **43**: 181-191.

Mellman DL, Gonzales ML, Song C, Barlow CA, Wang P, Kendziorski C, Anderson RA. 2008. A PtdIns4,5P2-regulated nuclear poly(A) polymerase controls expression of select mRNAs. *Nature* **451**: 1013-1017.

Mortier E, Wuytens G, Leenaerts I, Hannes F, Heung MY, Degeest G, David G, Zimmermann P. 2005. Nuclear speckles and nucleoli targeting by PIP2-PDZ domain interactions. *The EMBO journal* **24**: 2556-2565.

Osborne SL, Thomas CL, Gschmeissner S, Schiavo G. 2001. Nuclear PtdIns(4,5)P2 assembles in a mitotically regulated particle involved in pre-mRNA splicing. *Journal of cell science* **114**: 2501-2511.

Payrastre B, Nievers M, Boonstra J, Breton M, Verkleij AJ, Van Bergen en Henegouwen PM. 1992. A differential location of phosphoinositide kinases, diacylglycerol kinase, and phospholipase C in the nuclear matrix. *The Journal of biological chemistry* **267**: 5078-5084.

Percipalle P, Fomproix N, Cavellan E, Voit R, Reimer G, Kruger T, Thyberg J, Scheer U, Grummt I, Farrants AK. 2006. The chromatin remodelling complex WSTF-SNF2h interacts with nuclear myosin 1 and has a role in RNA polymerase I transcription. *EMBO Rep* **7**: 525-530.

Philimonenko VV, Zhao J, Iben S, Dingova H, Kysela K, Kahle M, Zentgraf H, Hofmann WA, de Lanerolle P, Hozak P et al. 2004. Nuclear actin and myosin I are required for RNA polymerase I transcription. *Nature cell biology* **6**: 1165-1172.

Rando OJ, Zhao K, Janmey P, Crabtree GR. 2002. Phosphatidylinositol-dependent actin filament binding by the SWI/SNF-like BAF chromatin remodeling complex. *Proc Natl Acad Sci U S A* **99**: 2824-2829.

Sarshad A, Sadeghifar F, Louvet E, Mori R, Bohm S, Al-Muzzaini B, Vintermist A, Fomproix N, Ostlund AK, Percipalle P. 2013. Nuclear myosin 1c facilitates the chromatin modifications required to activate rRNA gene transcription and cell cycle progression. *PLoS Genet* **9**: e1003397.

Scassellati C, Albi E, Cmarko D, Tiberi C, Cmarkova J, Bouchet-Marquis C, Verschure PJ, Driel R, Magni MV, Fakan S. 2010. Intranuclear sphingomyelin is associated with transcriptionally active chromatin and plays a role in nuclear integrity. *Biol Cell* **102**: 361-375.

Sobol M, Yildirim S, Philimonenko VV, Marasek P, Castano E, Hozak P. 2013. UBF complexes with phosphatidylinositol 4,5-bisphosphate in nucleolar organizer regions regardless of ongoing RNA polymerase I activity. *Nucleus* **4**: 478-486.

Sugi T, Oyama T, Morikawa K, Jingami H. 2008. Structural insights into the PIP2 recognition by syntenin-1 PDZ domain. *Biochemical and biophysical research communications* **366**: 373-378.

Tanaka T, Iwawaki D, Sakamoto M, Takai Y, Morishige J, Murakami K, Satouchi K. 2003. Mechanisms of accumulation of arachidonate in phosphatidylinositol in yellowtail. A comparative study of acylation systems of phospholipids in rat and the fish species Seriola quinqueradiata. *Eur J Biochem* **270**: 1466-1473.

Toska E, Campbell HA, Shandilya J, Goodfellow SJ, Shore P, Medler KF, Roberts SG. 2012. Repression of transcription by WT1-BASP1 requires the myristoylation of BASP1 and the PIP2-dependent recruitment of histone deacetylase. *Cell Rep* **2**: 462-469.

Vann LR, Wooding FB, Irvine RF, Divecha N. 1997. Metabolism and possible compartmentalization of inositol lipids in isolated rat-liver nuclei. *The Biochemical journal* **327 (Pt 2)**: 569-576.

Venit T, Dzijak R, Kalendová A, Kahle M, Rohožková J, Schmid tV, Rülicke T, Rathkolb B, Hans V, Bohla A et al. 2013. Mouse nuclear myosin I knock-out shows interchangeability and redundancy of myosin isoforms in the cell nucleus. *PloS one* **in press**.

Wang J, Arbuzova A, Hangyas-Mihalyne G, McLaughlin S. 2001. The effector domain of myristoylated alanine-rich C kinase substrate binds strongly to phosphatidylinositol 4,5-bisphosphate. *The Journal of biological chemistry* **276**: 5012-5019.

Watt SA, Kular G, Fleming IN, Downes CP, Lucocq JM. 2002. Subcellular localization of phosphatidylinositol 4,5-bisphosphate using the pleckstrin homology domain of phospholipase C delta1. *The Biochemical journal* **363**: 657-666.

Ye J, Zhao J, Hoffmann-Rohrer U, Grummt I. 2008. Nuclear myosin I acts in concert with polymeric actin to drive RNA polymerase I transcription. *Genes Dev* **22**: 322-330.

Yildirim S, Castano E, Sobol M, Philimonenko VV, Dzijak R, Venit T, Hozak P. 2013. Involvement of phosphatidylinositol 4,5-bisphosphate in RNA polymerase I transcription. *Journal of cell science* **126**: 2730-2739.

Yoo SH, Huh YH, Huh SK, Chu SY, Kim KD, Hur YS. 2014. Localization and projected role of phosphatidylinositol 4-kinases IIalpha and IIbeta in inositol 1,4,5-trisphosphate-sensitive nucleoplasmic Ca(2)(+) store vesicles. *Nucleus* **5**: 341-351.

Yu H, Fukami K, Watanabe Y, Ozaki C, Takenawa T. 1998. Phosphatidylinositol 4,5-bisphosphate reverses the inhibition of RNA transcription caused by histone H1. *Eur J Biochem* **251**: 281-287.

Zhao K, Wang W, Rando OJ, Xue Y, Swiderek K, Kuo A, Crabtree GR. 1998. Rapid and phosphoinositol-dependent binding of the SWI/SNF-like BAF complex to chromatin after T lymphocyte receptor signaling. *Cell* **95**: 625-636.

Zimmermann P, Meerschaert K, Reekmans G, Leenaerts I, Small JV, Vandekerckhove J, David G, Gettemans J. 2002. PIP(2)-PDZ domain binding controls the association of syntenin with the plasma membrane. *Molecular cell* **9**: 1215-1225.

Acknowledgements. We are very thankful to Ivana Nováková, Iva Jelínková, Lenka Jarolimová, and Pavel Kříž for the excellent technical work and to Irina Studenyak for the proofreading. We are thankful to Prof. Moise Bendayan for the methodological tips. We would like to thank for the financial support GACR (GAP305/11/2232), MIT (FR-TI3/588), TACR (TE01020118), GACR (GA15-08738S), project „BIOCEV – Biotechnology and Biomedicine Centre of the Academy of Sciences and Charles University“ (CZ.1.05/1.1.00/02.0109) from the European Regional Development Fund, IMG (RVO:68378050), CONACYT project 60223, Nikon spol. s r.o. The microscopy work was performed at the Microscopy Centre, Institute of Molecular Genetics AS CR.

Figure legends

Figure 1. Nucleoplasmic PIP2 appears as small roundish structures, which colocalize with nascent RNA and proteins involved in Pol II transcription. (a, b) Immunofluorescent labeling followed by SIM demonstrates that nucleoplasmic PIP2 forms small foci and colocalizes with both nascent RNA transcripts (BrRNA) and C-terminal domain of Pol II (Pol II CTD) as well as TATA-box binding protein (TBP) of the Pol II general transcription factor TFIID (TFIID TBP). This colocalization is supported by intensity profiles. General view: bar is 5 μm; magnified view corresponds to the area outlined by white rectangle, bar is 1 μm. (c) Manders' colocalization coefficients and Pearson's correlation coefficient, presented as mean ± standard deviation, illustrate colocalization between BrRNA and PIP2, *p value ≤ 0.05. (d) Cells transiently transfected with truncated form of NM1 fused to flag-tag (NM1(HDL)-flag) were processed for TEM and double labeled with anti-flag and anti-PIP2 antibodies. TEM showed more accurately that these PIP2 foci are roundish structures of 40-100 nm in size and revealed presence of NM1 at the periphery of these structures. Based on their roundish shape and size, we refer to them as PIP2 islets. Bar is 200 nm. Graph shows that PIP2 molecules and NM1 are colocalized at the distance of 25 – 75 nm (PCCF > 1, **p value ≤ 0.01).

Figure 2. NM1 associates with PIP2 islets and is anchored in nucleoplasm by PIP2. (a) NM1 was pulled-down with PIP2-coupled agarose beads from the nuclear extract and detected by immunoblotting. (b) Direct binding of NM1 to PIP2 was confirmed by incubation of recombinant wild-type NM1-flag and its PIP2-binding mutant NM1(K908A)-flag with PIP2 spotted on a nitrocellulose membrane. Recombinant NM1-flag and NM1(K908A)-flag were immunodetected by anti-flag antibody. (c) Mobility of NM1-EGFP significantly increases after mutation in PIP2-binding site (K908A), as measured by FRAP. Mobility of NM1-EGFP increases when nuclear PIP2 is converted to PI4P by inositol 5-phosphatase. When nuclear PIP2 is hindered by the binding of PLCδPH domain, NM1-EGFP mobility increases. As a control, PLCδPH domain with R40A mutation, which disables its binding to PIP2, was used. Results are presented as mean ± standard deviation, ***p value ≤ 0.001. (d) Nuclei extracted by Brij98 were subjected to a flotation on a sucrose density gradient. Nuclear extract was placed to the bottom of the gradient. After centrifugation, fractions were subjected to SDS-PAGE, transferred to a nitrocellulose membrane and immunodetected for the presence of NM1. To detect PIP2, fractions were spotted on a nitrocellulose membrane and labeled with anti-PIP2 antibody. Both NM1 and PIP2 are present in the light fraction 1 containing

detergent-insoluble lipoprotein complexes and also in the heavy fraction 10 composing of soluble complexes.

Figure 3. PIP2-NM1 interaction and integrity of PIP2 islets are important for Pol II-dependent transcription. (a) Cells stably expressing NM1-flag or NM1(K908A)-flag were prepared, lysed and subjected to the co-immunoprecipitation by anti-flag antibody. Immunoprecipitates were analyzed by anti-Pol II CTD S2 and anti-flag antibodies. (b) By shRNA-mediated knock-down, we generated stable cell line with decreased expression of NM1. On top of that, we further introduced NM1-flag, or NM1(K908A)-flag. As a control, cell line expressing non-targeting shRNA was used. (c) We monitored Pol II transcription level in these cell lines by short-pulse labeling of nascent transcripts with FU. We immunolabeled FU with anti-BrdU antibody and quantified intensity of the signal by indirect high-throughput immunofluorescent microscopy. Data are related to the control value and presented as mean ± standard deviation. (d) For PIP2 hydrolysis, cells were slightly permeabilized and incubated with PLC. As a control, cells were incubated with either PLC(R40A), which is unable to bind PIP2, or heat-inactivated PLC, or BSA, or buffer only. After 30 min, FU was added to the cells. FU as well as PIP2 were visualized and quantified as described above in (c). Data are related to the control value and presented for PIP2 islets area as mean ± standard deviation, *p value ≤ 0.05, **p value ≤ 0.01, ***p value ≤ 0.001, ****p value ≤ 0.0001. (e) Cells were incubated with BrUTP as a labeled precursor for the RNA synthesis. Cells were processed for TEM and double labeled with anti-BrdU and anti-PIP2 antibodies. We clearly showed that PIP2 molecules form the roundish islets colocalized at their periphery with nascent RNA transcripts. Bar is 100 nm. (f) The scheme shows PIP2 islet and neighbouring BrRNA over the distance, where their colocalization is significant. Graph represents the colocalization between PIP2 molecules and BrRNA at the distance of 25 – 75 nm (PCCF > 2, **p value ≤ 0.01). (g) Graph shows the relative colocalization of BrRNA and PIP2 molecules (BrRNA/PIP2) and *vice versa* (PIP2/BrRNA) as mean ± standard deviation (***p value ≤ 0.001). (h) Upon the inhibition of Pol II transcription with α-amanitin, the appearance and the quantity of PIP2 islets per μm^2 were not significantly changed as compared to the control. Bar is 100 nm. (i) Graph shows PIP2 islets quantity per μm^2 in the nuclei of control cells and cells treated with α-amanitin as mean ± standard devaition, ^{ns}p value ≥ 0.05.

Figure 4. PIP2 islets are chromatin-independent structures. Immunofluorescent labeling followed by SIM reveals that under isotonic conditions, PIP2 islets overlap with histone H1 (a). Under hypertonic conditions (final salt concentration 300 mM, 15 min), PIP2 islets minimally overlap and do not significantly colocalize with histone H1 (b). After 3 min of rescue under isotonic conditions, chromatin decondenses and PIP2 islets colocalize with histone H1 (c). General view: bar is 5 μm; magnified view corresponds to the area outlined by white rectangle, bar is 200 nm. These observations are supported by the intensity profiles, Manders' colocalization coefficients (d) and Pearson's correlation coefficient (e) in PIP2 islets area. (f) The volumes of chromatin and PIP2 islets related to the nuclear volume (relative volumes) under different experimental conditions. The left y-axis represents the percentage of histone H1, the right y-axis represents the percentage of PIP2. The values in (d-f) are presented as mean ± standard deviation (**p value ≤ 0.01, ***p value ≤ 0.001).

Figure 5. PIP2 islets are resistant to DNase treatment and are RNA-associated structures. Immunofluorescent labeling followed by SIM demonstrates that treatment of cells with 250 U/ml DNase for 30 min (b) has no significant effect on the arrangement of PIP2 islets as compared to control (a). Cells treated with 1 mg/ml RNase for 30 min display almost complete disappearance of PIP2 islets labeling (c). General view: bar is 5 μm; magnified view corresponds to the area outlined by white rectangle, bar is 200 nm. (d) Ultrathin sections were first labeled with anti-PIP2 antibody followed by secondary antibody conjugated with 6 nm gold nanoparticles. Then sections were labeled with RNase conjugated with 10 nm gold nanoparticles. TEM demonstrates that RNA molecules are located on the surface of PIP2 islets; bar is 100 nm. Graph shows the relative colocalization of RNA with PIP2 molecules (RNA/PIP2) and *vice versa* (PIP2/RNA) as mean ± standard deviation (***p value ≤ 0.001).

Figure 6. Morphology, composition and distribution of PIP2 islets. (a) PIP2 was visualized with anti-PIP2 antibody and z-stack was acquired using SIM. Nuclear PIP2 labeling was reconstructed in 3D and shown here as 2D maximum intensity projection image: N – nucleus, NS – nuclear speckles, NL – nucleolus; bar is 1 μm. Distribution of PIP2 in nuclear speckles, nucleoli, and nucleoplasm was calculated in 3D and color-coded using the software NIS-Elements and MATLAB. Color-coded original 2D image and diagram are shown below: nuclear speckles are in yellow, nucleoplasm is in red, nucleolar PIP2 is in blue. (b) TEM image of nuclear PIP2 labeling on the surface of ultrathin section. Abbreviations and color-coding are the same as in (a). Roundish PIP2 islets of 40-100 nm are shown below in

magnified view. Mapping was done using the commercially available software Ellips with the additionally installed software Gold plugins (Philimonenko et al. 2000; Schofer et al. 2004). General view: bar is 1 μm, magnified view: bar is 100 nm. (c) Ultrathin sections were first labeled with anti-PIP2 antibody and further subjected to elemental mapping by EELS; bar is 100 nm. (d) Mapping of the presence of nitrogen and phosphorus in PIP2 islets. (e, f) Magnified view of (d) shows PIP2 islet surrounded by nitrogen (e) and phosphorus (f); bar is 100 nm. The inner part of PIP2 islet appears to be devoid of them both. (g) Carbon mapping shows the inner space of PIP2 islet enriched with carbon-rich compounds; bar is 100 nm. (h, i) Immunofluorescent labeling followed by SIM reveals that PIP2 islets partially overlap with either histone H3K4me2 enriched in transcriptionally active genes (h) or histone H3K9me2 which is a heterochromatic marker (i) as confirmed by intensity profiles. General view: bar is 5 μm; magnified view corresponds to the area outlined by white rectangle: bar is 200 nm.

Supplementary Figure 1. The purity of recombinant PLC. Expressed and purified His-tagged PLC was detected in the eluted fraction using Coomassie staining and western blotting (WB) with anti-His antibody.

Supplementary Figure 2. The activity of RNase-gold complex and its specificity of labeling. (a) The enzymatic activity of RNase after the conjugation with gold nanoparticles was assessed using *in vitro* incubation with RNA followed by agarose gel electrophoresis; lane 1 – input RNA, lane 2 – RNA treated with RNase before conjugation, lane 3 – RNA treated with unbound RNase after conjugation, lane 4 – RNA treated with RNase-gold complex, lane 5 – marker. Cleaved 28 S (arrow) and 18S RNA (arrowhead) proves the activity of the complex. (b) The labeling specificity of RNase-gold complex was tested by TEM. Prior to labeling, RNase-gold complex was *in vitro* presaturated with RNA. This mixture was then used for the labeling of the sections. Apparent depletion of labeling proves the specificity of labeling by the RNase-gold complex. General view: bar is 200 nm; magnified view: bar is 100 nm.

Figure 1

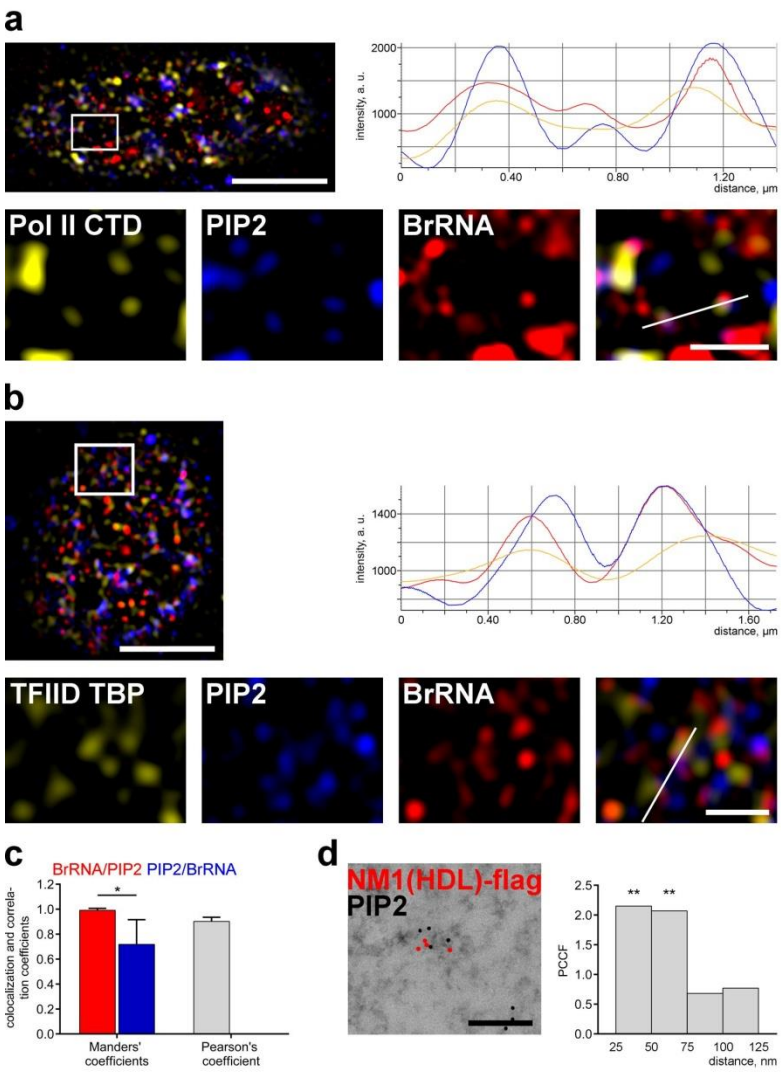
a
intensity, a. u.
distance, μm
Pol II CTD
PIP2
BrRNA
b
intensity, a. u.
distance, μm
TFIID TBP
PIP2
BrRNA
c
BrRNA/PIP2 PIP2/BrRNA
colocalization and correlation coefficients
Manders' coefficients
Pearson's coefficient
d
NM1(HDL)-flag
PIP2
PCCF
distance, nm

Figure 2

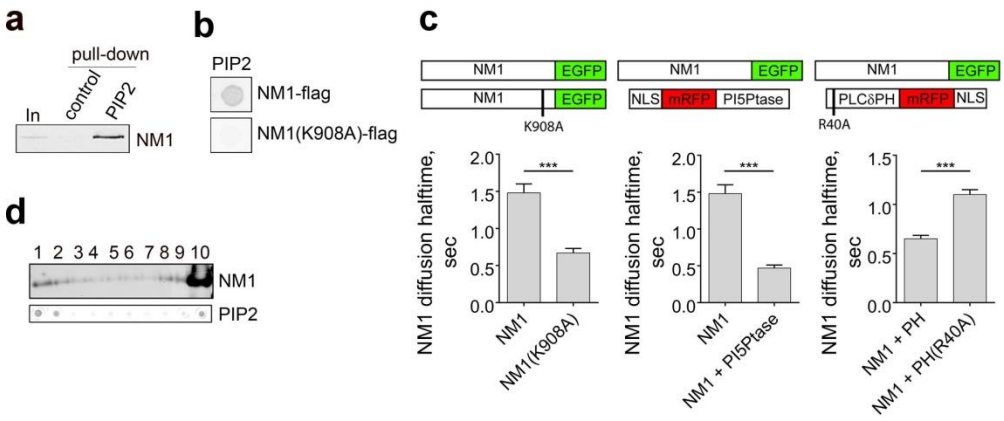
a
pull-down
In
control
PIP2
NM1
b
PIP2
NM1-flag
NM1(K908A)-flag
c
NM1
EGFP
K908A
NLS
mRFP
PI5Ptase
PLCδPH
R40A
NM1 diffusion halftime, sec
***
NM1
NM1(K908A)
NM1 + PI5Ptase
NM1 + PH
NM1 + PH(R40A)
d
1 2 3 4 5 6 7 8 9 10
NM1
PIP2

Figure 3

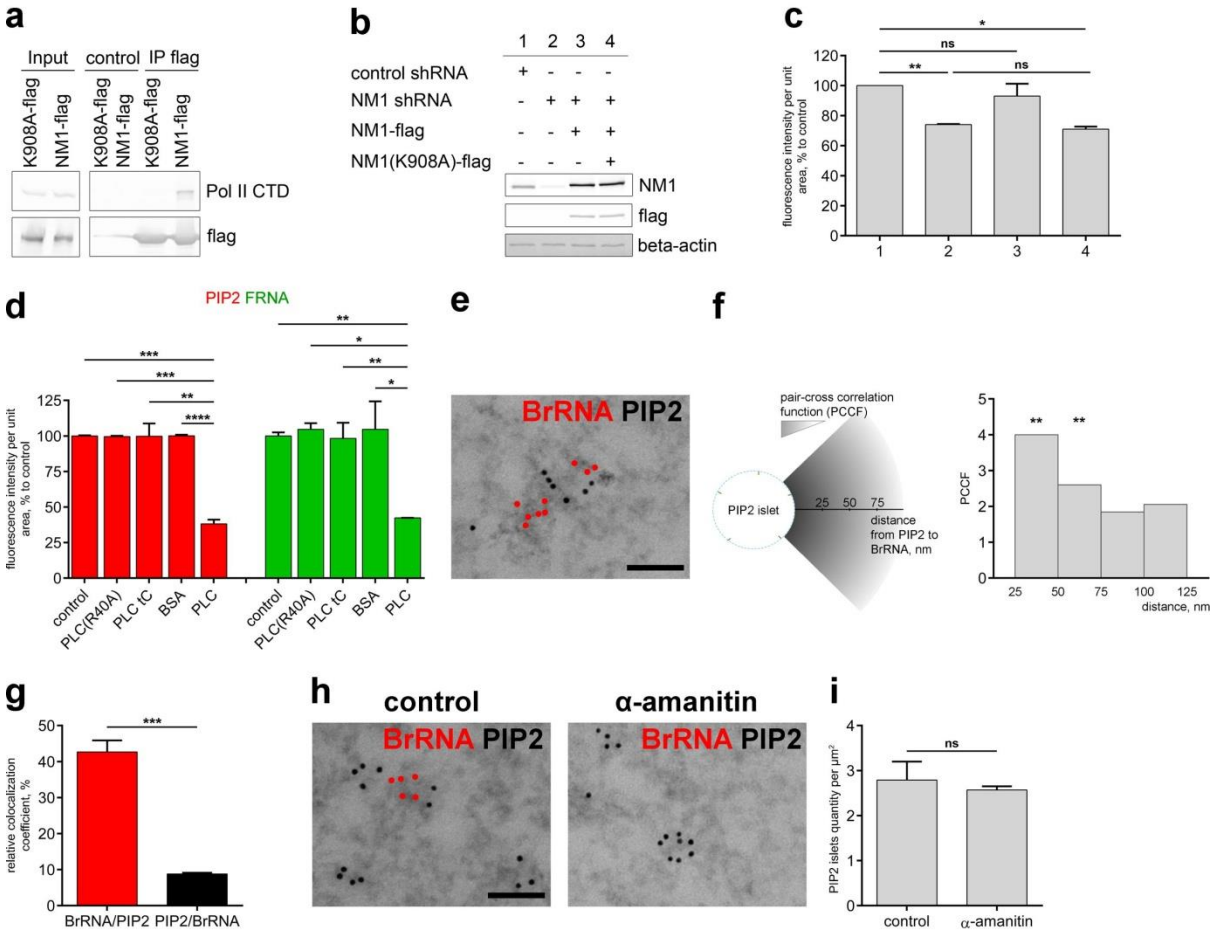
a
Input
control
IP flag
K908A-flag
NM1-flag
K908A-flag
NM1-flag
K908A-flag
NM1-flag
Pol II CTD
flag
b
1 2 3 4
control shRNA + - - -
NM1 shRNA - + + +
NM1-flag - - + +
NM1(K908A)-flag - - - +
NM1
flag
beta-actin
c
fluorescence intensity per unit area, % to control
ns
**
ns
*
d
PIP2 FRNA
fluorescence intensity per unit area, % to control
control
PLC(R40A)
PLC tC
BSA
PLC
e
BrRNA PIP2
f
pair-cross correlation function (PCCF)
PIP2 islet
25 50 75
distance from PIP2 to BrRNA, nm
PCCF
distance, nm
g
relative colocalization coefficient, %
BrRNA/PIP2
PIP2/BrRNA
h
control
α-amanitin
BrRNA PIP2
i
PIP2 islets quantity per μm²
ns
control
α-amanitin

Figure 4

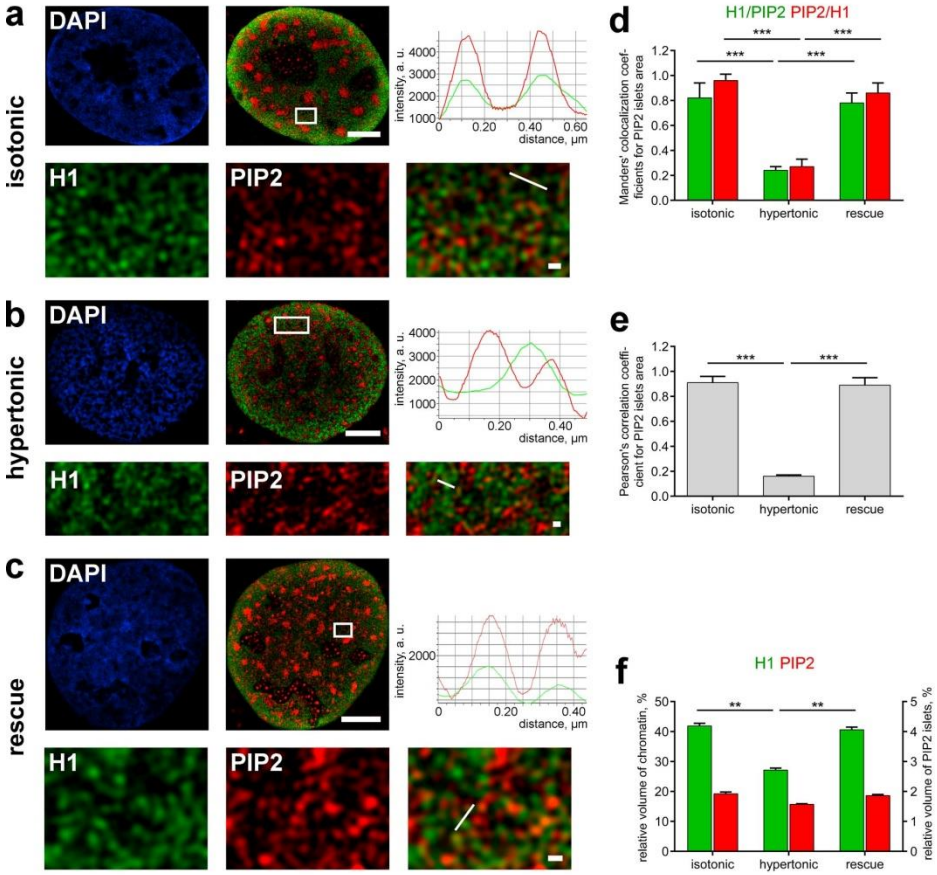
a
isotonic
DAPI
H1
PIP2
intensity, a. u.
distance, μm
b
hypertonic
c
rescue
d
H1/PIP2 PIP2/H1
Manders' colocalization coefficients for PIP2 islets area
isotonic
hypertonic
rescue
e
Pearson's correlation coefficient for PIP2 islets area
f
H1 PIP2
relative volume of chromatin, %
relative volume of PIP2 islets, %

Figure 5

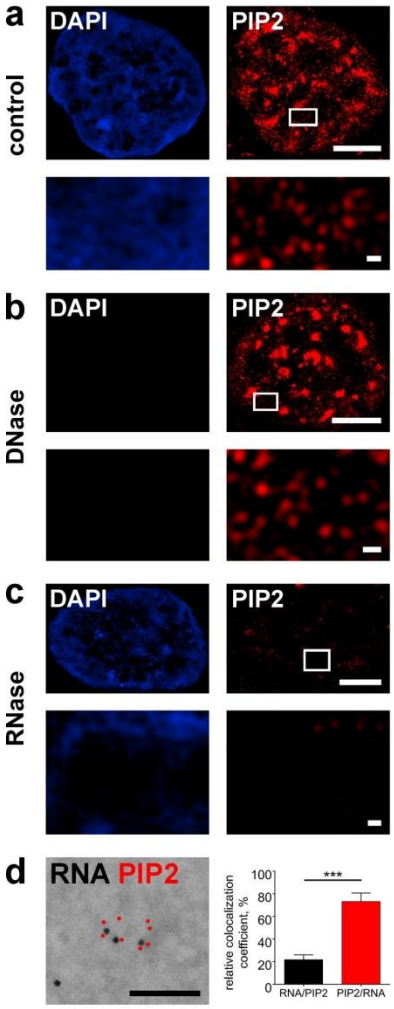
a
control
DAPI
PIP2
b
DNase
DAPI
PIP2
c
RNase
DAPI
PIP2
d
RNA PIP2
relative colocalization coefficient, %
100
80
60
40
20
0
***
RNA/PIP2
PIP2/RNA

Figure 6

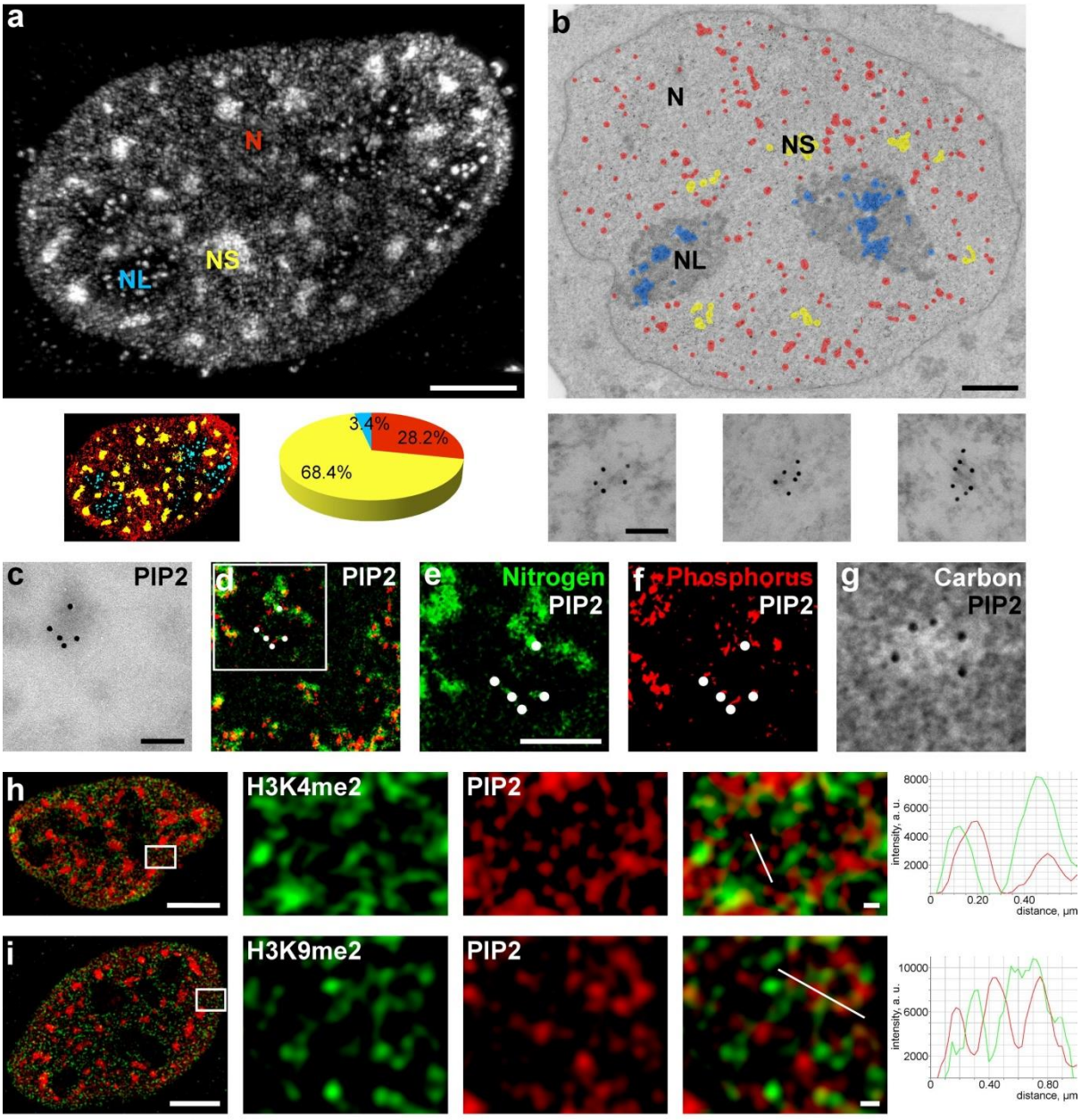
a
N
NS
NL
b
N
NS
NL
3.4%
28.2%
68.4%
c PIP2
d PIP2
e Nitrogen PIP2
f Phosphorus PIP2
g Carbon PIP2
h
H3K4me2
PIP2
intensity, a. u.
8000
6000
4000
2000
0
0.20
0.40
distance, µm
i
H3K9me2
PIP2
intensity, a. u.
10000
6000
2000
0
0.40
0.80
distance, µm

Supplementary Figure 1

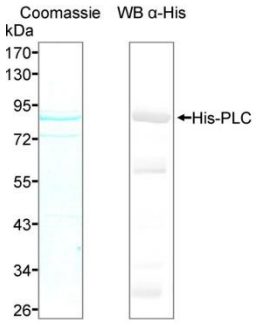

Supplementary Figure 2

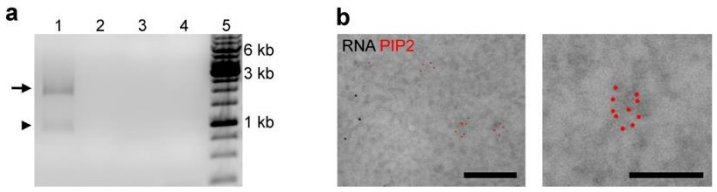

3.3 Chromatin associated PI(4)P regulates lysine-specific histone demethylase 1

Kalasova I, Kalendová A, Fáberová V, Marášek P, Uličná L, Vacík T and Hozák P

Manuscript.

I. K. designed and performed most of the experiments (DNA cloning, DNA mutagenesis, protein expression and purification, cellular fractionations, pull-down assays, fluorescence microscopy, western blotting, demethylation assays, qPCR) and wrote the manuscript.

Chromatin associated PI(4)P regulates lysine-specific histone demethylase 1.

Ilona Kalasova[1], Alžběta Kalendová[1], Veronika Fáberová[1], Lívia Uličná[1], Pavel Marášek[1], Tomáš Vacík[1], Pavel Hozák[1,*]

[1] Department of Biology of the Cell Nucleus, Institute of Molecular Genetics of the Academy of Sciences of the Czech Republic, v.v.i., Vídeňská 1083, 142 20, Prague, Czech Republic.

[*] **corresponding author, hozak@img.cas.cz, Tel.: +420 241 062 219, Fax: +420 241 062 289**

Abstract

Phosphoinositides (PIs) are negatively charged glycerol-based phospholipids. Their inositol head that can be reversibly phosphorylated at three positions generating 7 differently phosphorylated PIs. Approximately 15% of PIs localize to the nucleus. Nuclear PIs are implicated in essential nuclear processes as DNA damage response, and pre-rRNA and pre-mRNA processing. Moreover, they regulate DNA transcription either by interaction with RNA polymerases and transcription factors or by regulation of chromatin remodelling and modifications.

Phosphatidylinositol 4-phosphate (PI(4)P) is one of the most abundant PIs species. Although it can be actively metabolized within the nucleus, its nuclear functions are completely unknown. In this study, we show that PI(4)P is present in nuclear membrane, localizes to nuclear speckles and forms small nucleplasmic foci. The majority of PI(4) is associated with active chromatin. Lysine-specific histone demethylase 1 (LSD1), which demethylates H3K4me2 and H3K4me1, binds with the highest affinity to PI(4)P and binds also PI(3,4)P2, PI(3,5)P2, PI(4,5)P2 and PI(3,4,5)P3. While in a complex with PI(4)P, the activity of LSD1 is inhibited. On the other hand, the interaction with PI(4,5)P2 stimulates LSD1 demethylase activity *in vitro*. Since PI(4,5)P2 is a precursor/product of PI(4)P (de)phosphorylation, a single change in phosphorylation of inositol ring could provide a rapid regulation of LSD1 function also *in vivo*.

Keywords: nucleus, phosphoinositides, PI(4)P, PI(4,5)P2, LSD1

Introduction

Phosphoinositides (PIs) are negatively charged glycerol-based phospholipids. They consist of hydrophobic acyl tail and hydrophilic inositol head that can be reversibly phosphorylated at 3', 4', and 5' positions generating 7 differently phosphorylated PIs. Approximately 15% of PIs localize to the nucleus. Some PIs species associate with nuclear membrane however a large fraction of PIs occupies discrete nuclear domains (Vann et al. 1997), such as interchromatin and chromatin regions and nucleoli (Mazzotti et al. 1995; Boronenkov et al. 1998; Gillooly et al. 2000; Osborne et al. 2001; Watt et al. 2002; Lindsay et al. 2006; Hammond et al. 2009; Yildirim et al. 2013).

In agreement with their diverse nuclear localization, PIs display diverse nuclear functions. Nuclear PIs are implicated in cell differentiation, DNA damage response, apoptosis (Bertagnolo et al. 1999; Tanaka et al. 1999; Gozani et al. 2003; Ahn et al. 2004; Ahn et al. 2005; Jones et al. 2006; Zou et al. 2007; Li et al. 2012; Bua et al. 2013). They regulate pre-rRNA and pre-mRNA processing as well as DNA transcription (Osborne et al. 2001; Mellman et al. 2008; Okada et al. 2008; Wickramasinghe et al. 2013; Yildirim et al. 2013). PIs interact with both RNA Pol I and II (Osborne et al. 2001; Toska et al. 2012; Sobol et al. 2013; Yildirim et al. 2013) and regulate recruitment and activity of transcription factors (Toska et al. 2012; Blind et al. 2012; Yildirim et al. 2013; Stijf-Bultsma et al. 2015).

In addition, PIs can regulate gene expression also at epigenetic level. PI(4,5)P2 interacts with transcriptional co-repressor BASP1, facilitates BASP1 interaction with histone deacetylase 1 (HDAC1) and target BASP1-HDAC1 complex to chromatin (Toska et al. 2012). PI(4,5)P2 also interacts with SWI/SNF-like BAF remodelling complex and facilitates its association with chromatin during T cell activation (Rando et al. 2002). PI(5)P allosterically modulates ubiquitin-like PHD and RING finger domain-containing protein 1 (UHFR1), which can switch between two different histone binding modes. In absence of PI(5)P interaction, UHFR1 binds to unmodified histone H3 and recruits histone methyltransferases to establish heterochromatin marks. Upon PI(5)P binding, UHFR1 recognizes H3K9me3 and maintains heterochromatin state (Gelato et al. 2014).

Recently, we have detected nuclear PI(4)P by a specific anti-PI(4)P antibody (Kalasova et al. 2016). In the nucleus, PI(4)P can be formed by two different pathways. First, phosphatidylinositol (PI) is phosphorylated to PI(4)P by PI4Kα and PI4Kβ kinases (de Graaf et al. 2002; Strahl et al. 2005; Szivak et al. 2006; Kakuk et al. 2006). Second, PI(3,4)P2 and PI(4,5)P2 are dephosphorylated to PI(4)P by PTEN and SHIP phosphatases, respectively (Lachyankar et al. 2000; Gimm et al. 2000; Déléris et al. 2003; Lindsay et al. 2006; Elong Edimo et al. 2011; Nalaskowski et al. 2012; Ehm et al. 2015). These enzymes often localize to nuclear speckles (Boronenkov et al. 1998; Déléris et al. 2003; Szivak et al. 2006; Mellman et al. 2008; Elong Edimo et al. 2011) and nucleoli (Kakuk et al. 2006; Kakuk et al. 2008). Although PI(4)P is one of the most abundant nuclear PIs (Viaud et al. 2015)(Viaud et al. 2015), its role in the nucleus remains completely unknown.

In this study, we investigate localization and function of nuclear PI(4)P. We show that PI(4)P is present in nuclear membrane, localizes to nuclear speckles and forms small nucleoplasmic foci. Only a minority of nuclear PI(4)P resides in nuclear speckles. The majority localizes to other nuclear compartments and is associated with active chromatin. Lysine-specific histone demethylase 1 (LSD1), which demethylates H3K4me2 and H3K4me1 (Shi et al. 2004), interacts directly with PI(4)P, PI(3,4)P2, PI(3,5)P2, PI(4,5)P2 and PI(3,4,5)P3 but displays the highest affinity to PI(4)P. We demonstrate that the interaction with PI(4)P inhibits LSD1 *in vitro*. On the other hand, the interaction with PI(4,5)P2 stimulates LSD1 H3K4me2 demethylase activity. Since PI(4,5)P2 is a precursor/product of PI(4)P (de)phosphorylation, a single change in phosphorylation of inositol ring could provide rapid regulation of LSD1 function.

Results

PI(4)P localizes to nuclear membrane, nuclear speckles and nucleoplasm

We have previously detected PI(4)P in nuclei of U2OS cells (Kalasova et al. 2016). Here, we investigate PI(4)P localization in greater detail by stimulated emission depletion (STED) super-resolution microscopy. We show that PI(4)P is present in the nuclear membrane (Fig. 1a, insets), where it colocalizes with lamin A/C (Fig. 1a, arrowheads). In the nucleoplasm, PI(4)P localizes to nuclear speckles, where it colocalizes with Sm (Fig. 1b, upper inset) and Son (Fig. 1c, insets), nuclear speckles markers. Graphs show intensities of PI(4)P and Sm (Fig. 1b, right) or Son (Fig. 1c, right) signals along lines depicted in respective insets. The distribution of nuclear speckles-associated PI(4)P is not uniform, it rather forms foci inside of nuclear speckles (Figs. 2b,c, insets). Besides, bright foci of PI(4)P are often present at the edges of nuclear speckles (Fig. 2c, insets arrowheads), where the active transcription takes place (Spector and Lamond 2011). Although PI(4)P localizes to nuclear speckles, it does not localize to Cajal bodies, it rather forms foci around them (Fig. 1b, lower inset, arrowheads).

PI(4)P forms discrete foci dispersed throughout the nucleoplasm, which do not colocalize with any nuclear marker tested (Fig. 1). To determine the proportion of PI(4)P in nuclear speckles versus other nuclear regions, we performed high throughput microscopy and quantification of PI(4)P and Son labelled cells (Fig. 1d). We show that only 8 % of PI(4)P resides in nuclear speckles whereas 92 % of PI(4)P localizes outside of nuclear speckles, in other nuclear regions. Therefore, we believe that although PI(4)P is associated with nuclear speckles, its major roles are linked to processes outside of nuclear speckles.

PI(4)P associates with active chromatin.

To examine PI(4)P distribution, we fractionated cells into cytoplasm, soluble nuclear fraction, and chromatin-bound nuclear fraction (Fig. 1e). Following fractionation, an equal volume of each

fraction was spotted on a nitrocellulose membrane and loaded on SDS-PAGE. The purity of fractions was assayed by western blotting with specific cytoplasmic and nuclear markers, GAPDH and H3, respectively. PI(4)P was detected by a specific antibody (Fig. 3c, left). We show that approximately 7.3 ± 1.4 % of nuclear PI(4)P is in the soluble fraction while 92.7 ±1.4 % of PI(4)P is associated with chromatin (Fig. 1e, right).

To further investigate chromatin associated pool of PI(4)P, we performed colocalization with H3K4me2 (Fig. 2a) and H3K9me2 (Fig. 2b) markers of active and inactive chromatin, respectively. The values of Spearmans' coefficients show that PI(4)P partially colocalizes with H3K4me2 but not with H3K9me2 (Fig. 2c). Insets with details of PI(4)P and H3K4me2 signals are provided (Fig. 2a, insets). Graphs display intensities of PI(4)P and H3K4me2 signal along lines depicted in respective insets and overlapping peaks are marked with asterisks (Fig. 2a, right). Based on these results, we conclude that PI(4)P preferentially associates with active chromatin.

LSD1 is a general PIs interactor with the highest affinity for PI(4)P.

Since a pool of PI(4)P colocalizes with H3K4me2 (Figs. 3a,c), we searched for PI(4)P binding partners among proteins that establish, remove or bind H3K4me2. LSD1 is a histone demethylase, which demethylates H3K4me2 and H3K4me1 methylation marks (Shi et al. 2004) and was therefore one of the proteins we tested.

First, we performed pull-down experiments with agarose beads coupled to P(4)P and PI(4,5)P2 from HeLa nuclear extract. This initial experiment shows that LSD1 interacts with PI(4,5)P2 but not with PI(4)P in nuclear extracts (Fig. 3a). To test whether LSD1 interacts with PI(4,5)P2 directly, we incubated purified LSD1 coupled to GST (GST-LSD1) with beads coupled to all PIs, phosphatidylinositol (PI) and empty agarose beads as a control (C; Fig. 3b). The graph shows intensity of each band normalized to the signal from empty agarose beads (Fig. 3c). Surprisingly, purified GST-LSD1 interacts mostly with PI(4)P and binds also to PI(3,4)P2, PI(3,5)P2, PI(4,5)P2 and PI(3,4,5)P3 (Fig. 3b). Moreover, we observed that GST-LSD1 directly binds PI. Because the inositol ring of PI is not phosphorylated, we think that LSD1 probably contains two separate binding sites, one for phosphorylated PIs and another for PI.

These results show that although LSD1 is not pulled-down by PI(4)P from nuclear extract, it is able to bind PI(4)P directly. Since PI(4)P and PI(4,5)P2 are the most abundant PIs species (Viaud et al. 2015), we focused on the role of these PIs in LSD1 function.

LSD1 mutated in R310 and R312 does not bind PI(4)P.

In order to identify LSD1 PIs-binding site, we prepared 3 LSD1 truncations (Fig. 3d, top). The N-terminal truncation (1 - 297; LSD1-A) contains SWI3/RSC8/MOIRA (SWIRM) domain, the central

truncation (297 – 596; LSD1-B) contains N-terminal amino-oxidase domain (AOD), Tower domain and a short part of C-terminal AOD domain, and the C-terminal truncation (596 – 852; LSD1-C) contains the rest of the C-terminal AOD domain. We incubated these truncated forms with PI(4)P-coupled beads and compared the signal to the signal from empty agarose beads. We show that only GST-LSD1-B was enriched in PI(4)P pull-down (Fig. 3d, bottom). Therefore, the PI(4)P binding site is probably located in the central part of LSD1.

LSD1 does not possess any canonical PIs-binding domain or motif. In order to locate PIs-binding site, we used crystal structure of LSD1 (pdb2dw4), which was solved at 2.3 Å resolution (Mimasu et al. 2008). The positions of LSD1 truncated forms within full-length LSD1 are depicted in the model (Fig. 3e, left). LSD1-B is shown in yellow and positively charged amino acids, which could bind to negatively charged PIs, are highlighted in red (Fig. 3e, left). We inspected all positively charged residues within LSD1-B and compared their distances using PyMol software. We identified three arginine residues (R310, R312 and R316) with their side chains close enough (from 4.4 to 10.7 Å) to form a PIs binding pocket (Fig. 3e, inset). These residues are located in the N-terminal part of C-terminal AOD domain.

We prepared four different mutant GST-LSD1-B domains, which have positively charged arginine replaced by negatively charged glutamic acid residues (R310E, R310E, RR310,312EE and R316E). We purified these truncated forms and tested their PI(4)P binding ability in pull-down experiments. All four GST-LSD1-B mutants lost their binding towards PI(4)P (Fig. 3f).

To test whether mutation of the putative binding site affects PI(4)P binding by the whole protein, we prepared wild-type full-length LSD1 (LSD1-WT) and full-length LSD1 bearing RR310,312EE mutation (LSD1-MUT). We overexpressed LSD1-WT and LSD1-MUT fused with Flag-tag (Flag-LSD1-WT and Flag-LSD1-MUT) in HEK293 cells. Subsequently, we immunoprecipitated Flag-LSD1-WT and Flag-LSD1-MUT complexes (Fig. 3g, left) and assayed them for the presence of PI(4)P. We show that after overexpression, Flag-LSD1-WT forms a complex with PI(4)P in HEK293 cells. Moreover, double-mutation of R310 and R312 disturbs the interaction of the full-length LSD1 with PI(4)P (Fig. 3g, right).

PI(4)P and PI(4,5)P2 have opposing effects on LSD1 H3K4me2 demethylase activity.

To test PIs role in LSD1 function, we performed *in vitro* demethylation reaction. We prepared HEK293 cells stably expressing Flag-LSD1 and used this cell line for purification of the Flag-LSD1. The Flag-eluate was analyzed by SDS-PAGE and western blotting with antibodies against Flag-tag and CoREST (Fig. 4a). Interaction with CoREST corepressor is essential for LSD1 function (Amente et al. 2013). We show that CoREST (Fig. 4a, asterisks) is co-purified with Flag-LSD1 (Fig. 4a, arrows).

We preincubated Flag-LSD1 complex with increasing amounts of PI(4)P or PI(4,5)P2. Subsequently, we used these complexes for *in vitro* demethylation reaction with bulk histones (Fig.

4b). The intensity of H3K4me2 bands normalized to H3 signal is shown in the graph as percentage of normalized H3K4me2 signal in the input (Fig. 4b, bottom). The incubation of mock treated Flag-LSD1 results in a decrease of H3K4me2 to cca 80%. Pre-incubation of Flag-LSD1 with PI(4)P abolishes its H3K4me2 demethylase activity completely. However, pre-incubation of Flag-LSD1 with PI(4,5)P2 stimulates LSD1 activity and decreases H3K4me2 signal to cca 60 %. These results show that the activity of LSD1 in a complex with PI(4)P is inhibited. On the other hand, binding of PI(4,5)P2 stimulates LSD1H3K4me2 demethylase activity *in vitro*. Since the PI(4)P and PI(4,5)P2 can be easily interconverted by nuclear kinases or phosphatases, this mechanism could provide a very rapid regulation of LSD1 function and H3K4me2 level within the nucleus.

Discussion

PI(4)P is formed and metabolized in the nucleus (Vann et al. 1997; Clarke et al. 2001) by different nuclear kinases and phosphatases (Lachyankar et al. 2000; Gimm et al. 2000; Déléris et al. 2003; Lindsay et al. 2006; Elong Edimo et al. 2011; Nalaskowski et al. 2012; Ehm et al. 2015). However, its exact nuclear localization and function was unknown. Here, we show that nuclear PI(4)P localizes to nuclear membrane and nuclear speckles but not to Cajal bodies and it forms small foci in nucleoplasm and nucleoli (Fig. 1).

Nuclear speckles are highly dynamic structures enriched in splicing factors. They contain little or no DNA but they are often surrounded by actively transcribed chromatin. Electron microscopy revealed that nuclear speckles are composed of small granules connected by thin fibrils (Spector and Lamond 2011). When we closely examined PI(4)P pool in nuclear speckles, we observed that PI(4)P distribution is not homogenous. PI(4)P indeed forms small foci inside of nuclear speckles (Fig. 1b,c). Remarkably, PI(4)P also forms bright foci at the edges of nuclear speckles (Fig. 1c), where the active transcription takes place (Spector and Lamond 2011). PI(4,5)P2 and also enzymes, which convert PI(4,5)P2 to PI(4)P and *vice versa,* localize to nuclear speckles (Boronenkov et al. 1998; Déléris et al. 2003; Mellman et al. 2008; Schill and Anderson 2009; Elong Edimo et al. 2011). Therefore, it is possible that PI(4)P serve as a precursor and enables rapid formation of PI(4,5)P2 in nuclear speckles. On the other hand, cytoplasmic PI(4)P alone is an important signalling molecule and displays functions that are independent on PI(4,5)P2(Hammond et al. 2009). It is therefore possible that also PI(4)P in nuclear speckles has its unique roles in DNA transcription and pre-mRNA processing.

We show that only about 8 % of nuclear PI(4)P resides in nuclear speckles whereas 92 % localizes to other nuclear compartments (Fig. 1d) and that majority of nuclear PI(4)P is associated with chromatin (Fig. 1e). Small nucleoplasmic foci of PI(4)P partially colocalize with H3K4me2, a mark of active chromatin (Fig. 2a,c). Since PI(4)P localizes to active chromatin and forms foci at the edges

of nuclear speckles (Fig. 1c), where the active transcription takes place (Spector and Lamond 2011), we suggest that PI(4)P might be implicated in regulation or maintenance of active transcription.

Further, we searched for proteins that recognize or regulate H3K4me2 level in cells. We focused on LSD1 histone demethylase that demethylates H3K4me2 and H3K4me1 histone methylation marks (Shi 2004). Although LSD1 binds PI(4,5)P2 but not PI(4)P in nuclear extract (Fig. 3a), it directly interacts with PI(4)P, PI(3,4)P2, PI(3,5)P2, PI(4,5)P2 and PI(3,4,5)P3. Among these PIs, LSD1 displays the highest affinity to PI(4)P (Fig 3b,c). Interestingly, we found that LSD1 forms a complex with PI(4)P after overexpression. Mutation of two positively charged residues in the C-terminal AOD domain (R310 and R312) abolishes LDS1-PI(4)P interaction. Subsequently, we tested whether PI(4)P binding affects LSD1 activity. Using *in vitro* demethylation assay, we show that while LSD1 is in a complex with PI(4)P, its activity is inhibited. On the other hand, preincubation with PI(4,5)P2 stimulates LSD1 activity towards H3K4me2 (Fig. 4e). The mechanism how PIs regulate LSD1 function is currently unclear. However, it has been shown that a single change in phosphorylation of inositol ring can regulate affinity of a PIs-interacting protein to its binding partners (Blind et al. 2012). AOD domain is catalytically active domain and binding of PI(4)P or PI(4,5)P2 could alter its conformation and regulate its affinity for the histone substrate. Another possibility is that PIs regulate LSD1 interaction with other proteins in LSD1 complex. Since LSD1 has neither DNA nor histone binding domain, LSD1 function is highly dependent on its interacting partners (Baron and Vellore 2012). Therefore, a single phosphorylation of PI(4)P or dephosphorylation of PI(4,5)P2 by particular kinases or phosphatases could provide rapid and dynamic regulation of LSD1 function also *in vivo*.

Materials and methods

Cell cultures and transfection

U2OS, HEK293 and HeLa cells were cultured in D-MEM supplemented with 10 % FBS in 5 % CO_2/air, 37 °C and humidified atmosphere. Suspension HeLa cells were cultured in S-MEM supplemented with 5 % FBS in 5 % CO_2/air, 37 °C and humidified atmosphere. Plasmid transfection was performed using Lipofectamine 2000 (Invitrogen) according to manufacturer's protocol. Stable cell lines were established using G-418 (LifeTechnologies; 500 μg/ml).

Constructs

GST-LSD1 construct was prepared by ligation of full-length LSD1 amplified from HeLa cDNA into pET42a+ vector through EcoRI restriction sites (forward 5'-CCGGAATTCCGGATGTTATCTGGGAAGAAGGCGGC-3', reverse 5'-CCGGAATTCCGGTCACATGCTTGGGGACTGCTGTG-3'). GST-LSD1-A, GST-LSD1-B and GST-LD1-C were prepared by amplification from GST-LSD1 construct and inserted into pET42a+ vector trough EcoRI

restriction sites. Flag-LSD1 construct for mammalian expression was prepared by ligation of LSD1 cDNA into pCMV-Tag4B vector through EcoRI and XhoI restriction sites (forward 5'-CCGGAATTCATGTTATCTGGGAA-3', reverse 5'-AACCGCTCGAGCATGCTTGGGGA-3'). Mutated GST-LSD1-B R310E, R313E, RR310,312EE, R316E, and full-length GST-LSD1 RR310,312EE constructs were prepared by site-directed mutagenesis by Q5® Site-Directed Mutagenesis Kit (New England Biolabs, E0552S) according to the manufacturer's instructions.

Antibodies

Following primary antibodies were used: anti-PI(4)P (Echelon, Z-P004; 10 µg/ml for IF, 1 µg/ml for dot blot), anti-Son (Abcam, ab121759; 2 µg/ml for IF, 0.2 µg/ml for WB), anti-Lamin A/C (a kind gift from C.J. Hutchison; diluted 10x), anti-Sm (RayBiotech, MD-16-0062; diluted 400x), anti-H3K4me2 (Millipore, 07-030; 3 µg/ml for IF, 0.5 µg/ml for WB), anti-LSD1 (Abcam, ab17721; 8 µg/ml for IF, 0.8 µg/ml for WB), anti-H3 (Abcam, ab12079; 0.8 µg/ml), anti-Flag (Sigma, F1804; 1 µg/ml). For immunofluorescence, following secondary antibodies were used: goat anti-human IgG conjugated with Alexa Fluor 488, goat anti-rabbit conjugated with Alexa Fluor 488, goat anti-mouse IgG conjugated with DyLight 488, and goat anti-mouse IgM cojugated with Alexa Fluor 555 all purchased from Life Sciences. For western blotting, the following secondary antibodies were used: donkey anti-rabbit IgG IRDye®680RD, donkey anti-rabbit IgG IRDye®800CW, donkey anti-mouse IgG IRDye®680RD, and goat anti-mouse IgM IRDye® 680RD (LI-COR Biosciences).

Expression and purification of recombinant proteins

Recombinant GST-LSD1, GST-LSD1-A, GST-LSD1-B and GST-LD1-C were expressed in *E. coli* strain BL21-Gold(DE3). Bacteria transformed with GST-LSD1, GST-LSD1-A, GST-LSD1-B and GST-LD1-C constructs were grown overnight in 1 l of LB medium. Expression was induced by 0.5 mM IPTG for 48h at 4 ˚C. Cells were lysed in lysis buffer (PBS, 0.5 % Triton X-100, 1 mM DTT) containing EDTA-free protease inhibitor cocktail (cOmplete, Roche) and sonicated. Lysate was centrifuged at 16 000 g for 20 min at 4 ˚C and filtered through 0.22 µm filter. Cleared lysate was loaded on a GST-trap column and the column was washed by 10 volumes of lysis buffer. Bound proteins were eluted (PBS, 1 mM DTT, 10 mM reduced glutathione, pH 8.5).

Flag-LSD1 was stably expressed in HEK293 cell line. Cells were washed twice in PBS and lysed in lysis buffer (50 mM Tris pH 7.4, 150 mM NaCl, 1mM EDTA, 1% TRITON X-100, cOmplete) for 15 min at room temperature (RT) on a shaker. Cells were scraped and centrifuged at 12 000 g for 10 min at 4 ˚C. The supernatant was incubated with 50 µl of pre-equilibrated anti-Flag-M2 agarose beads (Sigma-Aldrich) for 4 h at 4 ˚C. Beads were washed three times in wash buffer (50mM Tris pH 7.4, 150 mM NaCl, 0.1 % NP-40, 10% glycerol) for 15 min at 4 ˚C on an orbital shaker. LSD1-Flag complex was eluted by wash buffer supplemented with 3x FLAG peptide (Sigma-Aldrich; 150 ng/µl) for 30 min at 4 ˚C on an orbital shaker.

Nuclear extract preparation and pull-down assays

Nuclear lysates were prepared from suspension HeLa cells as published previously (Trinkle-Mulcahy et al. 2008). Cells were spun down, washed twice in ice-cold PBS and once in hypotonic buffer (10 mM HEPES, pH 7.9, 1.5 mM $MgCl_2$, 10 mM KCl, 0.5 mM DTT, cOmplete). Cells were resuspended in hypotonic buffer, incubated on ice for 10 min and dounced to release the nuclei. Nuclei were pelleted at 200 g, for 5 min at 4 ˚C. Nuclei were resuspended (0.25 mM sucrose, 10 mM $MgCl_2$, cOmplete), layered over a sucrose buffer (0.88 mM sucrose, 0.5 mM $MgCl_2$, cOmplete) and centrifuged at 2800 g for 10 min at 4 ˚C. Purified nuclei were resuspended in lysis buffer (50 mM Tris, pH 7.5, 150 mM NaCl, 1 % NP-40, cOmplete) and sonicated. Lysate was centrifuged at 16 000 g for 10 min at 4 ˚C. PIs-coupled beads (Echelon) were pre-equilibrated in lysis buffer and blocked for 30 min on ice in lysis buffer supplemented with 1 % bovine serum albumin (BSA; Sigma, A-3059). Cleared lysate was incubated with pre-equilibrated PIs-coupled beads and incubated for 3 h at 4 ˚C on an orbital shaker. Beads were washed five times with lysis buffer and proteins were eluted in Laemmli buffer.

Purified proteins were diluted in binding buffer (10 mM HEPES, pH 7.5, 150 mM NaCl, 0.25% NP-40) and incubated with pre-equilibrated and blocked PIs-coupled beads for 3 h at 4 ˚C on an orbital shaker. Beads were washed five times in binding buffer and proteins were eluted in Laemmli buffer.

Nuclear fractionation and dot blot analysis

Soluble and chromatin-bound fractions were prepared as described previously (Mendez 2000). U2Os and HeLa cells were grown at 6 cm culture dish to 90 % confluence and lysed in 70 µl of lysis buffer (10 mM HEPES, pH 7.9, 10 mM KCl, 1.5 mM $MgCl_2$, 0.34 M sucrose, 10 % glycerol, 1 mM DTT, cOmplete). Triton X-100 was added to final concentration 0.1 % and cells were incubated for 5 min on ice. Nuclei were pelleted at 1300 g for 4 min at 4 ˚C and supernatant was kept as cytoplasmic fraction. Nuclei were washed in lysis buffer and resuspended in chromatin isolation buffer (3 mM EDTA, 0.2 mM EGTA, cOmplete). Insoluble chromatin was pelleted at 1700 g for 4 min at 4 ˚C and the supernatant was kept as soluble nuclear fraction. Chromatin was washed in chromatin isolation buffer, resuspended (50 mM Tris, pH 6.8, 2 % SDS) and sonicated. Cytoplasmic and soluble nuclear fractions were centrifuged at 16 000 g for 10 min at 4 ˚C and cleared supernatants were used in subsequent analysis. For detection of PI(4)P, 10 % of each fraction was spotted on a nitrocellulose membrane, blocked in 1 % BSA in PBS and incubated with anti-PI(4)P antibody. For the protein analysis, 10 % of each fraction was resolved by SDS-PAGE, transferred onto a nitrocellulose membrane, blocked with 3 % BSA and incubated with the antibodies against H3, Lamin A/C, Son and GAPDH. For the visualization, appropriate secondary antibodies conjugated to IRDye were used. Signal was detected by Odyssey Infrared Imaging System (LI-COR Biosciences).

Indirect immunofluorescence and fluorescence microscopy

Cells seeded on glass coverslips were washed with PBS, fixed with 3 % paraformaldehyde in PBS and permeabilized with 0.1 % Triton X-100 in PBS for 20 min. Coverslips were blocked with 5 % normal goat serum (Life Sciences) in PBS for 30 min. For protein detection, coverslips were incubated with primary antibodies diluted in PBS for 1 h at room temperature (RT) and then washed with PBS. After washes, coverslips were incubated with corresponding secondary antibodies diluted in PBS with 0.05% Tween 20 (PBS-T) for 1h at RT, washed with PBS-T and incubated with DAPI in PBS (1 µg/ µl). After final washes in PBS, coverslips were mounted in Vecta shield anti-fade reagent (Vector labs). Images were acquired using confocal microscopes Leica TCS SP8 and high-resolution Leica TCS SP8 STED with 63x (NA 1.4) immersion oil objective and Leica advanced fluorescence software (LAS AF). High-throughput microscopy images were taken by IX81 wide-field microscope with UPLSAPO 40x/0.90 oil objective (Olympus Corporation) and SCAN-R automated image and data analysis software. Images were taken as 1 µm z-stacks with 200 nm z-step.

***In vitro* demethylation assay**

Purified Flag-LSD1 complex (2 µg) was pre-incubated with 0, 100 or 200 µM PI(4)P diC8 (Echelon; P-4008) or PI(4,5)P2 diC8 (Echelon; P-4508) for 30 min at RT. Subsequently, the LSD1-Flag complex was incubated with 4 µg of calf thymus bulk histones (Sigma-Aldrich; H9250) in demethylation buffer (50 mM Tris, pH 8.5, 50 mM KCl, 5 mM $MgCl_2$, 5 % glycerol, 1 mM DTT, cOmplete) in a total volume of 25 µl for 16 h at 37 ˚C. Reaction was terminated by addition of Laemmli buffer and the individual reactions were analyzed for protein content by SDS-PAGE and wetern blotting.

Protein models

The crystal structure of LSD1 (pdb2dw4; Mimasu et al. 2008) was downloaded from PDB database. LSD1 models were made using The PyMol Molecular Graphic System, Schrödinger, LLC.

References

Ahn JY, Liu X, Cheng D, et al (2005) Nucleophosmin/B23, a nuclear PI(3,4,5)P3 receptor, mediates the antiapoptotic actions of NGF by inhibiting CAD. Mol Cell 18:435–445. doi: 10.1016/j.molcel.2005.04.010

Ahn J-Y, Rong R, Liu X, Ye K (2004) PIKE/nuclear PI 3-kinase signaling mediates the antiapoptotic actions of NGF in the nucleus. EMBO J 23:3995–4006. doi: 10.1038/sj.emboj.7600392

Amente S, Lania L, Majello B (2013) The histone LSD1 demethylase in stemness and cancer transcription programs. Biochim Biophys Acta 1829:981–6. doi: 10.1016/j.bbagrm.2013.05.002

Baron R, Vellore NA (2012) LSD1/CoREST is an allosteric nanoscale clamp regulated by H3-histone-tail molecular recognition. Proc Natl Acad Sci 109:12509–12514. doi: 10.1073/pnas.1207892109

Bertagnolo V, Neri LM, Marchisio M, et al (1999) Phosphoinositide 3-Kinase Activity Is Essential for all- trans -Retinoic Acid-induced Granulocytic Differentiation of HL-60 Cells Granulocytic Differentiation of HL-60 Cells. Cancer Res 59:542–546.

Blind RD, Suzawa M, Ingraham HA (2012) Direct modification and activation of a nuclear receptor-

PIP_2 complex by the inositol lipid kinase IPMK. Sci Signal 5:ra44. doi: 10.1126/scisignal.2003111
Boronenkov I V, Loijens JC, Umeda M, Anderson R a (1998) Phosphoinositide signaling pathways in nuclei are associated with nuclear speckles containing pre-mRNA processing factors. Mol Biol Cell 9:3547–3560.
Bua DJ, Martin GM, Binda O, Gozani O (2013) Nuclear phosphatidylinositol-5-phosphate regulates ING2 stability at discrete chromatin targets in response to DNA damage. Sci Rep 3:2137. doi: 10.1038/srep02137
Clarke JH, Letcher a J, D'santos CS, et al (2001) Inositol lipids are regulated during cell cycle progression in the nuclei of murine erythroleukaemia cells. Biochem J 357:905–910. doi: 10.1042/0264-6021:3570905
de Graaf P, Klapisz EE, Schulz TKF, et al (2002) Nuclear localization of phosphatidylinositol 4-kinase beta. J Cell Sci 115:1769–75.
Déléris P, Bacqueville D, Gayral S, et al (2003) SHIP-2 and PTEN are expressed and active in vascular smooth muscle cell nuclei, but only SHIP-2 is associated with nuclear speckles. J Biol Chem 278:38884–91. doi: 10.1074/jbc.M300816200
Ehm P, Nalaskowski MM, Wundenberg T, Jücker M (2015) The tumor suppressor SHIP1 colocalizes in nucleolar cavities with p53 and components of PML nuclear bodies. Nucleus 6:154–164. doi: 10.1080/19491034.2015.1022701
Elong Edimo W, Derua R, Janssens V, et al (2011) Evidence of SHIP2 Ser132 phosphorylation, its nuclear localization and stability. Biochem J 439:391–401. doi: 10.1042/BJ20110173
Gelato KA, Tauber M, Ong MS, et al (2014) Accessibility of different histone H3-binding domains of UHRF1 is allosterically regulated by phosphatidylinositol 5-phosphate. Mol Cell 54:905–19. doi: 10.1016/j.molcel.2014.04.004
Gillooly DJ, Morrow IC, Lindsay M, et al (2000) Localization of phosphatidylinositol 3-phosphate in yeast and mammalian cells. EMBO J 19:4577–4588. doi: 10.1093/emboj/19.17.4577
Gimm O, Perren A, Weng LP, et al (2000) Differential nuclear and cytoplasmic expression of PTEN in normal thyroid tissue, and benign and malignant epithelial thyroid tumors. Am J Pathol 156:1693–700. doi: 10.1016/S0002-9440(10)65040-7
Gozani O, Karuman P, Jones DR, et al (2003) The PHD finger of the chromatin-associated protein ING2 functions as a nuclear phosphoinositide receptor. Cell 114:99–111. doi: 10.1016/S0092-8674(03)00480-X
Hammond GR V., Schiavo G, Irvine RF (2009) Immunocytochemical techniques reveal multiple, distinct cellular pools of PtdIns4P and PtdIns(4,5)P 2. Biochem J 422:23–35. doi: 10.1042/BJ20090428
Jones DR, Bultsma Y, Keune W-J, et al (2006) Nuclear PtdIns5P as a Transducer of Stress Signaling: An In Vivo Role for PIP4Kbeta. Mol Cell 23:685–695. doi: 10.1016/j.molcel.2006.07.014
Kakuk A, Friedländer E, Vereb G, et al (2006) Nucleolar localization of phosphatidylinositol 4-kinase PI4K230 in various mammalian cells. Cytometry A 69:1174–83. doi: 10.1002/cyto.a.20347
Kakuk A, Friedländer E, Vereb G, et al (2008) Nuclear and nucleolar localization signals and their targeting function in phosphatidylinositol 4-kinase PI4K230. Exp Cell Res 314:2376–88. doi: 10.1016/j.yexcr.2008.05.006
Kalasova I, Fáberová V, Kalendová A, et al (2016) Tools for visualization of phosphoinositides in the cell nucleus. Histochem Cell Biol 1–12. doi: 10.1007/s00418-016-1409-8
Lachyankar MB, Sultana N, Schonhoff CM, et al (2000) A Role for Nuclear PTEN in Neuronal Differentiation. J Neurosci 20:1404–1413.
Li W, Laishram RS, Ji Z, et al (2012) Star-PAP control of BIK expression and apoptosis is regulated by nuclear PIPKIα and PKCδ signaling. Mol Cell 45:25–37. doi: 10.1016/j.molcel.2011.11.017
Lindsay Y, McCoull D, Davidson L, et al (2006) Localization of agonist-sensitive PtdIns(3,4,5)P3 reveals a nuclear pool that is insensitive to PTEN expression. J Cell Sci 119:5160–5168. doi: 10.1242/jcs.000133
Mazzotti G, Zini N, Rizzi E, et al (1995) Immunocytochemical detection of phosphatidylinositol 4,5-bisphosphate localization sites within the nucleus. J Histochem Cytochem 43:181–191. doi:

10.1177/43.2.7822774
Mellman DL, Gonzales ML, Song C, et al (2008) A PtdIns4,5P2-regulated nuclear poly(A) polymerase controls expression of select mRNAs. Nature 451:1013–1017. doi: 10.1038/nature06666
Mimasu S, Sengoku T, Fukuzawa S, et al (2008) Crystal structure of histone demethylase LSD1 and tranylcypromine at 2.25 A. Biochem Biophys Res Commun 366:15–22. doi: 10.1016/j.bbrc.2007.11.066
Nalaskowski MM, Metzner A, Brehm MA, et al (2012) The inositol 5-phosphatase SHIP1 is a nucleo-cytoplasmic shuttling protein and enzymatically active in cell nuclei. Cell Signal 24:621–8. doi: 10.1016/j.cellsig.2011.07.012
Okada M, Jang S-W, Ye K (2008) Akt phosphorylation and nuclear phosphoinositide association mediate mRNA export and cell proliferation activities by ALY. Proc Natl Acad Sci U S A 105:8649–8654. doi: 10.1073/pnas.0802533105
Osborne SL, Thomas CL, Gschmeissner S, Schiavo G (2001) Nuclear PtdIns(4,5)P2 assembles in a mitotically regulated particle involved in pre-mRNA splicing. J Cell Sci 114:2501–11.
Rando OJ, Zhao K, Janmey P, Crabtree GR (2002) Phosphatidylinositol-dependent actin filament binding by the SWI/SNF-like BAF chromatin remodeling complex. Proc Natl Acad Sci U S A 99:2824–9. doi: 10.1073/pnas.032662899
Shi Y, Lan F, Matson C, et al (2004) Histone demethylation mediated by the nuclear amine oxidase homolog LSD1. Cell 119:941–53. doi: 10.1016/j.cell.2004.12.012
Schill NJ, Anderson RA (2009) Two novel phosphatidylinositol-4-phosphate 5-kinase type Igamma splice variants expressed in human cells display distinctive cellular targeting. Biochem J 422:473–82. doi: 10.1042/BJ20090638
Sobol M, Yildirim S, Philimonenko V V, et al (2013) UBF complexes with phosphatidylinositol 4,5-bisphosphate in nucleolar organizer regions regardless of ongoing RNA polymerase I activity. Nucleus 4:478–86. doi: 10.4161/nucl.27154
Spector DL, Lamond AI (2011) Nuclear speckles. Cold Spring Harb Perspect Biol 3:a000646–. doi: 10.1101/cshperspect.a000646
Stijf-Bultsma Y, Sommer L, Fischle W, et al (2015) The Basal Transcription Complex Component TAF3 Transduces Changes in Nuclear Phosphoinositides into Transcriptional Output Article The Basal Transcription Complex Component TAF3 Transduces Changes in Nuclear Phosphoinositides into Transcriptional Output. Mol Cell 58:1–15. doi: 10.1016/j.molcel.2015.03.009
Strahl T, Hama H, DeWald DB, Thorner J (2005) Yeast phosphatidylinositol 4-kinase, Pik1, has essential roles at the Golgi and in the nucleus. J Cell Biol 171:967–979. doi: 10.1083/jcb.200504104
Szivak I, Lamb N, Heilmeyer LMG (2006) Subcellular localization and structural function of endogenous phosphorylated phosphatidylinositol 4-kinase (PI4K92). J Biol Chem 281:16740–16749. doi: 10.1074/jbc.M511645200
Tanaka K, Horiguchi K, Yoshida T, et al (1999) Evidence That a Phosphatidylinositol 3,4,5-Trisphosphate-binding Protein Can Function in Nucleus. J Biol Chem 274 :3919–3922. doi: 10.1074/jbc.274.7.3919
Toska E, Campbell HA, Shandilya J, et al (2012) Repression of Transcription by WT1-BASP1 Requires the Myristoylation of BASP1 and the PIP2-Dependent Recruitment of Histone Deacetylase. Cell Rep 2:462–469. doi: 10.1016/j.celrep.2012.08.005
Trinkle-Mulcahy L, Boulon S, Lam YW, et al (2008) Identifying specific protein interaction partners using quantitative mass spectrometry and bead proteomes. J Cell Biol 183:223–39. doi: 10.1083/jcb.200805092
Vann LR, Wooding FB, Irvine RF, Divecha N (1997) Metabolism and possible compartmentalization of inositol lipids in isolated rat-liver nuclei. Biochem J 327(2):569–576. doi: 10.1042/bj3270569
Viaud J, Mansour R, Antkowiak A, et al (2015) Phosphoinositides: Important lipids in the coordination of cell dynamics. Biochimie. doi: 10.1016/j.biochi.2015.09.005
Watt S a, Kular G, Fleming IN, et al (2002) Subcellular localization of phosphatidylinositol 4,5-bisphosphate using the pleckstrin homology domain of phospholipase C delta1. Biochem J

363:657–666. doi: 10.1074/jbc.M301418200
Wickramasinghe V, Savill J, Chavali S, et al (2013) Human Inositol Polyphosphate Multikinase Regulates Transcript-Selective Nuclear mRNA Export to Preserve Genome Integrity. Mol Cell 51:737–750. doi: 10.1016/j.molcel.2013.08.031
Yildirim S, Castano E, Sobol M, et al (2013) Involvement of phosphatidylinositol 4,5-bisphosphate in RNA polymerase I transcription. J Cell Sci 126:2730–9. doi: 10.1242/jcs.123661
Zou J, Marjanovic J, Kisseleva M V, et al (2007) Type I phosphatidylinositol-4,5-bisphosphate 4-phosphatase regulates stress-induced apoptosis. Proc Natl Acad Sci U S A 104:16834–16839. doi: 10.1073/pnas.0708189104

Acknowledgements

P. H., I. K., A.K., V. F., L. U., T.V., and P.M. were supported by the Grant agency of the Czech Republic (15-08738S, P305/11/2232, 16-03403S), P. H., L. U. were supported by Human Frontier Science Program (RGP0017/2013), I. K., A. K. and L. U. were supported by the Grant Agency of the Charles University (606112) and by the Charles University in Prague. This publication is supported by the project "BIOCEV – Biotechnology and Biomedicine Centre of the Academy of Sciences and Charles University" (CZ.1.05/1.1.00/02.0109), from the European Regional Development Fund. This research was performed with support of the Institute of Molecular Genetics, Academy of Sciences of the Czech Republic (RVO: 68378050). We would like to thank C.J. Hutchison for lamin A/C antibody, Iva Jelínková and Pavel Kříž for excellent technical assistance, Lenka Jarolímová for proofreading of the manuscript and Margarita Sobol for her advices.

Figure legends

Fig. 1. PI(4)P localizes to nuclear membrane, nuclear speckles and small nucleoplasmic foci and is associated with chromatin. STED super-resolution microscopy shows that PI(4)P is present in the nuclear membrane (a). Sites of PI(4)P colocalization with lamin a/c are incicated (insets, arrowheads). PI(4)P colocalizes with Sm in nuclear speckles (b, upper inset) but not in the Cajal bodies. Arrowheads indicate foci of PI(4)P around Cajal bodies (b, lower inset). Intensity plot shows localization of PI(4)P and Sm along the line drawn in the inset (b). PI(4)P colocalizes with Son in nuclear speckles (c, insets) and forms foci at the edges of nuclear speckles (arrowheads). Intensity plots show localization of PI(4)P and Son along the line drawn in insets (c). The distribution of PI(4)P in nuclear speckles (8.3 ± 1.5 %) and other nuclear regions (91.7 ± 1.5 %). Values are results of PI(4)P and Son signal analysis in 614 cells (d) Proportion of PI(4)P in soluble (7.3 ± 1.4 %) and chromatin-bound (92.7 ±1.4) fractions. Graph represents results of 4 experiments (e). Scale bar is 5 μm.

Fig. 2. Small nucleoplasmic foci of PI(4)P colocalize with active chromatin. STED super-resolution microscopy analysis of PI(4)P colocalization with H3K4me2, a mark of active chromatin (a). Details of PI(4)P and H3K4me2 colocalization are shown (insets), intensity graphs show PI(4)P and H3K4me2 signals along lines drawn in respective insets. Sites of intensity peak overlaps are

highlighted (asterisks). Colocalization of PI(4)P with H3K9me2, a mark of an inactive chromatin (b). Values of Spearman's coefficient show that PI(4)P colocalizes with H3K4me2 but not with H3K9me2 (c). Scale bar is 5 μm.

Fig. 3. LSD1 interacts with PI(4)P and other PIs. Pull-down with PI(4)P and PI(4,5)P2 beads show that LSD1 binds to PI(4,5)P2 but not to PI(4)P in HeLa nuclear extract (a). Purified GST-LSD1 binds specifically to beads coupled with PI, PI(4)P, PI(3,4)P2, PI(3,5)P2, PI(4,5)P2, and PI(3,4,5)P3 and displays the highest affinity to PI(4)P (b). Quantification GST-LSD1 bands intensities. Intensities are normalized to the signal form pull-down by control agarose beads. The level of signal in control pull-down is indicated by red line (c). A scheme of LSD1 full-length protein and its protein domain composition. LSD1 truncations (LSD1-A, LSD1-B. LSD1-C) are depicted. These truncated proteins were used for pull-down experiments with PI(4)P coupled beads and empty agarose beads as a control. LSD1-B is enriched in PI(4)P pulled-down fraction (d). The crystal structure of LSD1 downloaded from PDB database (pdb2dw4) and visualized by PyMol software (e) Position of LSD1 truncations are color-coded (left). LSD1-B is shown in yellow, all basic residues in LSD1-B are highlighted in red (right). Probable PIs-binding site formed by R310, R312 and R316 (inset). Pull-down of LSD1-B mutants by PI(4)P coupled beads (f). Pull-down of full-length LSD1 (Flag-LSD1-WT) and LSD1 RR310,312EE mutant (Flag-LSD1-MUT) (g). HEK293 cells were transfected by Flag-tag conjugated WT and MUT LSD1 and an empty vector as a control. LSD1 complexes were immunoprecipitated with anti-Flag antibody. Purified complexes were loaded on SDS-PAGE and assayed by anti-Flag antibody (left) and spotted on a nitrocellulose membrane. PI(4)P was detected by anti-PI(4)P antibody (right). PI(4)P associates with Flag-LSD1-WT but not with Flag-LSD1-MUT or empty vector. IN – input, C – control, SWIRM - SWI3/RSC8/MOIRA domain, AOD – amino-oxidase domain.

Fig. 4. PI(4)P inhibits and PI(4,5)P2 stimulates LSD1 activity. Flag-LSD1 was stably oveexpressed in HEK293 cells, purified and assayed on 10 % SDS-PAGE (a). Commasie stained Flag-eluate (left) and western blot analysis (right) show Flag-LSD1 (arrows) and CoREST (asterisks) in Flag-elution. Results of *in vitro* demethylation reaction (b, top) and graph representing quantification of H3K4me2 signal normalized to H3 signal and shown as percent of normalized input H3K4me2 signal (b, bottom). LSD1 was preincubated with indicated amount of PI(4)P di8 or PI(4,5)P2 di8. Incubation of bulk histones with Flag-LSD1 results in the decrease of H3K4me2 signal to 80 % of input signal. Preincubation with PI(4)P inhibits Flag-LSD1 activity. Preincubation with PI(4,5)P2 results in decrease of H3K4me2 to 60 %. IN – input, C – control, M-marker.

Figure 1

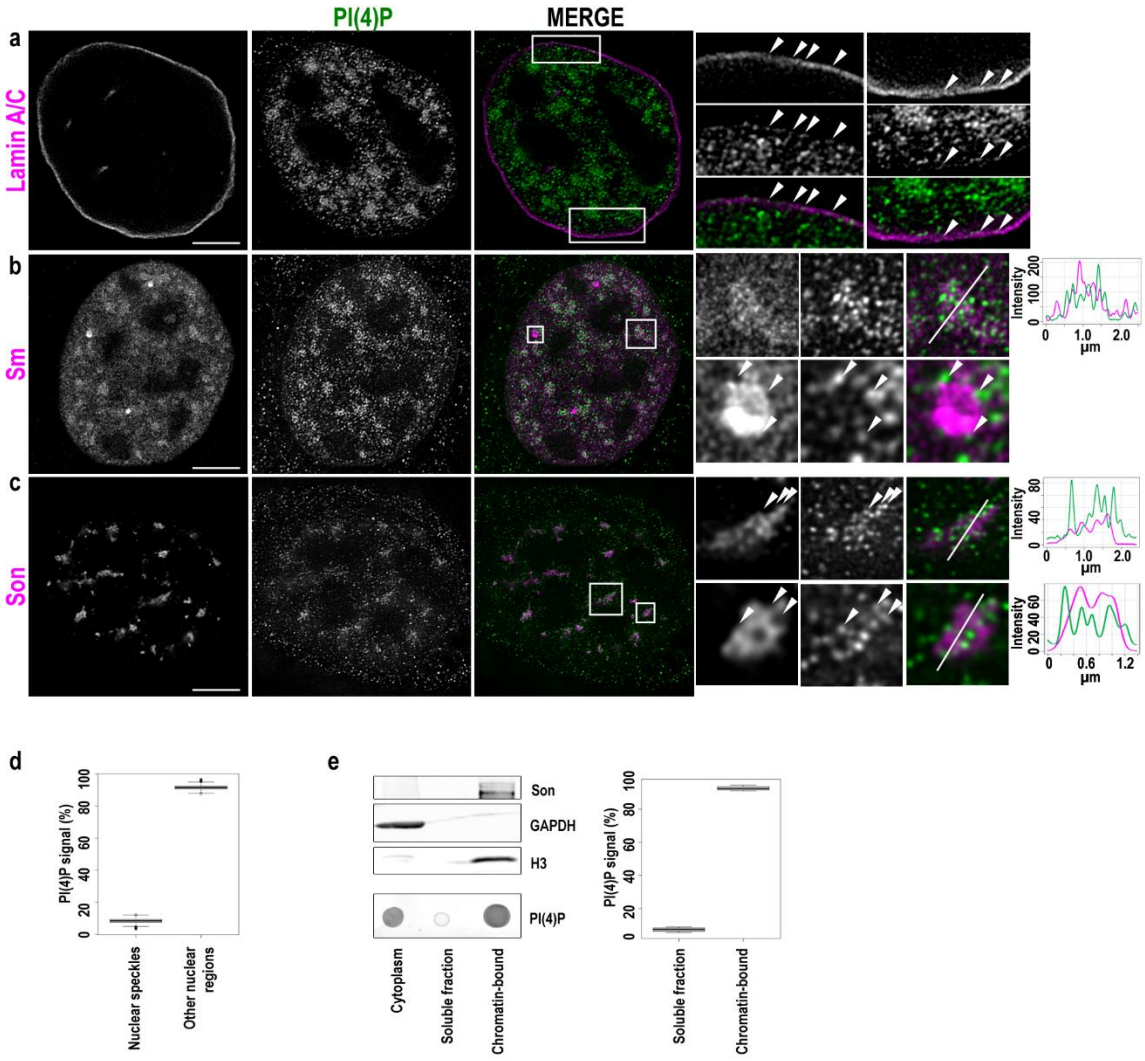
PI(4)P
MERGE
a
Lamin A/C
b
Sm
c
Son
Intensity
μm
d
PI(4)P signal (%)
Nuclear speckles
Other nuclear regions
e
Son
GAPDH
H3
PI(4)P
Cytoplasm
Soluble fraction
Chromatin-bound

Figure 2

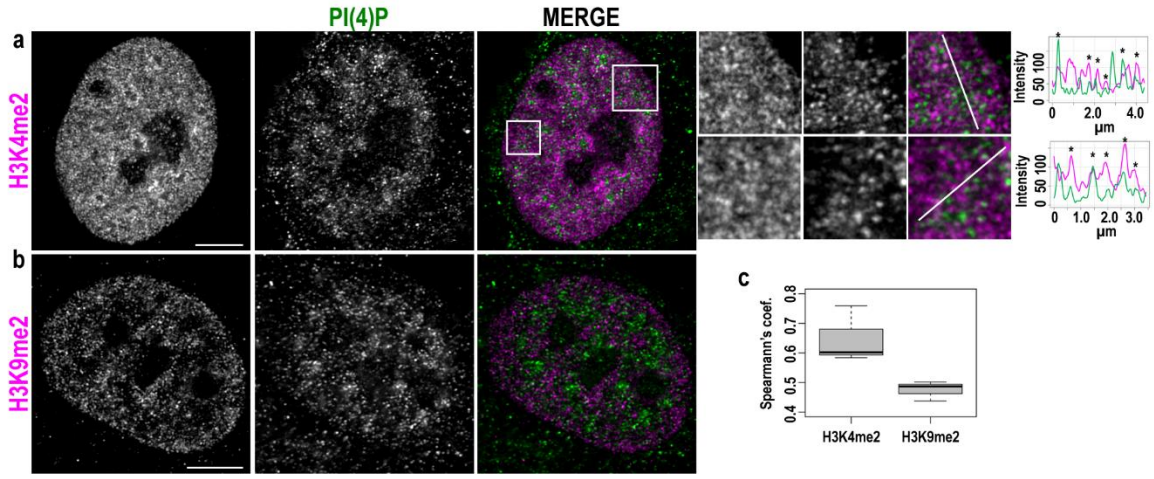
PI(4)P
MERGE
a
H3K4me2
b
H3K9me2
Intensity
0 50 100
0 2.0 4.0
µm
Intensity
0 50 100
0 1.0 2.0 3.0
µm
c
Spearmann's coef.
0.4 0.5 0.6 0.7 0.8
H3K4me2
H3K9me2

Figure 3

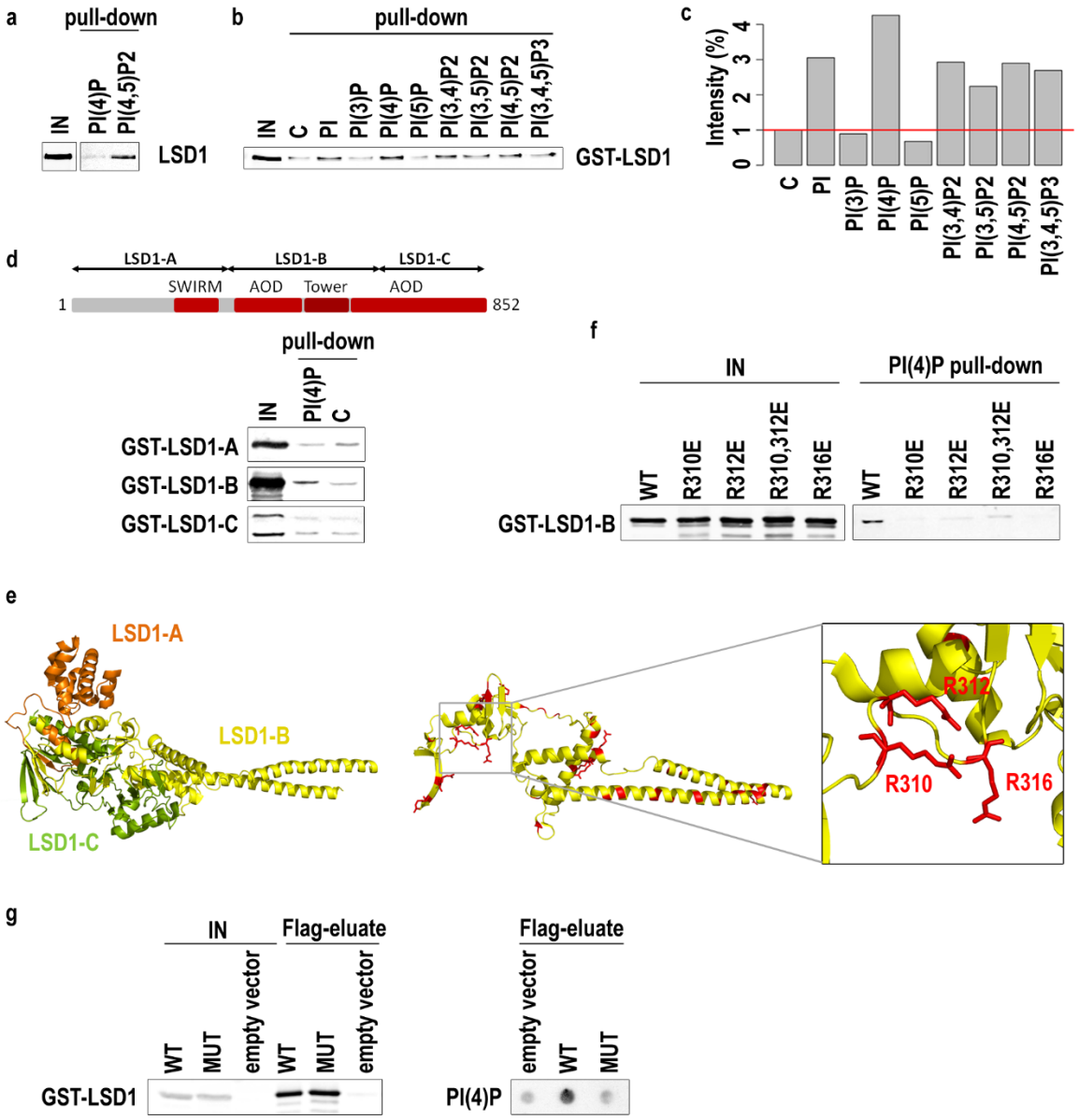
a
pull-down
IN
PI(4)P
PI(4,5)P2
LSD1
b
pull-down
IN
C
PI
PI(3)P
PI(4)P
PI(5)P
PI(3,4)P2
PI(3,5)P2
PI(4,5)P2
PI(3,4,5)P3
GST-LSD1
c
Intensity (%)
0 1 2 3 4
C
PI
PI(3)P
PI(4)P
PI(5)P
PI(3,4)P2
PI(3,5)P2
PI(4,5)P2
PI(3,4,5)P3
d
LSD1-A
LSD1-B
LSD1-C
SWIRM
AOD
Tower
AOD
1
852
pull-down
IN
PI(4)P
C
GST-LSD1-A
GST-LSD1-B
GST-LSD1-C
f
IN
PI(4)P pull-down
WT
R310E
R312E
R310,312E
R316E
GST-LSD1-B
e
LSD1-A
LSD1-B
LSD1-C
R312
R310
R316
g
IN
Flag-eluate
Flag-eluate
WT
MUT
empty vector
WT
MUT
empty vector
empty vector
WT
MUT
GST-LSD1
PI(4)P

Figure 4

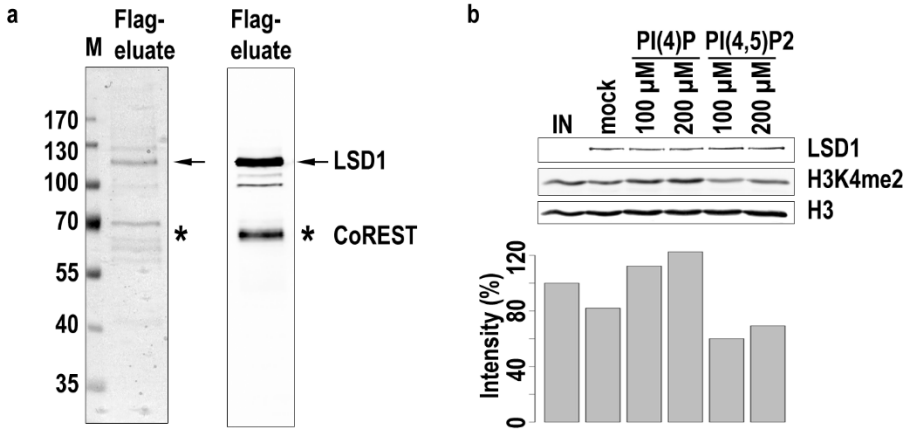
a
M
Flag-eluate
Flag-eluate
170
130
100
70
55
40
35
*
LSD1
* CoREST
b
IN
mock
PI(4)P
100 µM
200 µM
PI(4,5)P2
100 µM
200 µM
LSD1
H3K4me2
H3
Intensity (%)
0
40
80
120

3.4 Nuclear actin filaments recruit cofilin and Arp3 and their formation is connected with a mitotic block

Kalendová A, Kalasová I, Yamazaki S, Uličná L, Harata M and Hozák P

Histochem Cell Biol. 2014 Aug;142(2):139-52. doi: 10.1007/s00418-014-1243-9.

IF: 3.054 (2014)

I. K. performed experiments (fluorescence microscopy)

Histochem Cell Biol (2014) 142:139–152
DOI 10.1007/s00418-014-1243-9

ORIGINAL PAPER

Nuclear actin filaments recruit cofilin and actin-related protein 3, and their formation is connected with a mitotic block

Alžběta Kalendová · Ilona Kalasová · Shota Yamazaki · Lívia Uličná · Masahiko Harata · Pavel Hozák

Accepted: 25 June 2014 / Published online: 8 July 2014

Abstract Although actin monomers polymerize into filaments in the cytoplasm, the form of actin in the nucleus remains elusive. We searched for the form and function of β-actin fused to nuclear localization signal and to enhanced yellow fluorescent protein (EN-actin). Our results reveal that EN-actin is either dispersed in the nucleoplasm (homogenous EN-actin) or forms bundled filaments in the nucleus (EN-actin filaments). Formation of such filaments was not connected with increased EN-actin levels. Among numerous actin-binding proteins tested, only cofilin is recruited to the EN-actin filaments. Overexpression of EN-actin causes increase in the nuclear levels of actin-related protein 3 (Arp3). Although Arp3, a member of actin nucleation complex Arp2/3, is responsible for EN-actin filament nucleation and bundling, the way cofilin affects nuclear EN-actin filaments dynamics is not clear. While cells with homogenous EN-actin maintained unaffected mitosis during which EN-actin re-localizes to the plasma membrane, generation of nuclear EN-actin filaments severely decreases cell proliferation and interferes with mitotic progress. The introduction of EN-actin manifests in two mitotic-inborn defects—formation of binucleic cells and generation of micronuclei—suggesting that cells suffer aberrant cytokinesis and/or impaired chromosomal segregation. In interphase, nuclear EN-actin filaments passed through chromatin region, but do not co-localize with either chromatin remodeling complexes or RNA polymerases I and II. Surprisingly presence of EN-actin filaments was connected with increase in the overall transcription levels in the S-phase by yet unknown mechanism. Taken together, EN-actin can form filaments in the nucleus which affect important cellular processes such as transcription and mitosis.

Keywords Nuclear actin · Transcription · Mitosis · Actin-related protein 3 · Cofilin

A. Kalendová · I. Kalasová · L. Uličná · P. Hozák (✉)
Department of Biology of the Cell Nucleus, Institute of Molecular Genetics of the Academy of Sciences of the Czech Republic, v.v.i., Vídeňská 1083, 142 20 Prague, Czech Republic
e-mail: hozak@img.cas.cz

S. Yamazaki · M. Harata
Laboratory of Molecular Biology, Graduate School of Agricultural Science, Tohoku University, Tsutsumidori-Amamiyamachi 1-1, Aoba-ku, Sendai 981-8555, Japan

Introduction

Actin is a highly abundant intracellular protein essential for maintenance of many cellular functions. It is widely expressed across the species and present in all eukaryotic cell types. In the cytoplasm, actin is present in the form of monomers (globular actin, G-actin), which can polymerize to form filaments (F-actin) that can be specifically visualized by phalloidin. The formation of F-actin is driven by the availability of G-actin subunits—a filament grows when G-actin levels exceed the critical concentration required for polymerization, and a filament shrinks if the critical concentration was not reached. Actin filaments are highly dynamic structures that can assemble or disassemble rapidly based on cell needs.

There are many actin-binding proteins available in the cytoplasm. Depending on their relative binding affinities, they can promote, block or alter the formation of actin filaments. In addition, various actin-binding proteins cross-link actin filaments to form bundles or networks (reviewed in Winder and Ayscough 2005). Such structures are important for the maintenance of cell shape, polarity, mechanical resistance, adhesion and movement.

Actin shuttles between cytoplasm and nucleus employing importin 9 and exportin 6 (Dopie et al. 2012). In the nucleus, actin is present in the form of monomers (Jockusch et al. 2006; Kukalev et al. 2005; McDonald et al. 2006; Obrdlik et al. 2008; Pendleton et al. 2003), yet its ability to form nuclear filaments has been questioned for a long time due to the lack of nuclear phalloidin staining. Eventually, several conditions leading to the formation of nuclear actin polymers have been described. Under various stress conditions (e.g., heat shock, DMSO treatment, virus infection etc.), nuclear actin rods and paracrystals were observed in numerous cell types (reviewed in Hofmann 2009). Moreover, a recent study revealed the presence of actin filaments in nuclei of NIH3T3 cells after overexpression of LifeAct, an F-actin marker, fused to nuclear localization signal (NLS). These filaments were formed after serum induction in a formin-dependent manner (Baarlink et al. 2013). Accumulation and subsequent polymerization of the overexpressed actin in the nucleus was also reported after the disruption of the actin export (Dopie et al. 2012; Stuven et al. 2003). Additionally, Miyamoto et al. (2011) detected actin filaments in nuclei of somatic cells transplanted into oocytes of *Xenopus leavis* using an actin-binding domain of utrophin fused to NLS. Interestingly, the same probe revealed the presence of punctate structures in the nuclei of U2OS cells under physiological conditions which were moreover susceptible to phalloidin staining (Belin et al. 2013). Even though these polymeric structures do not co-localize with any actin-binding proteins, they are found predominantly in the interchromatin space and probably serve as a structural platform that facilitates nuclear organization (Belin et al. 2013).

Even though the state of nuclear actin is not entirely clear, its functional importance has been known for some time. Actin is together with the actin-related proteins required for chromatin remodeling (Ikura et al. 2000; Kapoor et al. 2013; Mizuguchi et al. 2004; Shen et al. 2000; Szerlong et al. 2008; Zhao et al. 1998). Actin also associates with all three RNA polymerases (Hofmann et al. 2004; Hu et al. 2004; Philimonenko et al. 2004) and in cooperation with nuclear myosin 1 (NM1) facilitates transcription initiation and recruitment of chromatin modifying complexes during the elongation phase (reviewed in de Lanerolle and Serebryannyy 2011). Furthermore, actin also participates in RNA processing and export by interacting with heterogenous ribonucleoproteins (hnRNPs; Obrdlik et al. 2008; Percipalle et al. 2002).

From the data available, it seems that the state of nuclear actin engaged in chromatin remodeling complexes and in complex with hnRNPs (Kapoor et al. 2013; Obrdlik et al. 2008; Percipalle et al. 2002) is rather monomeric, whereas in transcription both forms seem to be involved (Miyamoto et al. 2011; Obrdlik and Percipalle 2011; Qi et al. 2011; Wu et al. 2006; Ye et al. 2008; Yoo et al. 2007). Similarly, actin in its polymeric form is essential for the movement of genomic loci throughout the nucleus during transcriptional activation (Dundr et al. 2007; Hu et al. 2008). The presence of polymeric actin in the nucleus is also supported by the findings that various proteins known to bind F-actin in the cytoplasm also localize to the nucleus (reviewed in Castano et al. 2010)) and are implicated in nuclear processes such as transcription (Baarlink et al. 2013; Miyamoto et al. 2011; Obrdlik and Percipalle 2011; Wu et al. 2006; Yoo et al. 2007).

Kokai et al. (2014) have previously reported that ectopically expressed β-actin fused to NLS is imported into the nucleus, where it forms filamentous network. Detailed analysis of the network revealed that distinct actin filaments are branched and cross-linked into parallel bundles. The formation of such structures alters the shape of neuronal-like rat PC12 cells and activates serum response factor (SRF)-mediated transcription. In this study, we employed a similar fusion protein, β-actin fused to enhanced yellow fluorescent protein (EYFP) and to NLS (EN-actin), aiming to explore (1) the formation of EN-actin filaments in the nucleus, (2) contribution of actin-binding proteins to the EN-actin filaments formation and dynamics, (3) association of nuclear EN-actin filaments with complexes where endogenous actin is known to localize, and (4) an effect of the nuclear EN-actin filaments formation on cell cycle and transcription in human osteosarcoma cells (U2OS).

Materials and methods

Cells and transfections

U2OS, H1299, HEK293 and human skin fibroblasts were cultured in D-MEM supplemented with 10 % FBS in 5 % CO2/air, 37 °C and humidified atmosphere. Cells were transfected with Lipofectamine 2000 (Life Technologies) and TurboFect (Thermo Scientific) according to manufacturer's protocol. 2 μg of DNA and 5 μl of Lipofectamine or 3 μl of TurboFect was used to transfect 5×10^5 cells. Cells were incubated for 6 to 12 h with a transfection mix and additional 36 h before fixation and imaging. Linear polyethylenimine (PEI), 25 kDa, was purchased from Polysciences. 1 mg/ml stock solution was prepared and pH adjusted to 7. 9 μl of this solution was mixed with 1.5 μg DNA in serum-free media and incubated for 15 min at room temperature. 5×10^5 cells were incubated with transfection mix for 4 h and then grown for 48 h before imaging.

5 μg of exogenous DNA was delivered into 5×10^5 primary mouse skin fibroblasts by nucleofection using Amaxa nucleofector (Lonza), programme C005. Cells were seeded onto coverslips and imaged 48 h after nucleofection.

Constructs used in this study

EN-actin was generated as described previously (Hofmann et al. 2009). Shortly, NLS was inserted between the EYFP and actin into the plasmid pEYFP-actin (Clontech). cDNA of mouse NM1 was cloned into pCDNA3.1-mCherry using NheI and HindIII by standard methods of molecular biology.

Indirect immunofluorescence and confocal fluorescence microscopy

U2OS cells seeded on glass coverslips were fixed with 4 % paraformaldehyde in PBS for 20 min and permeabilized with 0.1 % Triton X-100 in PBS for 10 min afterward. Non-specific labeling was further blocked with 5 % BSA in PBS for 30 min. After washes with PBS, coverslips were incubated with the respective primary antibodies diluted in PBS for 1 h at RT in a wet chamber and washed with PBST (PBS supplemented with 0.05 % Tween 20). Subsequently, coverslips were incubated with corresponding secondary antibodies for 1 h at RT in a wet chamber. After final washes in PBST, coverslips were mounted in ProLong Gold anti-fade reagent with DAPI. For detection of emerin, cells were fixed with ice-cold methanol for 5 min without additional permeabilization. Images were acquired using confocal microscope Leica TCS SP5 AOBS TANDEM with 63× (NA 1.4) immersion oil objective lens with 405, 512, 561 and 631 laser excitations, and LAS AF software.

Antibodies

Following primary antibodies were used in this study: lamin B (Santa Cruz cat. no. sc-6217); filamin (Santa Cruz cat. no. sc-28284); alpha-actinin-4 (Abcam cat. no. ab96866); spectrin (Sigma Aldrich cat. no. S1390); paxillin (Millipore cat. no. 05-471); vinculin (Sigma Aldrich cat. no. V4505); mDia1 (BD Biosciences cat. no. P66520-050); SUN2 (Abcam cat. no. ab124916); emerin (Abcam cat. no. ab40688); Arp3 (Welch et al. 1997); cofilin (Abcam cat. no. ab11062); P-cofilin (Cell Signaling cat. no. 3313); Arp6 (Sigma Aldrich cat. no. R35554); Arp5 (Kitayama et al. 2009); Arp8 (Aoyama et al. 2008); Brg1 (Abcam cat. no. ab70558); hnRNP U (Santa Cruz, clone 3G6); H3K9Me2 (Millipore cat. no. 17-648); H3K4Me2 (Millipore cat. no. 07-030); CTD-phosphoS2 (Abcam cat. no. ab24758); RPA194 (Santa Cruz, cat. no. sc-28714); and BrdU (Sigma Aldrich, clone BU-33).

Secondary antibodies used in this study are donkey anti-rabbit IgG conjugated with Alexa Fluor 568 (A10042), goat anti-mouse IgG conjugated with Alexa Fluor 647 (A21236) and donkey anti-goat IgG cojugated with Alexa Fluor 647 (A21447) all purchased from Life Sciences.

5-Fluorouridine, 5-ethynyl-2′-deoxyuridine incorporation and EN-actin fluorescence measurements

U2OS cells grown on coverslips were transfected with EN-actin using Lipofectamine as described above. 48 h after the transfection, cells were incubated for 30 min or 1 h at 37 °C, 5 % CO_2/air with 2 mM 5-fluorouridine (FU) or 5-ethynyl-2′-deoxyuridine (EdU), respectively. After this time period, cells were washed, fixed and permeabilized as mentioned above. FU incorporated into nascent transcripts was detected using anti-BrdU antibody as described above. EdU was directly labeled in a click reaction using ClickiT EdU Alexa Fluor 647 Flow Cytometry Assay kit (Life Technologies). Images were acquired as four 200-nm optical stacks of a total thickness of 2 μm using the above mentioned fluorescence confocal microscope. Total intensity of FU/EdU fluorescence in the nucleus was integrated from 3D reconstruction (maximal projection) of all four optical stacks in LAS AF, background subtracted and normalized to the nuclear area. The measurement was repeated three times, and fluorescence intensities of the cells expressing EN-actin were in each replicate normalized to the controls to prevent variations caused by antibodies dilutions, etc. Results are presented as a mean of three experiments ± standard deviation (SD) and were plotted using Prism GraphPad. *T* test was used to determine the statistical significance. Each cell imaged was manually classified according to the EN-actin expression pattern as G-actin (homogenous signal), F-actin (nuclear filaments) or control (no expression of EN-actin). Fluorescence of EN-actin was quantified in the same way.

Results

EN-actin forms filaments in the nucleus

We studied the behavior of exogenous β-actin in the nucleus. In order to achieve its nuclear localization, we fused β-actin with NLS and EYFP (EN-actin). It has been observed previously that the overexpression of NLS-β-actin leads to the formation of filamentous structures inside of the nucleus in various cell lines (Kokai et al. 2014). When we overexpressed EN-actin in human osteosarcoma cell line (U2OS), majority of cells (95 to 99 %) exhibited homogenously dispersed nuclear signal, apparently corresponding to the free G-actin or short actin polymers (Fig. 1a). However, in 1–5 % of cells, EN-actin assembled into filamentous structures which stretched through the whole nuclear volume with the exception of nucleoli (Fig. 1b, c). The EN-actin filaments adopt various shapes from straight long (Fig. 8h) to curved (Fig. 1b), or they form a dense meshwork (Fig. 1c). These nuclear actin filaments are phalloidin-positive structures (Fig. 2a) which in some cases run at the nuclear periphery

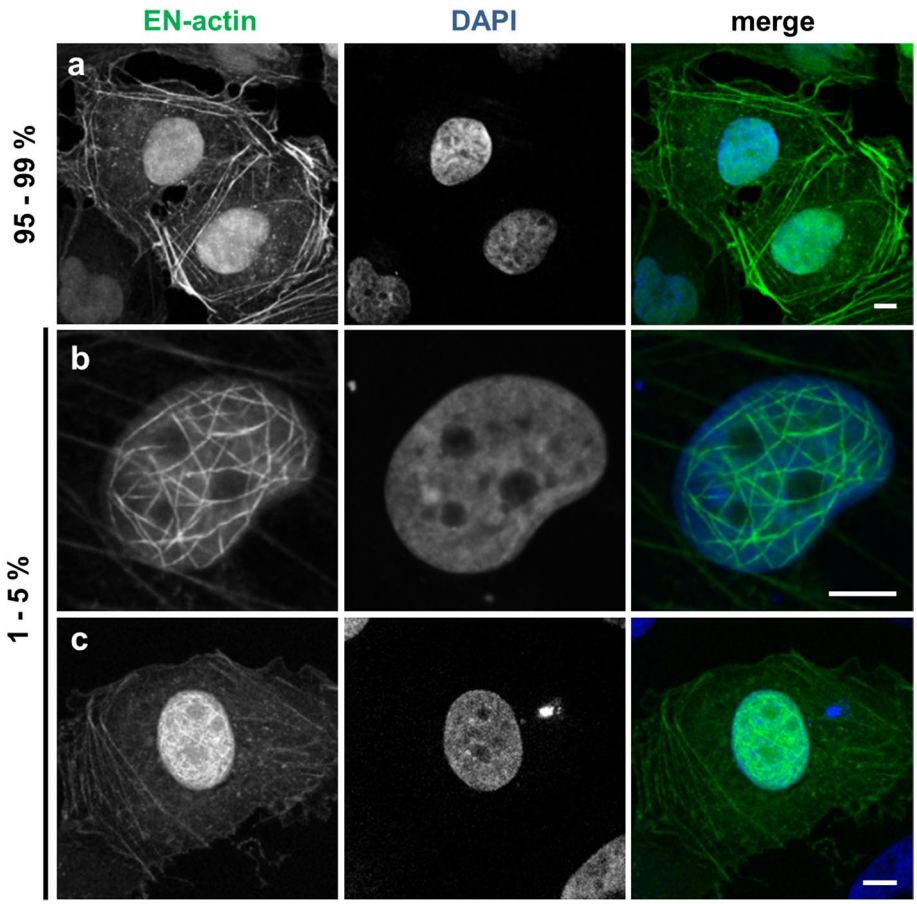

Fig. 1 Overexpressed EN-actin forms filaments in the nucleus of U2OS cells. In vast majority of cells (95–99 %), EN-actin was imported into the nucleus, where it was homogenously dispersed throughout the nucleoplasm (**a**). Minority of cells (1–5 %) displayed EN-actin assembled into thick nuclear filaments (**b**). At the same time, EN-actin was also incorporated into cytoplasmic filaments (**a**, **c**). Single focal plane in the equatorial position (**b**) and 3D reconstructions of the entire cells (**a**, **c**) are shown. *Scale bars* 5 μm

along the nuclear lamina (Fig. 2b, white arrows), occasionally even reaching the nuclear lamina (Fig. 2c, d). The thickness of and the length of the filaments range from 50 to 100 nm and 1 to 15 μm, respectively, which corresponds to actin bundles rather than single filaments, as has been concluded previously (Kokai et al. 2014).

In parallel to its nuclear localization, EN-actin was also incorporated into canonical cytoplasmic filaments in both cells with homogenous nuclear pattern (Fig. 1a), as well as in the cells that contained nuclear EN-actin filaments (Fig. 1c). This suggests that the presence of cytoplasmic EN-actin filaments does not restrict nuclear EN-actin filaments formation, and vice versa.

Since nuclear EN-actin filaments are present only in a small fraction of cells, this raises the question which stimulus triggers their formation. One could predict that when the critical concentration of actin monomers inside a compartment is reached, the polymerization process starts. To find out whether there is a difference in the amount of EN-actin in the nucleus between the cells forming filaments and those having homogenous dispersion of EN-actin, we measured the total fluorescence intensity of EN-actin in the nuclei of those cells. Because there is a variability in size of the nuclei among the cells, we normalized total fluorescence intensity to the nuclear area after background subtraction. We found that there is no significant difference in normalized fluorescence intensity between nuclei with homogenously dispersed EN-actin (G-actin) and filaments-forming nuclei (F-actin; Fig. 2e).

In addition, we tested the impact of transfection method on the filament formation. For this purpose, we used Lipofectamine 2000 (Life Technologies), TurboFect (Thermo Scientific) and linear polyethylenimine (Polysciences) according to the manufacturers' protocols (see Materials and methods). Even though the efficiencies of the transfections varied, the percentage of transfected cells containing nuclear actin filaments did not change significantly (data not shown).

Taken together, after overexpression of EN-actin, 1–5 % of cells contain nuclear EN-actin filaments assembled into bundles. Formation of these filaments is dependent neither on the intranuclear concentration of EN-actin nor on the transfection method.

Formation of nuclear EN-actin filaments varies among cell types

We analyzed the formation of nuclear EN-actin filaments in various cell types. The pattern of overexpressed EN-actin

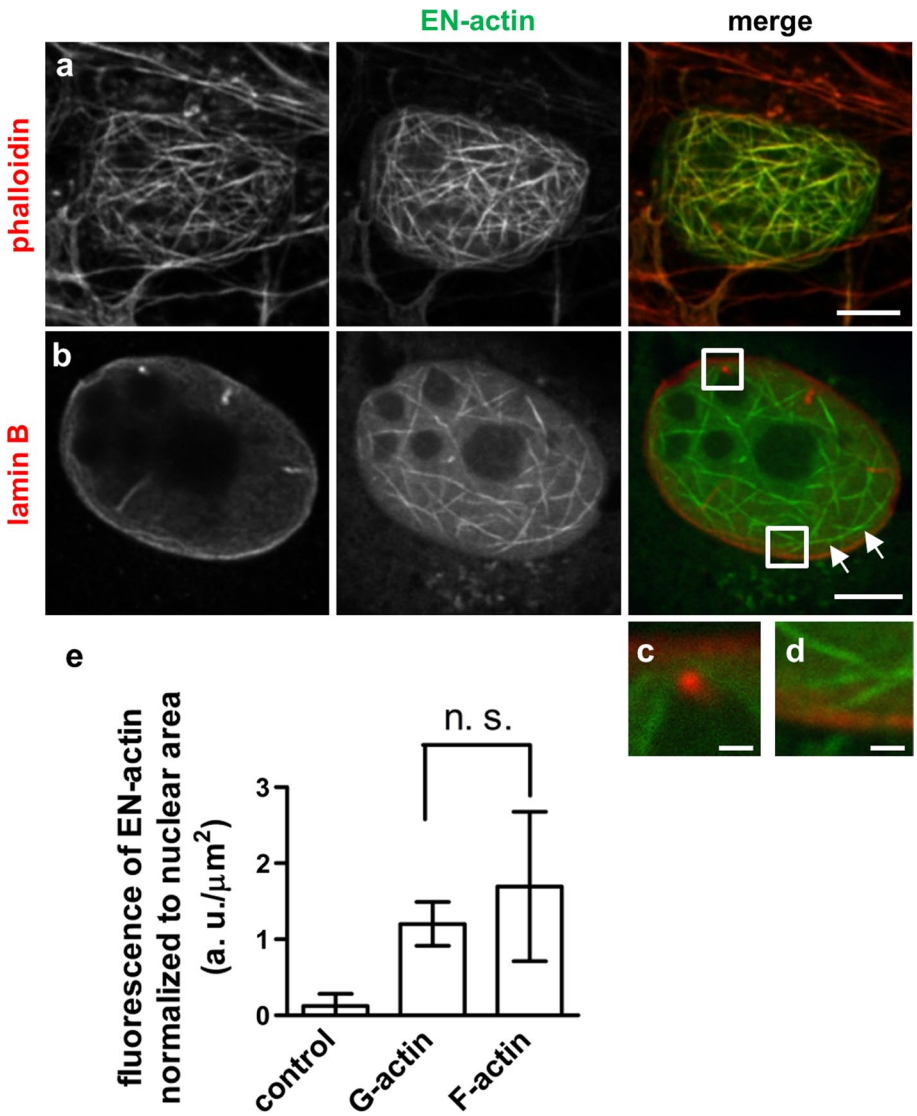

Fig. 2 Properties of nuclear EN-actin filaments formed in U2OS cells. Nuclear EN-actin filaments are susceptible to phalloidin staining (**a**), run along the nuclear lamina (**b** *white arrows*) and occasionally join the nuclear lamina (**c**–**d**). No significant difference in the total nuclear fluorescence intensity of EN-actin normalized to the nuclear area was found between the cells forming EN-actin filaments (F-actin; **e**) and cells containing homogenously dispersed EN-actin (G-actin; **e**). As a control, cells having no expression of EN-actin but present within the same coverslip were used. Results are presented as mean ± SD of three independent experiments, whiskers indicate minimal and maximal values. In total, 30 cells for F-actin, 69 cells for G-actin and 130 control cells were analyzed (**e**). *Scale bars* 5 μm (**a**–**e**), 1.25 μm (**f**–**g**), *n. s. p*>0.05

was inspected in immortalized human embryonic kidney cell line (HEK293), human cervical carcinoma cell line (HeLa), human non-small cell lung carcinoma cell line (H1299) and primary mouse skin fibroblasts. Formation of nuclear actin filaments was noticed in all immortalized human cell lines (HEK293, HeLa, H1299; Fig. 3c–e); however, no nuclear filaments were found in primary mouse fibroblasts (Fig. 3a, b). In mouse fibroblasts, EN-actin was preferentially incorporated into cytoplasmic fibers (Fig. 3a, optical section focused to the cytoplasmic fibers), while only a small portion was imported into the nucleus, where it stayed homogenously dispersed in the monomeric form (Fig. 3b, the same cell—optical section in the equatorial position).

However, we noticed some differences between the immortalized cell lines. HEK293 cells (Fig. 3e) formed nuclear actin filaments more readily than U20S cells, reaching up to 10–20 % of cells with filaments. On the other hand, the proportion of H1299 cells forming nuclear actin filaments was only around 0.5 % (Fig. 3d). Even though we found nuclear EN-actin filaments in some H1299 cells, EN-actin was not imported into the nucleus efficiently; it rather stayed in the cytoplasmic filaments in majority of cells (not shown).

Altogether, we conclude that the ability to translocate EN-actin into the nucleus and form nuclear EN-actin filaments is cell-type specific and reflects diverse nuclear environment and/or nucleocytoplasmic transport properties.

Cells with nuclear EN-actin filaments undergo a mitotic block

In order to investigate the behavior of nuclear EN-actin during cell cycle, we observed localization of homogenously dispersed EN-actin and EN-actin incorporated into the filaments at various stages of mitosis by light

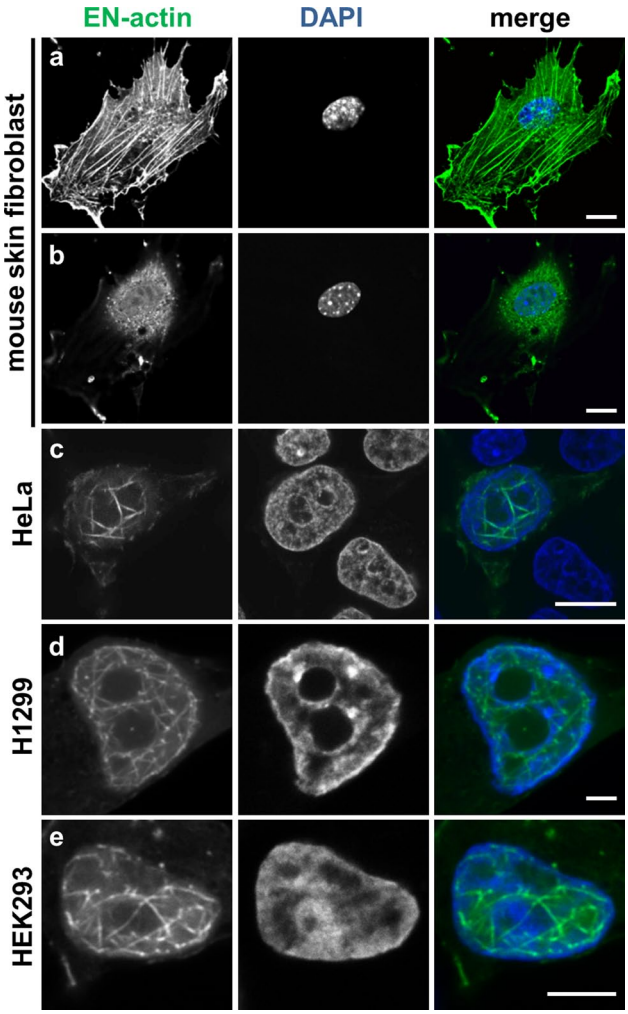

Fig. 3 Formation of nuclear EN-actin filaments varies among cell types. In primary mouse skin fibroblasts, EN-actin (delivered by nucleofection) incorporates preferentially into cytoplasmic fibers (**a** optical section focused on the cytoplasmic fibers) and does not form filaments in the nucleus (**b** optical section of the same cell in the equatorial position). EN-actin, delivered by transfection, assembled into filaments in the nuclei of Hela (**c**), H1299 (**d**) and HEK293 (**e**) cells. *Scale bars* 10 μm (**a**–**c**), 5 μm (**d**–**e**)

microscopy (Fig. 4a–f). We revealed that homogenously dispersed EN-actin is at the onset of mitosis exported from the nucleus (Fig. 4b). In later phases of mitosis, EN-actin is not associated with chromosomes; it is enriched at the plasma membrane and in plasma membrane protrusions instead (Fig. 4c–e). EN-actin is imported into the nucleus after the re-assembly of the nuclear envelope during cytokinesis (Fig. 4f).

Interestingly, when we monitored cells by a long-term live-cell observations, we did not observe any cells containing EN-actin filaments to progress through mitosis. At the same time, other cells in the field of view which contained cytoplasmic EN-actin filaments or homogenous nuclear EN-actin divided normally (data not shown). This suggests a block in mitosis caused by the presence of EN-actin filaments in the nucleus. Indeed, when we measured proliferation rate by EdU incorporation, 53 % of the control or homogenous nuclear EN-actin containing cells incorporated EdU (Fig. 5c, control and G-actin, respectively). After the formation of nuclear EN-actin filaments, the EdU incorporation decreased by a half, to 24 % (Fig. 5c, F-actin). We furthermore noticed that many cells carrying nuclear actin filaments exhibited two types of morphological abnormalities: in the first case, additional micronuclei was formed. This micronuclei contained DAPI-stainable chromatin and also a homogenous or filamentous EN-actin (Fig. 5a). Second, some cells did not complete cytokinesis resulting in retention of both daughter nuclei within one cell (Fig. 5b). Of the binucleic cells, 90 % contained nuclear EN-actin filaments in both nuclei, while only 10 % of cells had homogenous EN-actin. The other way around, of all the nuclear EN-actin filament-containing cells, 10 % were binucleic, while only 1 % of cells with homogenous nuclear EN-actin were binucleic. In the binucleic cells, both nuclei always contained the same pattern of EN-actin—either filamentous or homogenous.

Based on the results, we propose that the presence of the EN-actin filaments in the cell nucleus may disturb progress into mitotic phase of a cell cycle. In case the cell still undergoes mitosis, irregularities in structure of daughter cells or aberrant cytokinesis appear as a consequence.

Cofilin co-localizes with nuclear EN-actin filaments, and Arp3 is enriched in cells with EN-actin

The initial experiment (Fig. 2e) showed that the concentration of EN-actin is not the only factor which triggers assembly of nuclear EN-actin filaments. To see whether actin-binding proteins participate in the regulation of EN-actin filaments formation in the nucleus, we observed their localization in respect of the nuclear EN-actin filaments by confocal light microscopy (Fig. 6). We considered particular protein as co-localizing when it was accumulated or enriched at the EN-actin filaments or in their close vicinity.

As we have established that EN-actin does not form individual filaments but bundles instead, we explored the localization of F-actin cross-linking proteins filamin, α-actinin and spectrin (Fig. 6a–c) which are known to localize to the nucleus (Bedolla et al. 2009; Dingova et al. 2009). None of these actin cross-linkers, however, showed preferential co-localization with nuclear EN-actin filaments; therefore, it remains unclear by which mechanism nuclear EN-actin filaments become bundled.

Next, we explored the localization of the F-actin-binding proteins paxillin and vinculin (Fig. 6d, e). These two proteins typically associate with focal adhesions, where

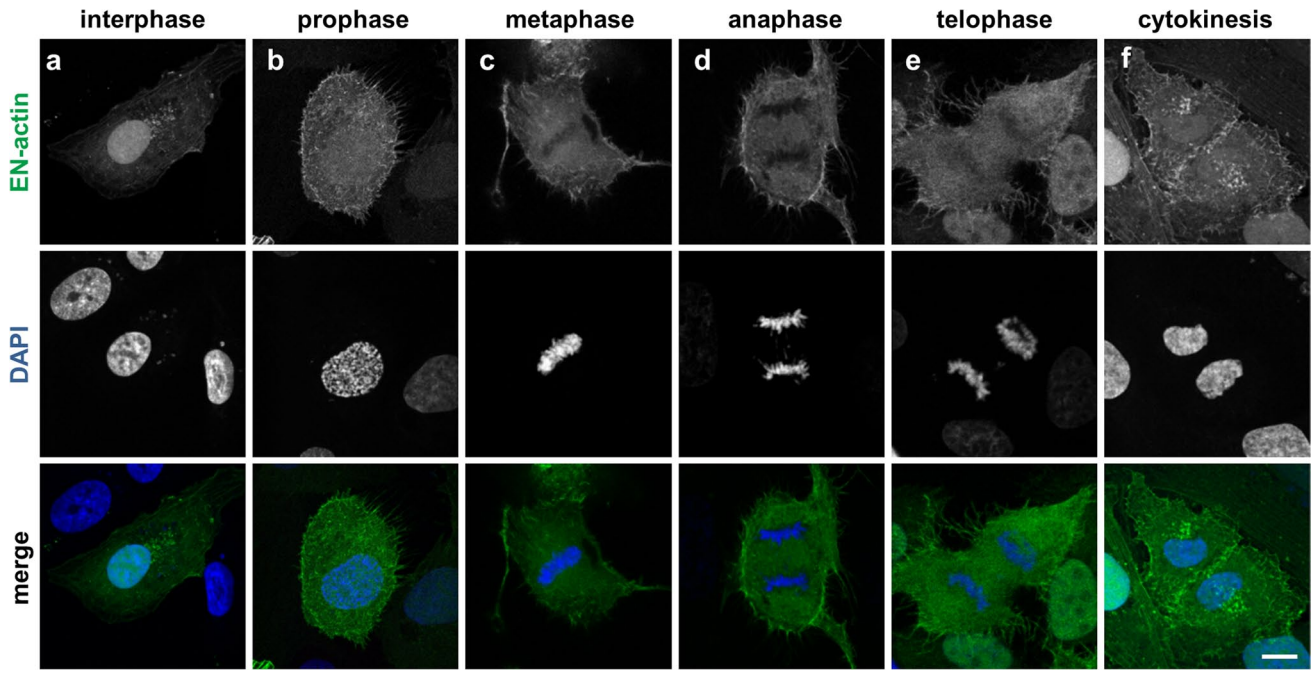

Fig. 4 EN-actin is enriched at the plasma membrane during mitosis. Localization of overexpressed EN-actin was observed at various stages of mitosis in U2OS cells (**a**–**f**). At the onset of mitosis, EN-actin is exported from the nucleus to the plasma membrane (**b**–**e**). When the nuclear envelope re-assembles, EN-actin is imported back into the nucleus (**f**). Maximal projections of five optical sections are shown. *Scale bars* 10 μm

vinculin mediates the association between integrin and F-actin and binds also paxillin (Turner et al. 1990). Despite the fact that both vinculin and paxillin were previously reported to localize in the nucleus (Dingova et al. 2009; Dong et al. 2009; Kano et al. 1996), we detected only a negligible amount of nuclear paxillin. Yet, neither of them co-localized with the nuclear filaments formed after the overexpression of EN-actin (Fig. 6d, e). Therefore, we speculate that nuclear-specific isoforms of actin-bundling proteins assist in cross-linking of EN-actin filaments.

In a recent study, Baarlink et al. (2013) showed that formation of the actin filaments in the nucleus is dependent on the presence of nuclear formins. Since we observed neither co-localization of formin mDia1 with the EN-actin filaments nor any change in pattern of mDia upon EN-actin filaments formation (Fig. 6f), we concluded that mDia1 does not assist in EN-actin polymerization.

Our results show that nuclear EN-actin filaments join nuclear lamina occasionally (Fig. 2b–d). Therefore, we also tested their association with two other nuclear envelope-associated proteins—SUN2, a member of linker of nucleoskeleton and cytoskeleton complex (LINC; Fig. 6g); and emerin, an inner nuclear membrane protein, which binds lamin A/C (Fig. 7a, b). Of these proteins, nuclear EN-actin filaments join in some cases emerin (Fig. 7a, b) in a similar manner as lamin B (Fig. 2b–d).

Next, we investigated the localization of proteins which affect F-actin assembly. First of them, cofilin binds to the pointed end of F-actin filaments and causes their disassembly. Surprisingly, cofilin co-localized with the nuclear EN-actin filaments (Fig. 7c, arrowheads) not only at the ends, but along the entire length of the filament (Fig. 7d, arrowheads). On the contrary, phosphorylated form of cofilin (P-cofilin), which becomes incapable of F-actin binding, did not co-localize with EN-actin filaments (Fig. 7e), even though it was present in the nucleus.

Since the previous study suggested that NLS-actin filaments are branched (Kokai et al. 2014), we explored also localization of branching proteins which area able to bind to the existing filaments in order to trigger nucleation and growth of new branches of the actin filaments. We found that levels of Arp3, a member of Arp2/3 nucleation complex (Pantaloni et al. 2000), are increased upon expression of EN-actin (Fig. 7f, g). It is therefore plausible that Arp3 re-localizes to the nucleus after elevation of EN-actin to assist in the growth of new filaments.

Among the actin-binding proteins analyzed, only Arp3 and cofilin seem to be in relation with the nuclear EN-actin filaments. Such limited co-localization indicates that assembly and bundling of nuclear EN-filaments are controlled by nuclear-specific regulators or nuclear-specific isoforms of actin-associated proteins.

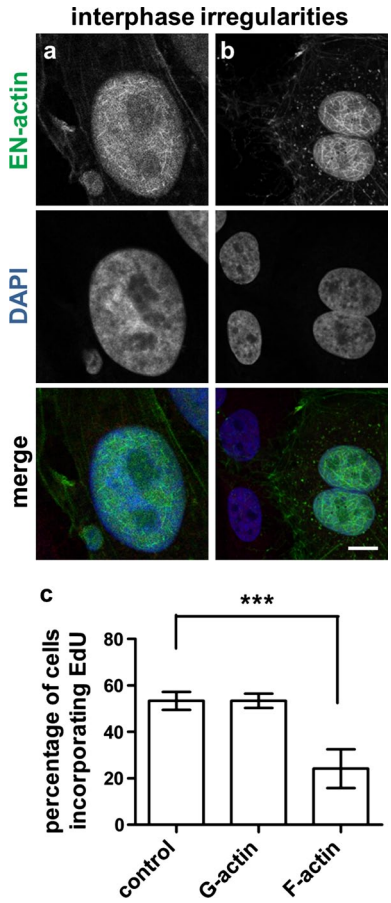

Fig. 5 Cells with EN-actin filaments exhibit irregularities in the interphase. U2OS cells with EN-actin filaments exhibit two phenomena originated in mitosis—presence of DAPI-stainable micronuclei (**a**) and retention of both daughter nuclei within a single cell (**b**). Cell proliferation was measured by EdU incorporation. After labeling, fluorescence of EdU was measured and percentage of EdU-positive cells is shown for cells containing EN-actin filaments (F-actin, **c**), homogenous EN-actin (G-actin, **c**) and control. Results are presented as mean ± SD of three independent experiments. More than 50 cells were analyzed in each experiment (**c**). *Scale bars* 10 μm, ***$p < 0.001$

Nuclear EN-actin filaments formation enhances transcription in the S-phase

It is known that actin is found in chromatin remodeling complexes (Szerlong et al. 2008; Zhao et al. 1998). To test the functional involvement of the EN-actin filaments in chromatin remodeling, we performed co-localization studies with protein hallmarks of chromatin remodeling using confocal microscopy. However, no significant co-localization was observed with the actin-related proteins (Arp5, Arp8 and Arp6), brahma-related gene 1 (Brg1) or hnRNP U (Fig. 8a–e).

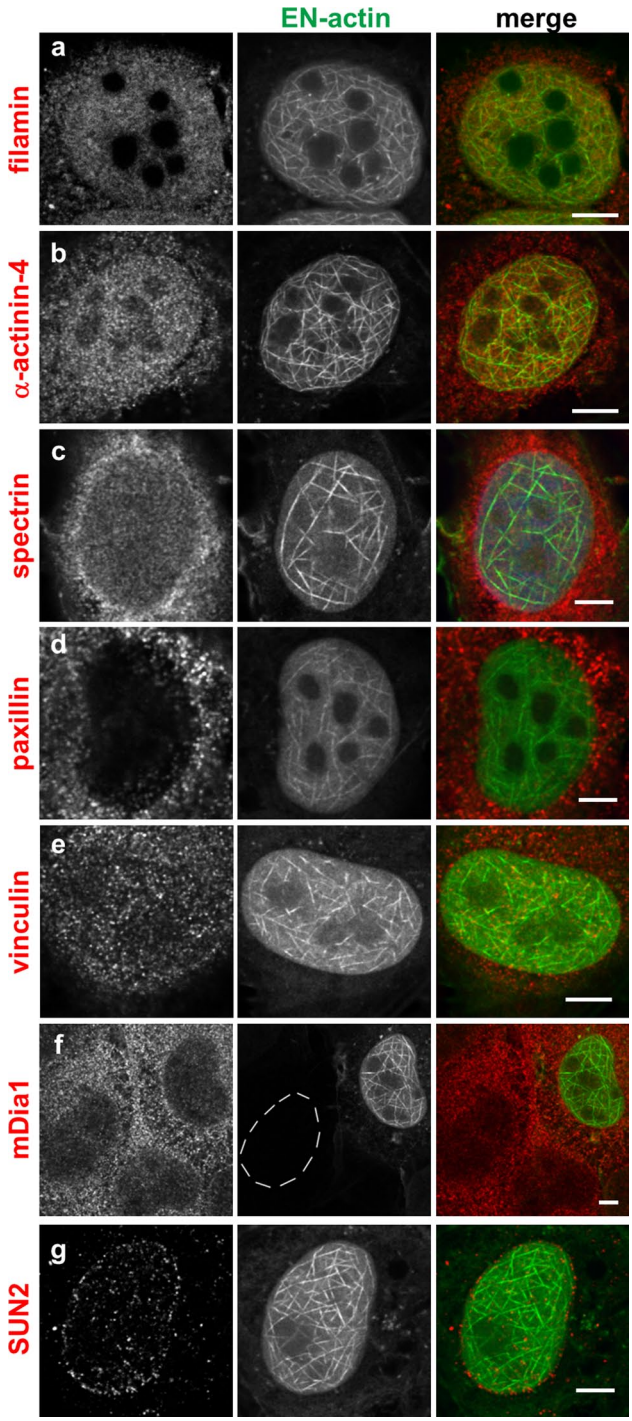

Fig. 6 Nuclear EN-actin filaments do not co-localize with the actin-binding proteins tested. Co-localization of the nuclear EN-actin filaments with various actin-binding proteins was tested by indirect immunofluorescence microscopy in the U2OS cells (**a**–**g**). A protein was considered as co-localizing when it predominantly accumulated at the nuclear EN-filaments or was enriched in their close vicinity. Nucleus of cell with no EN-actin expression is labelled by a *dashed line*. *Scale bars* 5 μm

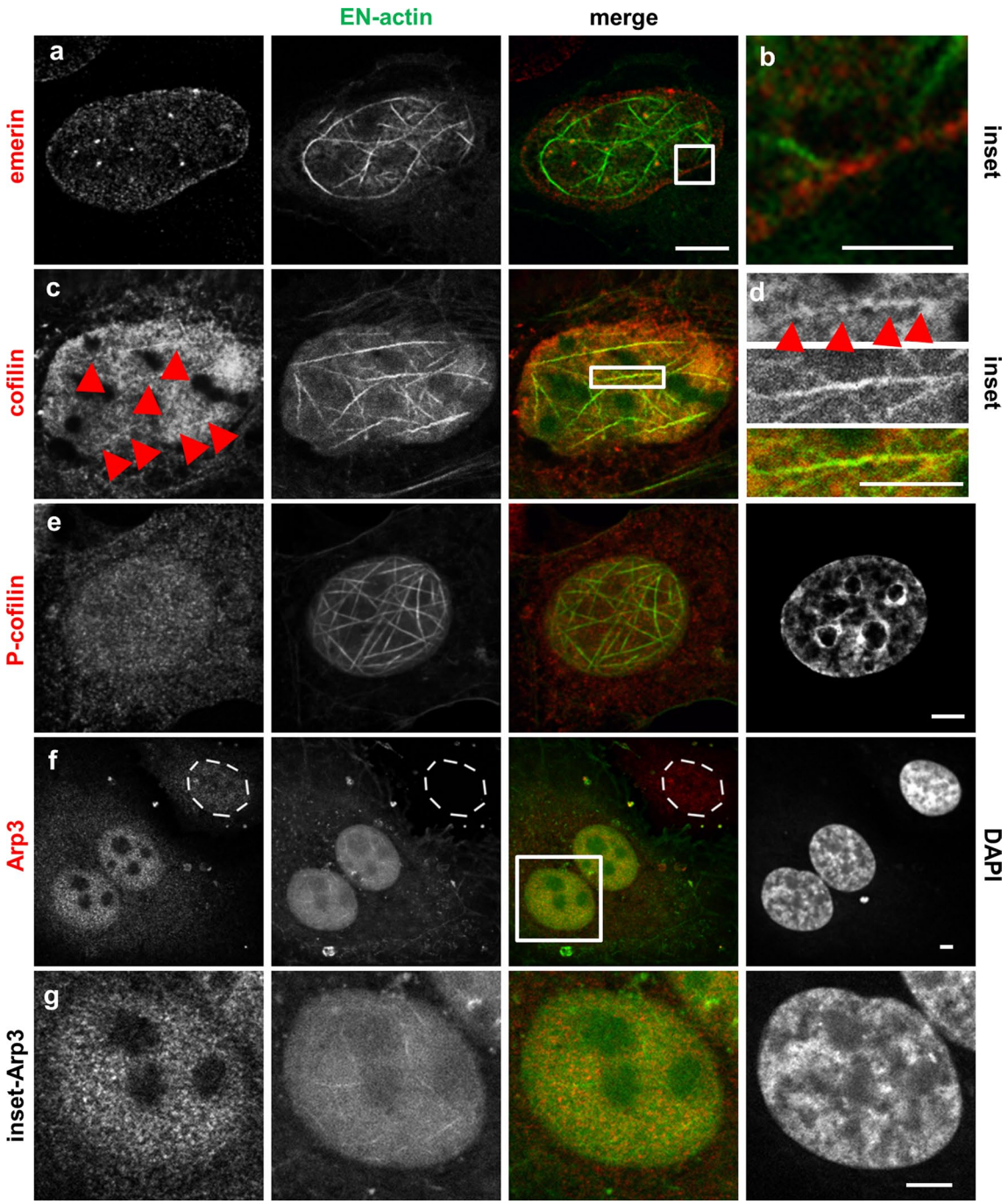

Fig. 7 Nuclear EN-actin filaments recruit Arp3 and cofilin. Co-localization of the nuclear EN-actin filaments with various actin-binding proteins was tested by indirect immunofluorescence microscopy in the U2OS cells (**a**–**g**). EN-actin filaments occasionally come into contact with emerin (**a** and **b** *inset*). EN-actin filaments co-localize with cofilin in the nucleus (**c** and **d**, *arrowheads*). *Inset* of the EN-actin filaments (**d**). EN-actin filaments do not co-localize with P-cofilin (**e**), but recruit Arp3 into the nucleus (**f**). Nucleus of cell with no expression of EN-actin is labeled by dashed line (**f**). *Inset* of the cell with increased Arp3 levels and EN-actin filaments (**g**). *Scale bars* 2.5 μm

Numerous studies have repeatedly emphasized the importance of actin in transcription (Hofmann et al. 2004; Hu et al. 2004; Philimonenko et al. 2004). NM1 is a transcription factor, which exerts its function in cooperation with actin (Ye et al. 2008). Even though one would expect NM1, which requires oligo- or polymeric actin for its function, to be predominantly found on the EN-actin filaments, it is not the case (Fig. 8f). Overexpressed NM1-mCherry is in the nucleoplasm present in the vicinity of the EN-actin filaments, but no evidence points toward their association.

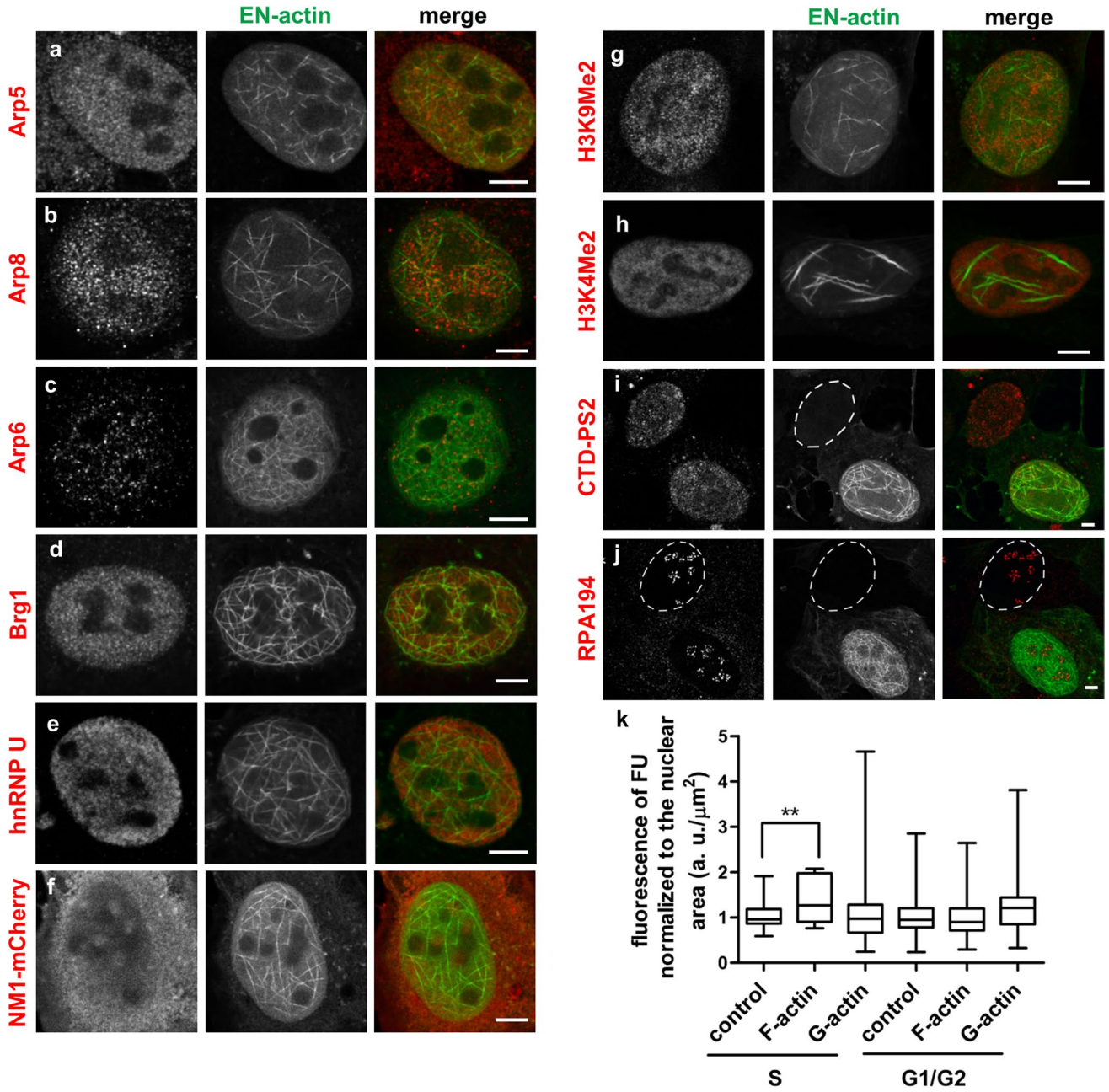

Fig. 8 Nuclear EN-actin filaments enhance DNA transcription. Co-localization of overexpressed nuclear EN-actin and hallmarks of various nuclear functional complexes was observed in U2OS cells by indirect immunofluorescence microscopy. A protein was considered as co-localizing when it predominantly accumulated at the nuclear EN-filaments or was enriched in their close vicinity. Nuclear EN-actin filaments do not co-localize with components of chromatin remodeling complexes (**a**–**f**), but passed through both transcriptionally inactive (**g**) and active chromatin (**h**). Formation of EN-actin filaments does not affect either localization of C-terminal domain of RNA polymerase II phosporylated on serine 2 (CTD-PS2, **i**) or the catalytic subunit of RNA polymerase I (RPA194, **j**). Generation of nuclear EN-actin filaments causes increase in the overall transcription levels in the S-phase (**k**). In this experiment, transcription levels of cells containing EN-actin filaments (**k** F-actin) were compared to cells with homogenous EN-actin (**k** G-actin) and to cells with no expression of EN-actin, which resided within the same coverslips (**k** control). Nascent transcripts were labeled by FU in the U2OS cells and their amounts were then quantified by indirect immunofluorescence using anti-BrdU antibody. Total fluorescence intensity in the nucleus was normalized to the nuclear area. The experiment was repeated three times and the values in each replicate were further normalized to the control. Normalized mean values ± SD of three independent experiments are shown in the graph where whiskers represent the minimum and maximum values. More than 20 cells were analyzed in each experiment. S and G1/G2 phases of the cell cycle were analyzed separately. No significant changes ($p < 0.05$) were observed unless indicated by *asterisks*. **$p = 0.01$-0.001. *Scale bars* 5 μm

We then proceeded with the study of participation of EN-actin in transcription and observed its occurrence in transcriptionally inactive and active chromatin regions, marked by H3K9Me2 and H3K4Me2 histone modification, respectively. Nuclear EN-actin filaments did not show any preferential enrichment in either type of chromatin, neither did homogenously dispersed EN-actin (Fig. 8g, h). On the other hand, EN-actin filaments did not avoid either type of chromatin; they passed through both chromatin regions instead. Therefore, we asked whether EN-actin filaments or free EN-actin do indeed affect transcription as has been previously published (Miyamoto et al. 2011; Wu et al. 2006; Ye et al. 2008). To answer this question, we explored the presence of the catalytic subunit of RNA polymerase I (RPA194) as well as the active form of RNA polymerase II phosphorylated on serine 2 (CTD-PS2), as these would indicate active transcription. Both CTD-PS2 and RPA194 were present in the cells containing nuclear EN-actin filaments (Fig. 8i, j), and no obvious changes in their localization were noticed in comparison with non-transfected cells. In order to assess the impact of homogenous and filamentous EN-actin on transcription, we compared transcription levels of those cells with cells having no overexpression of actin (control). As it is known that transcription is inactivated during mitosis, gradually activated during G1 and its levels are maximal in S and G2 phases (Klein and Grummt 1999; Oelgeschlager 2002; White et al. 1995), we measured the transcription levels in different stages of the cell cycle based on the proliferating cell-nuclear antigen (PCNA) pattern. Nascent transcripts were labeled with fluorouridine (FU) in vivo, which was then detected by indirect immunofluorescence microscopy. Total fluorescence intensity of FU in the nucleus was quantified and normalized to the nuclear area. Transcription levels of cells expressing either homogenous EN-actin (Fig. 8k, G-actin) or EN-actin filaments (Fig. 8k, F-actin) did not significantly differ from the control (Fig. 8k, control) cells in the G1 and G2 phases of the cell cycle. However, we detected changes in transcription in the S-phase when cells forming nuclear EN-actin filaments significantly increased their transcription levels by 30 % (Fig. 8k) in comparison with control cells. On the other hand, S-phase transcription of cells having homogenous nuclear EN-actin did not significantly differ either from control cells or from the cells with EN-actin filaments.

In conclusion, nuclear EN-actin filaments do not participate in chromatin remodeling, do not preferentially associate with transcriptionally active or inactive chromatin, but their presence causes increase in general transcription levels in the S-phase in comparison with control cells.

Discussion

The fundamental ability of actin is to form polymers. Although polymeric structures are long known to exist in the cytoplasm, their presence and form in the nucleus remains unclear.

We showed that the overexpression of EN-actin triggers formation of bundled filaments in the nucleus bearing various shapes from straight long (Figs. 7e, 8h) to curved (Fig. 7a) and dense meshwork (Figs. 1c, 6e). This observation is in agreement with a previous work by Kokai et al. (2014), which moreover proposed that some of the filaments are even branched. Even though we did not study this feature in greater detail, we support the notion that some of the filaments are indeed branched, not only crossing each other (Fig. 2b–c).

In U2OS cells, EN-actin localizes not only to the nucleus, but is also incorporated into cytoplasmic filaments (Fig. 1a and c). The incorporation of EN-actin into the cytoplasmic fibers affected neither formation of EN-actin nuclear filaments nor its nuclear translocation, which was indeed favored (Fig. 1c). The distribution of EN-actin within a cell seems to be cell-type specific, because cytoplasmic retention was not observed in rat PC12 cells (Kokai et al. 2014), whereas in primary mouse skin fibroblasts (Fig. 3a, b) EN-actin resided preferentially in the cytoplasm and did not form nuclear filaments. At the same time, EN-actin was readily imported into the nucleus of HEK293 cells (Fig. 3e). This may reflect differential requirements of actin in the nuclear processes in various cell types.

The formation of nuclear filaments after expression of exogenous EN-actin is relatively rare in U2OS cells, since only 1–5 % of cells show such phenomenon. Such a low incidence of EN-actin filament formation suggests that specific conditions are required to trigger polymerization. It is known that actin begins to polymerize when the critical concentration of free actin monomers is achieved. However, we did not observe such concentration dependency, since the expression levels of EN-actin normalized to nuclear area did not differ significantly in cells with homogenous EN-actin versus cells containing EN-actin filaments (Fig. 2e). This indicates that the amount of actin in the nucleus is not the only factor determining the filament formation, but seems to be a prerequisite. In agreement, blocking the actin export has been reported to cause actin polymerization inside of the nucleus (Dopie et al. 2012; Stuven et al. 2003).

While we observed that cells containing homogenous EN-actin progressed through mitosis (Fig. 4), during which EN-actin mimicked localization of the endogenous actin (Yang et al. 2004), the presence of nuclear EN-actin filaments decreased cell proliferation rate by a half (Fig. 5c). Moreover, we observed two abnormalities in the interphase

cells which seem to originate in mitosis—formation of additional micronuclei or retention of both daughter nuclei within one cell (Fig. 5a, b). These two irregularities were previously observed by Moulding et al. (2007) as a consequence of increase in cytoplasmic F-actin assembly, which caused its mislocalization and led to delay in mitosis and defects in cytokinesis. Besides, both micronuclei formation and bridging the two daughter nuclei together are also results of improper chromosome segregation, which is caused by aberrant centromeric incidence (reviewed in Fenech et al. 2011). Because F-actin is as well required for the anchoring of mitotic spindle to the cell cortex and moreover to establish the direction of spindle movement (Woolner and Bement 2009), it is plausible that the excessive amount of overexpressed EN-actin (which may form filaments during mitosis) prevents correct spindle positioning and manifests in chromosome segregation errors. Since 90 % of the binucleic cells contained nuclear EN-actin filaments, whereas only 10 % of the cells contained homogenous nuclear EN-actin, we speculate that the effect is reinforced with increasing filamentous EN-actin levels. In conclusion, multiple aspects seem to contribute to the defects in mitosis; however, the severity is related to the amount of EN-actin which is available for polymerization into nuclear filaments.

It has been shown that the increase in cofilin expression causes arrest in G1 phase of a cell cycle by a mechanism which involves cyclin-dependent kinase inhibitor $p27^{Kip1}$ (Tsai et al. 2009). Although we did not observe elevated levels of cofilin, we showed a co-localization between cofilin and the nuclear EN-actin filaments (Fig. 7c, d). Therefore, we speculate that cofilin might trigger the nuclear $p27^{Kip1}$ leading to G1 arrest. In conclusion, the defective mitosis is probably a result of more than one aspect and additional experiments need to be performed to understand this issue clearly.

Numerous actin-binding proteins localize and exert their functions in the nucleus (reviewed in Castano et al. 2010). Among those tested in this study, cofilin co-localized with the nuclear EN-actin filaments (Fig. 7c, d,), whereas its phosphorylated form (P-cofilin) did not (Fig. 7e). Besides its involvement in cell cycle progression, cofilin employs multiple modes of action—upon increase in G-actin amount, cofilin maintains actin import into the nucleus (Pendleton et al. 2003) and, at the same time, regulates actin dynamics. Cofilin severs actin filaments at low actin concentrations and nucleates actin filaments at high actin concentrations (Andrianantoandro and Pollard 2006). When filaments are bundled, they become more resistant to cofilin severing (Michelot et al. 2007). Therefore, we suggest that cofilin promotes EN-actin filament formation.

We also found Arp3 upregulated upon EN-actin overexpression (Fig. 7f, g). Arp3 is a member of Arp2/3 complex, which triggers nucleation of the new or branching of the existing actin filaments (Pantaloni et al. 2000). Although we did not study branching of the EN-actin filaments, analysis of nuclear NLS-actin filaments performed by Kokai et al. (2014) revealed that the filaments are most likely branched. Hence, we propose that Arp3 might assist in EN-actin filament nucleation and branching.

Besides cofilin and Arp3, we did not identify any other actin-associated protein to co-localize with the EN-actin filaments, despite testing many potential candidates. However, as recent studies identified nuclear actin filament formation being dependent on nuclear formin (Baarlink et al. 2013), Toca-1, (Miyamoto et al. 2011), N-WASP (Wu et al. 2006) and JMY (Zuchero et al. 2009), we assume that other nuclear-specific actin-binding proteins assist in EN-actin dynamics too.

We showed here that both homogenous and filamentous forms of EN-actin are preferentially neither enriched nor excluded from the chromatin regardless of its transcriptional state (Fig. 8g, h). Noteworthy, we observed that EN-actin filaments seem to avoid only densely packed heterochromatin (Figs. 1c, 3c–e, 7g), which indeed occurs rarely in the U2OS cells as revealed by the electron microscopy (not shown). Based on the absence of co-localization between nuclear EN-actin filaments and chromatin remodeling complexes (Fig. 8a–f), we support the notion that the actin in chromatin remodeling complexes and in complex with hnRNPs is monomeric (Obrdlik et al. 2008; Percipalle et al. 2002) and nuclear EN-actin filaments do not seem to affect chromatin state.

Similarly, formation of nuclear EN-actin filaments did not affect the gross localization of active forms of RNA polymerases I and II (Fig. 8i, j), which were concentrated in discrete foci throughout the nucleolus and nucleoplasm, respectively. The pattern of transcription foci was identical to the control cells, and all the cells were transcriptionally active. After we quantified transcription levels, we found that there is an elevation in the S-phase of the cell cycle in the presence of nuclear EN-actin filaments by 30 % in comparison with control, whereas the presence of homogenous EN-actin did not affect transcription significantly (Fig. 8k). In G1 and G2 phases, the transcription levels did not differ significantly from control. It is plausible that recruitment of EN-actin filaments to the transcription complexes in the S-phase is enabled by a more permissive state of chromatin in the S-phase. This finding also points toward the possibility that polymeric state of actin is required for transcription as has been suggested previously (Miyamoto et al. 2011; Obrdlik and Percipalle 2011; Wu et al. 2006; Ye et al. 2008; Yoo et al. 2007). Up to date, numerous studies focused on the involvement of actin in transcription of SRF-regulated genes. To trigger transcription, SRF requires its cofactor

MAL which is only imported into the nucleus when free of G-actin (Miralles et al. 2003; Vartiainen et al. 2007). Collectively, these studies revealed that formation of F-actin in the nucleus or in the cytoplasm depletes levels of G-actin, which cannot sequester MAL. MAL is in turn imported into the nucleus leading to upregulation of SRF-mediated transcription (Baarlink et al. 2013; Kokai et al. 2014; Stern et al. 2009; Vartiainen et al. 2007). It is therefore reasonable to speculate that the elevation of transcription upon EN-actin filaments formation that we observed occurs via exhaustion of free G-actin monomers. However, to answer this clearly, more experiments need to be performed.

To sum up, our study documents a potential for EN-actin to form filaments in the nucleus closely resembling actin filaments in the cytoplasm. Generation of nuclear EN-actin filaments recruits cofilin and Arp3 into the nucleus and affects cellular processes. Since our observations of the EN-actin polymerization, its behavior during cell cycle, co-localization with actin-binding proteins and transcriptional activity are in agreement with previous studies, we suggest that EN-actin fusion protein mimics the endogenous actin and may be used as a tool for future challenging research focusing on actin functions in the nucleus.

Acknowledgments P. H., A. K. and L. U. were supported by the Grant agency of the Czech Republic (P305/11/2232), P. H. and I. K. were supported by the Ministry of Youth, Sports and Education of the Czech Republic (LD12063); P. H., L. U. and M. H. were supported by Human Frontier Science Program (RGP0017/2013). A. K., I. K. and L. U. were supported by the Charles University in Prague. This publication is supported by the project "BIOCEV – Biotechnology and Biomedicine Centre of the Academy of Sciences and Charles University" (CZ.1.05/1.1.00/02.0109), from the European Regional Development Fund. This research was performed with support of the Institute of Molecular Genetics, Academy of Sciences of the Czech Republic (RVO: 68378050). We are very grateful to Prof. Primal de Lanerolle (University of Illinois at Chicago) for providing us the EN-actin plasmid and Prof. Matthew Welch (University of California, Berkeley) for providing us the Arp3 antibody. We would like to thank Iva Jelínková for excellent technical assistance and Irina Studenyak for critical reading of the manuscript.

References

Andrianantoandro E, Pollard TD (2006) Mechanism of actin filament turnover by severing and nucleation at different concentrations of ADF/cofilin. Mol Cell 24:13–23. doi:10.1016/j.molcel.2006.08.006

Aoyama N, Oka A, Kitayama K, Kurumizaka H, Harata M (2008) The actin-related protein hArp8 accumulates on the mitotic chromosomes and functions in chromosome alignment. Exp Cell Res 314:859–868. doi:10.1016/j.yexcr.2007.11.020

Baarlink C, Wang H, Grosse R (2013) Nuclear actin network assembly by formins regulates the SRF coactivator MAL. Science 340:864–867. doi:10.1126/science.1235038

Bedolla RG et al (2009) Nuclear versus cytoplasmic localization of filamin A in prostate cancer: immunohistochemical correlation with metastases Clinical cancer research : an official journal of the American Association for. Cancer Res 15:788–796. doi:10.1158/1078-0432.CCR-08-1402

Belin BJ, Cimini BA, Blackburn EH, Mullins RD (2013) Visualization of actin filaments and monomers in somatic cell nuclei. Mol Biol Cell 24:982–994. doi:10.1091/mbc.E12-09-0685

Castano E et al (2010) Actin complexes in the cell nucleus: new stones in an old field. Histochem Cell Biol 133:607–626. doi:10.1007/s00418-010-0701-2

de Lanerolle P, Serebryannyy L (2011) Nuclear actin and myosins: life without filaments. Nat Cell Biol 13:1282–1288. doi:10.1038/ncb2364

Dingova H, Fukalova J, Maninova M, Philimonenko VV, Hozak P (2009) Ultrastructural localization of actin and actin-binding proteins in the nucleus. Histochem Cell Biol 131:425–434. doi:10.1007/s00418-008-0539-z

Dong JM, Lau LS, Ng YW, Lim L, Manser E (2009) Paxillin nuclear-cytoplasmic localization is regulated by phosphorylation of the LD4 motif: evidence that nuclear paxillin promotes cell proliferation. Biochem J 418:173–184. doi:10.1042/BJ20080170

Dopie J, Skarp KP, Rajakyla EK, Tanhuanpaa K, Vartiainen MK (2012) Active maintenance of nuclear actin by importin 9 supports transcription. Proc Natl Acad Sci USA 109:E544–E552. doi:10.1073/pnas.1118880109

Dundr M et al (2007) Actin-dependent intranuclear repositioning of an active gene locus in vivo. J Cell Biol 179:1095–1103. doi:10.1083/jcb.200710058

Fenech M et al (2011) Molecular mechanisms of micronucleus, nucleoplasmic bridge and nuclear bud formation in mammalian and human cells. Mutagenesis 26:125–132. doi:10.1093/mutage/geq052

Hofmann WA (2009) Cell and molecular biology of nuclear actin. Int Rev Cell Mol Biol 273:219–263. doi:10.1016/S1937-6448(08)01806-6

Hofmann WA et al (2004) Actin is part of pre-initiation complexes and is necessary for transcription by RNA polymerase II. Nat Cell Biol 6:1094–1101. doi:10.1038/ncb1182

Hofmann WA, Arduini A, Nicol SM, Camacho CJ, Lessard JL, Fuller-Pace FV, de Lanerolle P (2009) SUMOylation of nuclear actin. J Cell Biol 186:193–200. doi:10.1083/jcb.200905016

Hu P, Wu S, Hernandez N (2004) A role for beta-actin in RNA polymerase III transcription. Genes Dev 18:3010–3015. doi:10.1101/gad.1250804

Hu Q et al (2008) Enhancing nuclear receptor-induced transcription requires nuclear motor and LSD1-dependent gene networking in interchromatin granules. Proc Natl Acad Sci USA 105:19199–19204. doi:10.1073/pnas.0810634105

Ikura T et al (2000) Involvement of the TIP60 histone acetylase complex in DNA repair and apoptosis. Cell 102:463–473

Jockusch BM, Schoenenberger CA, Stetefeld J, Aebi U (2006) Tracking down the different forms of nuclear actin. Trends Cell Biol 16:391–396. doi:10.1016/j.tcb.2006.06.006

Kano Y, Katoh K, Masuda M, Fujiwara K (1996) Macromolecular composition of stress fiber-plasma membrane attachment sites in endothelial cells in situ. Circ Res 79:1000–1006

Kapoor P, Chen M, Winkler DD, Luger K, Shen X (2013) Evidence for monomeric actin function in INO80 chromatin remodeling. Nat Struct Mol Biol 20:426–432. doi:10.1038/nsmb.2529

Kitayama K et al (2009) The human actin-related protein hArp5: nucleo-cytoplasmic shuttling and involvement in DNA repair. Exp Cell Res 315:206–217. doi:10.1016/j.yexcr.2008.10.028

Klein J, Grummt I (1999) Cell cycle-dependent regulation of RNA polymerase I transcription: the nucleolar transcription factor UBF is inactive in mitosis and early G1. Proc Natl Acad Sci USA 96:6096–6101

Kokai E et al (2014) Analysis of nuclear actin by overexpression of wild-type and actin mutant proteins. Histochem Cell Biol 141:123–135. doi:10.1007/s00418-013-1151-4

Kukalev A, Nord Y, Palmberg C, Bergman T, Percipalle P (2005) Actin and hnRNP U cooperate for productive transcription by RNA polymerase II. Nat Struct Mol Biol 12:238–244. doi:10.1038/nsmb904

McDonald D, Carrero G, Andrin C, de Vries G, Hendzel MJ (2006) Nucleoplasmic beta-actin exists in a dynamic equilibrium between low-mobility polymeric species and rapidly diffusing populations. J Cell Biol 172:541–552. doi:10.1083/jcb.200507101

Michelot A, Berro J, Guerin C, Boujemaa-Paterski R, Staiger CJ, Martiel JL, Blanchoin L (2007) Actin-filament stochastic dynamics mediated by ADF/cofilin. Curr Biol: CB 17:825–833. doi:10.1016/j.cub.2007.04.037

Miralles F, Posern G, Zaromytidou AI, Treisman R (2003) Actin dynamics control SRF activity by regulation of its coactivator MAL. Cell 113:329–342

Miyamoto K, Pasque V, Jullien J, Gurdon JB (2011) Nuclear actin polymerization is required for transcriptional reprogramming of Oct4 by oocytes. Genes Dev 25:946–958. doi:10.1101/gad.615211

Mizuguchi G, Shen X, Landry J, Wu WH, Sen S, Wu C (2004) ATP-driven exchange of histone H2AZ variant catalyzed by SWR1 chromatin remodeling complex. Science 303:343–348. doi:10.1126/science.1090701

Moulding DA et al (2007) Unregulated actin polymerization by WASp causes defects of mitosis and cytokinesis in X-linked neutropenia. J Exp Med 204:2213–2224. doi:10.1084/jem.20062324

Obrdlik A, Percipalle P (2011) The F-actin severing protein cofilin-1 is required for RNA polymerase II transcription elongation. Nucleus 2:72–79. doi:10.4161/nucl.2.1.14508

Obrdlik A, Kukalev A, Louvet E, Farrants AK, Caputo L, Percipalle P (2008) The histone acetyltransferase PCAF associates with actin and hnRNP U for RNA polymerase II transcription. Mol Cell Biol 28:6342–6357. doi:10.1128/MCB.00766-08

Oelgeschlager T (2002) Regulation of RNA polymerase II activity by CTD phosphorylation and cell cycle control. J Cell Physiol 190:160–169. doi:10.1002/jcp.10058

Pantaloni D, Boujemaa R, Didry D, Gounon P, Carlier MF (2000) The Arp2/3 complex branches filament barbed ends: functional antagonism with capping proteins. Nature Cell Biol 2:385–391. doi:10.1038/35017011

Pendleton A, Pope B, Weeds A, Koffer A (2003) Latrunculin B or ATP depletion induces cofilin-dependent translocation of actin into nuclei of mast cells. J Biol Chem 278:14394–14400. doi:10.1074/jbc.M206393200

Percipalle P, Jonsson A, Nashchekin D, Karlsson C, Bergman T, Guialis A, Daneholt B (2002) Nuclear actin is associated with a specific subset of hnRNP A/B-type proteins. Nucleic Acids Res 30:1725–1734

Philimonenko VV et al (2004) Nuclear actin and myosin I are required for RNA polymerase I transcription. Nat Cell Biol 6:1165–1172. doi:10.1038/ncb1190

Qi T, Tang W, Wang L, Zhai L, Guo L, Zeng X (2011) G-actin participates in RNA polymerase II-dependent transcription elongation by recruiting positive transcription elongation factor b (P-TEFb). J Biol Chem 286:15171–15181. doi:10.1074/jbc.M110.184374

Shen X, Mizuguchi G, Hamiche A, Wu C (2000) A chromatin remodelling complex involved in transcription and DNA processing Nature 406:541–544. doi:10.1038/35020123

Stern S, Debre E, Stritt C, Berger J, Posern G, Knoll B (2009) A nuclear actin function regulates neuronal motility by serum response factor-dependent gene transcription. J Neurosci 29:4512–4518. doi:10.1523/JNEUROSCI.0333-09.2009

Stuven T, Hartmann E, Gorlich D (2003) Exportin 6: a novel nuclear export receptor that is specific for profilin. Actin complexes. EMBO J 22:5928–5940. doi:10.1093/emboj/cdg565

Szerlong H, Hinata K, Viswanathan R, Erdjument-Bromage H, Tempst P, Cairns BR (2008) The HSA domain binds nuclear actin-related proteins to regulate chromatin-remodeling ATPases. Nat Struct Mol Biol 15:469–476. doi:10.1038/nsmb.1403

Tsai CH, Chiu SJ, Liu CC, Sheu TJ, Hsieh CH, Keng PC, Lee YJ (2009) Regulated expression of cofilin and the consequent regulation of p27(kip1) are essential for G(1) phase progression. Cell Cycle 8:2365–2374

Turner CE, Glenney JR Jr, Burridge K (1990) Paxillin: a new vinculin-binding protein present in focal adhesions. J Cell Biol 111:1059–1068

Vartiainen MK, Guettler S, Larijani B, Treisman R (2007) Nuclear actin regulates dynamic subcellular localization and activity of the SRF cofactor MAL. Science 316:1749–1752. doi:10.1126/science.1141084

Welch MD, Iwamatsu A, Mitchison TJ (1997) Actin polymerization is induced by Arp2/3 protein complex at the surface of Listeria monocytogenes. Nature 385:265–269. doi:10.1038/385265a0

White RJ, Gottlieb TM, Downes CS, Jackson SP (1995) Cell cycle regulation of RNA polymerase III transcription. Mol Cell Biol 15:6653–6662

Winder SJ, Ayscough KR (2005) Actin-binding proteins. J Cell Sci 118:651–654. doi:10.1242/jcs.01670

Woolner S, Bement WM (2009) Unconventional myosins acting unconventionally. Trends Cell Biol 19:245–252. doi:10.1016/j.tcb.2009.03.003

Wu X, Yoo Y, Okuhama NN, Tucker PW, Liu G, Guan JL (2006) Regulation of RNA-polymerase-II-dependent transcription by N-WASP and its nuclear-binding partners. Nat Cell Biol 8:756–763. doi:10.1038/ncb1433

Yang X, Yu K, Hao Y, Li DM, Stewart R, Insogna KL, Xu T (2004) LATS1 tumour suppressor affects cytokinesis by inhibiting LIMK1. Nat Cell Biol 6:609–617. doi:10.1038/ncb1140

Ye J, Zhao J, Hoffmann-Rohrer U, Grummt I (2008) Nuclear myosin I acts in concert with polymeric actin to drive RNA polymerase I transcription. Genes Dev 22:322–330. doi:10.1101/gad.455908

Yoo Y, Wu X, Guan JL (2007) A novel role of the actin-nucleating Arp2/3 complex in the regulation of RNA polymerase II-dependent transcription. J Biol Chem 282:7616–7623. doi:10.1074/jbc.M607596200

Zhao K, Wang W, Rando OJ, Xue Y, Swiderek K, Kuo A, Crabtree GR (1998) Rapid and phosphoinositol-dependent binding of the SWI/SNF-like BAF complex to chromatin after T lymphocyte receptor signaling. Cell 95:625–636

Zuchero JB, Coutts AS, Quinlan ME, Thangue NB, Mullins RD (2009) p53-cofactor JMY is a multifunctional actin nucleation factor. Nat Cell Biol 11:451–459. doi:10.1038/ncb1852

5. DISCUSSION

5.1 Phosphoinositides and their localization in the nucleus

Nuclear PIs are important regulators of various nuclear processes (reviewed in Shah et al. 2013). To better understand their role in the nucleus, tools for nuclear PIs visualization both *in vivo* and *in vitro* are needed.

In order to detect nuclear PIs, we tested several antibodies and PIs-binding protein domains. Overexpressed PIs-binding domains conjugated with GFP are widely used for detection of PIs in cellular membranes. They often localize also to the nucleus however their nuclear localization is probably a result of unspecific accumulation after overexpression (Hammond and Balla 2015). Indeed, most of PIs-binding domains we tested display the same nuclear pattern as their mutant forms, which are not able to bind PIs. Only EEA1-FYVE domain specifically detected PI(3)P foci in nucleoli of U2OS cells. In support of our data, PI(3)P has been previously detected in nucleoli of human fibroblasts and baby hamster kidney cells (Gillooly et al. 2000). The function of nucleolar PI(3)P is completely unknown and will be a subject of our future research.

As most of the overexpressed PIs-binding domains are not suitable for PIs detection in the nucleus, we prepared purified PLCδ1-PH, Tubby and OSH1-PH domains fused with eGFP, which recognize PI(4,5)P2 and PI(4)P, respectively. We compared a nuclear pattern of these domains with patterns of anti-PI(4,5)P2 and anti-PI(4)P antibodies.

Using OSH1-PH and anti-PI(4)P, we demonstrate for the first time that nuclear PI(4)P can be visualized in the cell nucleus. PI(4)P is present in the nuclear membrane, it localizes to the nuclear speckles and forms small nucleoplasmic foci. The pattern of PI(4)P in nuclear speckles is not homogenous, it forms small foci inside and at the edges of nuclear speckles, where the active transcription takes place (reviewed in Spector and Lamond 2011). Only a minority of nuclear PI(4)P resides in nuclear speckles. The majority of nuclear PI(4)P localizes to other nuclear compartments and most of nuclear PI(4)P is associated with chromatin. Moreover, small nucleoplasmic foci of PI(4)P partially colocalize with H3K4me2, the mark of active chromatin (Wang et al. 2014).

PI(4)P localization to the active chromatin and to the edges of nuclear speckles indicates that PI(4)P might play a role in the regulation of DNA transcription. In addition,

PI(4)P in the nuclear speckles could be implicated in splicing of newly transcribed pre-mRNA. The other possibility is that PI(4)P in nuclear speckles serves as a precursor for PI(4,5)P2. Enzymes, which convert PI(4,5)P2 to PI(4)P and *vice versa,* localize to the nuclear speckles (Boronenkov et al. 1998; Déléris et al. 2003; Mellman et al. 2008; Schill and Anderson 2009; Elong Edimo et al. 2011) and therefore it is highly probable that an active metabolism of these PIs in nuclear speckles indeed occurs.

Using PLCδ1-PH and Tubby domains and anti-PI(4,5)P2 antibody we detected PI(4,5)P2 in nucleoli, nuclear speckles and nucleoplasm. In agreement, localization of PI(4,5)P2 in nuclear speckles and nucleoli has been described (Osborne et al. 2001; Yildirim et al. 2013; Sobol et al. 2016). Moreover, we show that nearly 30 % of total nuclear PI(4,5)P2 detected by anti-PI(4,5)P2 antibody is located in foci outside of these structures. This nucleoplasmic PI(4,5)P2 forms 40-100 nm roundish structures, which we termed PI(4,5)P2 islets. They have carbon-rich interior and phosphorus- and nitrogen-rich exterior. Therefore, we suggest that the inner core of PI(4,5)P2 islets is composed of lipids while their outer surface is surrounded by proteins and nucleic acids.

Recently, nuclear lipid droplets (nLDs) have been described in rat and human liver hepatocytes (Layerenza et al. 2013). Their hydrophobic lipid core is formed by triacylglycerols and cholesterol and is surrounded by a hydrophilic outer monolayer from polar lipids and proteins. Yoo et al. (2014) showed that PI(4,5)P2 can form membrane enclosed nucleoplasmic vesicles in the bovine adrenal chromaffin cells (Yoo et al. 2014). However, PI(4,5)P2 islets are approximately 10-times smaller than nLDs and are not surrounded by a membrane. These results suggest that PI(4,5)P2 islets are a novel type of phospholipid-containing foci in the nucleus.

We show that the active form of RNA Pol II and transcription machinery proteins as well as nascent RNA are associated with PI(4,5)P2 islets. PI(4,5)P2 islets are RNA but not DNA dependent structures. The majority of PI(4,5)P2 islets colocalizes with RNA and can be disturbed by RNase treatment. Therefore, PI(4,5)P2 islets might serve as a scaffold for the arrangement of RNA Pol II transcription machinery. In agreement, PI(4,5)P2 hydrolysis results in a significant decrease of transcription level. Similarly, several studies demonstrated a contribution of other lipid-based structures in transcription (Scassellati et al. 2010; Layerenza et al. 2013; Yoo et al. 2014).

We show that the inhibition of RNA Pol II transcription does not disturb PI(4,5)P2 islets. Hence, PI(4,5)P2 islets are stable nuclear structures independent of ongoing transcription. Therefore, we suggest that PI(4,5)P2 islets facilitate spatial-temporal arrangement of transcription complexes assembly.

5.2 Binding partners of phosphoinositides in the nucleus and their functions

Nuclear phosphoinositides associate with histones and other chromosomal proteins to regulate chromatin remodelling, DNA modifications and transcription (reviewed in Viiri et al. 2012). However, their functions in the nucleus are still poorly understood. Here, we describe two novel PIs interacting proteins - nuclear myosin 1 (NM1) and lysine-specific histone demethylase 1 (LSD1).

NM1 contains C-terminal PH domain that specifically binds PI(4,5)P2 and tethers NM1 to the plasma membrane (Hokanson and Ostap 2006; Hokanson et al. 2006). In the nucleus, NM1 is involved in chromatin remodelling and RNA Pol II transcription. The C-terminal part of NM1 containing PI(4,5)P2-binding site is essential for these functions (Hofmann et al. 2006; Almuzzaini et al. 2015).

We show that NM1 interacts with PI(4,5)P2 also in the cell nucleus and this interaction anchors NM1 to bigger nuclear complexes. The mutation of PI(4,5)P2 binding site results in a loss of interaction with RNA Pol II and downregulation of transcription. We show that NM1 localizes to the surface of PI(4,5)P2 islets. Therefore we hypothesize that NM1 is sequestered to PI(4,5)P2 islets through the interactions with PI(4,5)P2. In such way, NM1 could recruit chromatin remodelling complexes to PI(4,5)P2 islets to create an open chromatin structure and promote transcription. We speculate that after disruption of NM1 association with PI(4,5)P2 islets, RNA Pol II complexes remain attached to the surface of PI(4,5)P2 islets. However, transcription cannot occur probably due to the lack of chromatin remodelling factors.

We found that PI(4)P associates with chromatin and colocalizes with H3K4me2. We show that PI(4)P interacts with LSD1, which demethylates H3K4me2 and H3K4me1 histone methylation marks and therefore represses transcription of its target genes (Shi et al. 2004). By direct binding assay, we show that LSD1 interacts directly with PI, PI(4)P, PI(3,4)P2, PI(3,5)P2, PI(4,5)P2 and PI(3,4,5)P3 but displays the highest affinity towards PI(4)P. As PI(4)P and PI(4,5)P2 are the most abundant PIs species (reviewed in Viaud et al. 2015), we studied

how these two PIs regulate LSD1 activity. We demonstrate that PI(4)P binding inhibits LSD1 activity *in vitro* whereas PI(4,5)P2 binding has a stimulatory effect. Interestingly, LSD1 binds PI(4,5)P2 but not PI(4)P in nuclear lysates. Since LSD1 interacts with PI(4)P after overexpression, we hypothesize that PI(4)P binds to LSD1 only when downregulation of H3K4me2 demethylase activity is necessary.

It has been shown that a single change in phosphorylation of inositol ring can regulate the affinity of a PIs-interacting protein to its binding partners (Blind et al. 2012). Since LSD1 has neither DNA nor histone binding domain, its function is highly dependent on its interacting partners in transcriptional repression complexes (reviewed in Amente et al. 2013). Therefore, a single phosphorylation of PI(4)P or dephosphorylation of PI(4,5)P2 by particular kinases or phosphatases could provide a rapid and dynamic regulation of LSD1 function also *in vivo*. Such regulation could provide a fine adjustment of LSD1 functions and expression of its target genes.

5.3 Actin in the nucleus

In the cytoplasm, actin is present in two different forms - as monomeric globular actin (G-actin), which can polymerize and form actin filaments (F-actin). In the nucleus, actin is present in monomeric form (reviewed in Jockusch et al. 2006). Initially, it was uncertain whether actin polymerization can occur in the nucleus. Eventually, several studies reported F-actin formation in the nucleus (Miyamoto et al. 2011; Belin et al. 2013; Baarlink et al. 2013; Kokai et al. 2014). We investigated whether nuclear actin filaments recruit actin-binding proteins and affect the nuclear processes. After over-expression of EYEP-NLS-actin (EN-actin), 1 to 5 % of cells formed long thick nuclear filaments, which in their length and thickness resembled cytoplasmic F-actin. The rest of the cells displayed diffused nuclear actin signal. We show that cofilin, actin-depolymerizing factor, and Arp3, a component of actin nucleation complex Arp2/3 colocalizes with nuclear actin filaments. EN-filaments do not preferentially localize to either active or inactive chromatin. Although EN-actin does not colocalize with RNA polymerases, the level of transcription increases in S-phase in the presence of EN-actin filaments. In support of this finding, earlier studies reported an increased transcription in the presence of polymeric actin in the nucleus (Ye et al. 2008; Baarlink et al. 2013; Kokai et al. 2014).

The formation of EN-actin filaments decreases the cell proliferation rate and increases incidence of formation of additional micronuclei or retention of both daughter nuclei within one cell. Similar results were reported previously as a consequence of cytoplasmic F-actin assembly (Moulding et al. 2007). However, it could be also a result of aberrant chromosome segregation (reviewed in Fenech et al. 2011). Since EN-actin polymerization, its behaviour during the cell cycle, colocalization with actin-binding protein, and transcriptional activity are in agreement with previous studies, we suggest that EN-actin could be used as a tool in future research regarding actin functions in the nucleus.

6. SUMMARY AND CONCLUSIONS

6.1 PI(4,5)P2 islets are associated with active transcription

PI(4,5)P2 forms 40-100 nm large structures in the nucleoplasm, which we call PI(4,5)P2 islets. Their interior is composed of carbon rich structures, probably lipids. They are surrounded by proteins and nucleic acids. PI(4,5)P2 islets surface is associated with active form of RNA polymerase II, transcription machinery proteins and nascent RNA.

6.2 NM1 interacts with PI(4,5)P2 in the nucleus

NM1 interacts with PI(4,5)P2 in the nucleus through its PH domain. PI(4,5)P2 anchors NM1 to PI(4,5)P2 islets and is essential for NM1 interaction with transcription machinery. The mutation of PI(4,5)P2 binding site results in loss of interaction with RNA Pol II and decreased transcription.

6.3 PI(4)P localizes to the nucleus and is associated with chromatin

In the nucleus, PI(4)P is present in the nuclear membrane, nuclear speckles and small nucleoplasmic foci. The majority of nuclear PI(4)P is associated with chromatin and colocalizes with H3K4me2, a mark of active chromatin.

6.4 LSD1 is regulated by nuclear phosphoinositides

LSD1 binds directly to both PI(4)P and PI(4,5)P2. While the interaction with PI(4)P leads to the inhibition of LSD1, the interaction with PI(4,5)P2 stimulates LSD1 H3K4me2 demethylase activity.

6.5 Nuclear actin filaments alter cellular behaviour

After overexpression of nuclear targeted EN-actin, 1-5 % of cells display formation of nuclear actin filaments. These filaments resemble cytoplasmic F-actin and recruit cofilin and Arp3 actin binding proteins. A formation of actin filaments in the nucleus results in an increased transcription in S-phase, decreased cell proliferation and aberrant mitosis.

7. FUTURE PROSPECTS

Our results demonstrate that nuclear phosphoinositides can regulate DNA transcription directly by interaction with RNA polymerase and transcription factors or indirectly by the alteration of epigenetic regulation. Further, we would like to answer the following questions:

7.1 What is the composition of PI(4,5)P2 lipid islets? Which genes are transcribed at their surface?

The core of PI(4,5)P2 islets is enriched in carbon and probably contains lipids. We would like to investigate the composition of PI(4,5)P2 islets core in greater detail. Moreover, the surface of PI(4,5)P2 islets is associated with actively transcribing RNA Pol II. However, it remains unknown whether certain genes are transcribed in the vicinity of PI(4,5)P2 islets. We would like to identify genes which are associated with nuclear PI(4,5)P2 and whose transcription is connected to PI(4,5)P2 islets.

7.2 What are the other binding partners of nuclear PI(4)P?

Although it is known that PI(4)P is metabolized in the nucleus, its localization, binding partners and functions were unknown. We showed for the first time that PI(4)P localizes to nuclear membrane, nuclear speckles and forms small nucleoplasmic foci that partially colocalize with H3K4me2. Moreover, we demonstrated that PI(4)P interacts with LSD1. In our future research, we would like to analyse other possible binding partners and identify PI(4)P role in their function.

7.3 How do PIs regulate LSD1 activity?

PIs regulate nuclear processes by two different mechanisms. First, PIs target their binding partners to the sites of their action. Second, PIs bind proteins partners and allosterically regulate their functions. We showed that H3K4me2 demethylase activity of LSD1 can be donwregulated or upregulated by PI(4)P or PI(4,5)P2, respectively. However, how this regulation is achieved is unclear. We would like to elucidate the mechanism of LSD1 regulation. Moreover, LSD1 can bind also other PIs as PI(3,4)P2, PI(3,5)P2 and PI(3,4,5)P3. Although these PIs are present in minor amounts in the cell, we would like to investigate whether and to which extend they can regulate LSD1 function.

7.4 What is the role of PI(3)P in nucleolus?

Previously, we have shown that PI(4,5)P2 is synthesized at rDNA promoter and regulates RNA Pol I transcription (Yildirim et al. 2013). Here, we have detected PI(3)P in nucleoli of U2Os cells by specific EEA1-FYVE domain. Since PI(3)P is not a direct product of PI(4,5)P2 (de)phosphorylation, it has probably its own unique roles in the nucleolus. We would like to investigate these functions.

8. REFERENCES

Ahn JY, Liu X, Cheng D, et al (2005) Nucleophosmin/B23, a nuclear PI(3,4,5)P3 receptor, mediates the antiapoptotic actions of NGF by inhibiting CAD. Mol Cell 18:435–445. doi: 10.1016/j.molcel.2005.04.010

Ahn J-Y, Rong R, Liu X, Ye K (2004) PIKE/nuclear PI 3-kinase signaling mediates the antiapoptotic actions of NGF in the nucleus. EMBO J 23:3995–4006. doi: 10.1038/sj.emboj.7600392

Almuzzaini B, Sarshad AA, Farrants A-KÖ, Percipalle P (2015) Nuclear myosin 1 contributes to a chromatin landscape compatible with RNA polymerase II transcription activation. BMC Biol 13:35. doi: 10.1186/s12915-015-0147-z

Amente S, Lania L, Majello B (2013) The histone LSD1 demethylase in stemness and cancer transcription programs. Biochim Biophys Acta 1829:981–6. doi: 10.1016/j.bbagrm.2013.05.002

Baarlink C, Wang H, Grosse R (2013) Nuclear actin network assembly by formins regulates the SRF coactivator MAL. Science 340:864–7. doi: 10.1126/science.1235038

Bacqueville D, Déléris P, Mendre C, et al (2001) Characterization of a G protein-activated phosphoinositide 3-kinase in vascular smooth muscle cell nuclei. J Biol Chem 276:22170–6. doi: 10.1074/jbc.M011572200

Balla T (2013) Phosphoinositides: Tiny Lipids With Giant Impact on Cell Regulation. Physiol Rev 93:1019–1137. doi: 10.1152/physrev.00028.2012

Balla T, Várnai P (2009) Visualization of cellular phosphoinositide pools with GFP-fused protein-domains. Curr Protoc Cell Biol Chapter 24:Unit 24.4. doi: 10.1002/0471143030.cb2404s42

Beh CT, Rine J (2004) A role for yeast oxysterol-binding protein homologs in endocytosis and in the maintenance of intracellular sterol-lipid distribution. J Cell Sci 117:2983–96. doi: 10.1242/jcs.01157

Belin BJ, Cimini BA, Blackburn EH, Mullins RD (2013) Visualization of actin filaments and monomers in somatic cell nuclei. Mol Biol Cell 24:982–94. doi: 10.1091/mbc.E12-09-0685

Bell SP, Learned RM, Jantzen HM, Tjian R (1988) Functional cooperativity between transcription factors UBF1 and SL1 mediates human ribosomal RNA synthesis. Science 241:1192–7.

Bertagnolo V, Marchisio M, Capitani S, Neri LM (1997) Intranuclear translocation of phospholipase C beta2 during HL-60 myeloid differentiation. Biochem Biophys Res Commun 235:831–7. doi: 10.1006/bbrc.1997.6893

Bertagnolo V, Mazzoni M, Ricci D, et al (1995) Identification of PI-PLC beta 1, gamma 1, and delta 1 in rat liver: subcellular distribution and relationship to inositol lipid nuclear signalling. Cell Signal 7:669–78.

Bertagnolo V, Neri LM, Marchisio M, et al (1999) Phosphoinositide 3-Kinase Activity Is Essential for all- trans -Retinoic Acid-induced Granulocytic Differentiation of HL-60 Cells Granulocytic Differentiation of HL-60 Cells. Cancer Res 59:542–546.

Blagoveshchenskaya A, Fei YC, Rohde HM, et al (2008) Integration of Golgi trafficking and growth factor signaling by the lipid phosphatase SAC1. J Cell Biol 180:803–812. doi: 10.1083/jcb.200708109

Blind RD, Sablin EP, Kuchenbecker KM, et al (2014) The signaling phospholipid PIP3 creates a new interaction surface on the nuclear receptor SF-1. Proc Natl Acad Sci U S A 111:15054–9. doi: 10.1073/pnas.1416740111

Blind RD, Suzawa M, Ingraham HA (2012) Direct modification and activation of a nuclear receptor-PIP_2 complex by the inositol lipid kinase IPMK. Sci Signal 5:ra44. doi: 10.1126/scisignal.2003111

Borgatti P, Martelli AM, Tabellini G, et al (2003) Threonine 308 phosphorylated form of Akt translocates to the nucleus of PC12 cells under nerve growth factor stimulation and associates with the nuclear matrix protein nucleolin. J Cell Physiol 196:79–88. doi: 10.1002/jcp.10279

Boronenkov I V, Loijens JC, Umeda M, Anderson R a (1998) Phosphoinositide signaling pathways in nuclei are associated with nuclear speckles containing pre-mRNA processing factors. Mol Biol Cell 9:3547–3560.

Boucrot E, Ferreira APA, Almeida-Souza L, et al (2015) Endophilin marks and controls a clathrin-

independent endocytic pathway. Nature 517:460–5. doi: 10.1038/nature14067
Brodie C, Blumberg PM (2003) Regulation of cell apoptosis by protein kinase c. Apoptosis 8:19–27. doi: 10.1023/A:1021640817208
Bronner C, Krifa M, Mousli M (2013) Increasing role of UHRF1 in the reading and inheritance of the epigenetic code as well as in tumorogenesis. Biochem Pharmacol 86:1643–1649. doi: 10.1016/j.bcp.2013.10.002
Bua DJ, Martin GM, Binda O, Gozani O (2013) Nuclear phosphatidylinositol-5-phosphate regulates ING2 stability at discrete chromatin targets in response to DNA damage. Sci Rep 3:2137. doi: 10.1038/srep02137
Clarke JH, Emson PC, Irvine RF (2009) Distribution and neuronal expression of phosphatidylinositol phosphate kinase IIγ in the mouse brain. J Comp Neurol 517:296–312. doi: 10.1002/cne.22161
Clarke JH, Irvine RF (2012) The activity, evolution and association of phosphatidylinositol 5-phosphate 4-kinases. Adv Biol Regul 52:40–5. doi: 10.1016/j.advenzreg.2011.09.002
Cocco L, Gilmour RS, Ognibene A, et al (1987) Synthesis of polyphosphoinositides in nuclei of Friend cells. Evidence for polyphosphoinositide metabolism inside the nucleus which changes with cell differentiation. Biochem J 248:765–70.
Cooney MA, Malcuit C, Cheon B, et al (2010) Species-specific differences in the activity and nuclear localization of murine and bovine phospholipase C zeta 1. Biol Reprod 83:92–101. doi: 10.1095/biolreprod.109.079814
Croston GE, Kerrigan LA, Lira LM, et al (1991) Sequence-specific antirepression of histone H1-mediated inhibition of basal RNA polymerase II transcription. Science 251:643–9.
Damen JE, Liu L, Rosten P, et al (1996) The 145-kDa protein induced to associate with Shc by multiple cytokines is an inositol tetraphosphate and phosphatidylinositol 3,4,5-triphosphate 5-phosphatase. Proc Natl Acad Sci U S A 93:1689–93.
de Graaf P, Klapisz EE, Schulz TKF, et al (2002) Nuclear localization of phosphatidylinositol 4-kinase beta. J Cell Sci 115:1769–75.
de Lartigue J, Polson H, Feldman M, et al (2009) PIKfyve regulation of endosome-linked pathways. Traffic 10:883–893. doi: 10.1111/j.1600-0854.2009.00915.x
de Saint-Jean M, Delfosse V, Douguet D, et al (2011) Osh4p exchanges sterols for phosphatidylinositol 4-phosphate between lipid bilayers. J Cell Biol 195:965–78. doi: 10.1083/jcb.201104062
De Vries KJ, Westerman J, Bastiaens PI, et al (1996) Fluorescently labeled phosphatidylinositol transfer protein isoforms (alpha and beta), microinjected into fetal bovine heart endothelial cells, are targeted to distinct intracellular sites. Exp Cell Res 227:33–9. doi: 10.1006/excr.1996.0246
Déléris P, Bacqueville D, Gayral S, et al (2003) SHIP-2 and PTEN are expressed and active in vascular smooth muscle cell nuclei, but only SHIP-2 is associated with nuclear speckles. J Biol Chem 278:38884–91. doi: 10.1074/jbc.M300816200
Didichenko S a, Thelen M (2001) Phosphatidylinositol 3-kinase c2alpha contains a nuclear localization sequence and associates with nuclear speckles. J Biol Chem 276:48135–42. doi: 10.1074/jbc.M104610200
Dove SK, Cooke FT, Douglas MR, et al (1997) Osmotic stress activates phosphatidylinositol-3,5-bisphosphate synthesis. Nature 390:187–192. doi: 10.1038/36613
Duex JE, Nau JJ, Kauffman EJ, Weisman LS (2006) Phosphoinositide 5-phosphatase Fig 4p is required for both acute rise and subsequent fall in stress-induced phosphatidylinositol 3,5-bisphosphate levels. Eukaryot Cell 5:723–31. doi: 10.1128/EC.5.4.723-731.2006
Dupuis-Coronas S, Lagarrigue F, Ramel D, et al (2011) The nucleophosmin-anaplastic lymphoma kinase oncogene interacts, activates, and uses the kinase PIKfyve to increase invasiveness. J Biol Chem 286:32105–14. doi: 10.1074/jbc.M111.227512
Ehm P, Nalaskowski MM, Wundenberg T, Jücker M (2015) The tumor suppressor SHIP1 colocalizes in nucleolar cavities with p53 and components of PML nuclear bodies. Nucleus 6:154–164. doi: 10.1080/19491034.2015.1022701

Ellson C, Davidson K, Anderson K, et al (2006) PtdIns3P binding to the PX domain of p40phox is a physiological signal in NADPH oxidase activation. EMBO J 25:4468–78. doi: 10.1038/sj.emboj.7601346
Ellson CD, Gobert-Gosse S, Anderson KE, et al (2001) PtdIns(3)P regulates the neutrophil oxidase complex by binding to the PX domain of p40(phox). Nat Cell Biol 3:679–82. doi: 10.1038/35083076
Elong Edimo W, Derua R, Janssens V, et al (2011) Evidence of SHIP2 Ser132 phosphorylation, its nuclear localization and stability. Biochem J 439:391–401. doi: 10.1042/BJ20110173
Fenech M, Kirsch-Volders M, Natarajan AT, et al (2011) Molecular mechanisms of micronucleus, nucleoplasmic bridge and nuclear bud formation in mammalian and human cells. Mutagenesis 26:125–32. doi: 10.1093/mutage/geq052
Fiume R, Ramazzotti G, Faenza I, et al (2012) Nuclear PLCs affect insulin secretion by targeting PPARγ in pancreatic β cells. FASEB J 26:203–10. doi: 10.1096/fj.11-186510
Fuke H, Ohno M (2008) Role of poly (A) tail as an identity element for mRNA nuclear export. Nucleic Acids Res 36:1037–49. doi: 10.1093/nar/gkm1120
Garcia-Ramirez M, Rocchini C, Ausio J (1995) Modulation of chromatin folding by histone acetylation. J Biol Chem 270:17923–8.
Gaullier JM, Simonsen A, D'Arrigo A, et al (1998) FYVE fingers bind PtdIns(3)P. Nature 394:432–3. doi: 10.1038/28767
Gelato KA, Tauber M, Ong MS, et al (2014) Accessibility of different histone H3-binding domains of UHRF1 is allosterically regulated by phosphatidylinositol 5-phosphate. Mol Cell 54:905–19. doi: 10.1016/j.molcel.2014.04.004
Gillooly DJ, Morrow IC, Lindsay M, et al (2000) Localization of phosphatidylinositol 3-phosphate in yeast and mammalian cells. EMBO J 19:4577–4588. doi: 10.1093/emboj/19.17.4577
Gimm O, Perren A, Weng LP, et al (2000) Differential nuclear and cytoplasmic expression of PTEN in normal thyroid tissue, and benign and malignant epithelial thyroid tumors. Am J Pathol 156:1693–700. doi: 10.1016/S0002-9440(10)65040-7
Godi A, Di Campli A, Konstantakopoulos A, et al (2004) FAPPs control Golgi-to-cell-surface membrane traffic by binding to ARF and PtdIns(4)P. Nat Cell Biol 6:393–404. doi: 10.1038/ncb1119
Gozani O, Karuman P, Jones DR, et al (2003) The PHD finger of the chromatin-associated protein ING2 functions as a nuclear phosphoinositide receptor. Cell 114:99–111. doi: 10.1016/S0092-8674(03)00480-X
Guittard G, Gérard A, Dupuis-Coronas S, et al (2009) Cutting edge: Dok-1 and Dok-2 adaptor molecules are regulated by phosphatidylinositol 5-phosphate production in T cells. J Immunol 182:3974–8. doi: 10.4049/jimmunol.0804172
Guittard G, Mortier E, Tronchère H, et al (2010) Evidence for a positive role of PtdIns5P in T-cell signal transduction pathways. FEBS Lett 584:2455–60. doi: 10.1016/j.febslet.2010.04.051
Hammond GR V, Balla T (2015) Polyphosphoinositide binding domains: Key to inositol lipid biology. Biochim Biophys Acta 1851:746–758. doi: 10.1016/j.bbalip.2015.02.013.Polyphosphoinositide
Han BK, Emr SD (2011) Phosphoinositide [PI(3,5)P2] lipid-dependent regulation of the general transcriptional regulator Tup1. Genes Dev 25:984–995. doi: 10.1101/gad.1998611
Hofmann WA, Vargas GM, Ramchandran R, et al (2006) Nuclear myosin I is necessary for the formation of the first phosphodiester bond during transcription initiation by RNA polymerase II. J Cell Biochem 99:1001–9. doi: 10.1002/jcb.21035
Hokanson DE, Laakso JM, Lin T, et al (2006) Myo1c binds phosphoinositides through a putative pleckstrin homology domain. Mol Biol Cell 17:4856–65. doi: 10.1091/mbc.E06-05-0449
Hokanson DE, Ostap EM (2006) Myo1c binds tightly and specifically to phosphatidylinositol 4,5-bisphosphate and inositol 1,4,5-trisphosphate. Proc Natl Acad Sci U S A 103:3118–23. doi: 10.1073/pnas.0505685103
Cheever ML, Sato TK, de Beer T, et al (2001) Phox domain interaction with PtdIns(3)P targets the Vam7 t-SNARE to vacuole membranes. Nat Cell Biol 3:613–8. doi: 10.1038/35083000
Itoh F, Divecha N, Brocks L, et al (2002) The FYVE domain in Smad anchor for receptor activation

(SARA) is sufficient for localization of SARA in early endosomes and regulates TGF-beta/Smad signalling. Genes to Cells 7:321–331. doi: 10.1046/j.1365-2443.2002.00519.x
Ivetac I, Munday AD, Kisseleva M V, et al (2005) The type Ialpha inositol polyphosphate 4-phosphatase generates and terminates phosphoinositide 3-kinase signals on endosomes and the plasma membrane. Mol Biol Cell 16:2218–33. doi: 10.1091/mbc.E04-09-0799
Jean S, Kiger A a. (2012) Coordination between RAB GTPase and phosphoinositide regulation and functions. Nat Rev Mol Cell Biol 13:463–470. doi: 10.1038/nrm3379
Jockusch BM, Schoenenberger C-A, Stetefeld J, Aebi U (2006) Tracking down the different forms of nuclear actin. Trends Cell Biol 16:391–6. doi: 10.1016/j.tcb.2006.06.006
Johnson CA, Goddard JP, Adams RL (1995) The effect of histone H1 and DNA methylation on transcription. Biochem J 305 (Pt 3:791–8.
Jones DR, Bultsma Y, Keune W-J, et al (2006) Nuclear PtdIns5P as a Transducer of Stress Signaling: An In Vivo Role for PIP4Kbeta. Mol Cell 23:685–695. doi: 10.1016/j.molcel.2006.07.014
Jones DR, Foulger R, Keune W-J, et al (2013) PtdIns5P is an oxidative stress-induced second messenger that regulates PKB activation. FASEB J 27:1644–56. doi: 10.1096/fj.12-218842
Jones DR, Gonzalez-Garcia A, Diez E, et al (1999) The Identification of Phosphatidylinositol 3,5-bisphosphate in T-lymphocytes and Its Regulation by Interleukin-2. J Biol Chem 274:18407–18413. doi: 10.1074/jbc.274.26.18407
Jungmichel S, Sylvestersen KB, Choudhary C, et al (2014) Specificity and commonality of the phosphoinositide-binding proteome analyzed by quantitative mass spectrometry. Cell Rep 6:578–91. doi: 10.1016/j.celrep.2013.12.038
Kakuk A, Friedländer E, Vereb G, et al (2006) Nucleolar localization of phosphatidylinositol 4-kinase PI4K230 in various mammalian cells. Cytometry A 69:1174–83. doi: 10.1002/cyto.a.20347
Kakuk A, Friedländer E, Vereb G, et al (2008) Nuclear and nucleolar localization signals and their targeting function in phosphatidylinositol 4-kinase PI4K230. Exp Cell Res 314:2376–88. doi: 10.1016/j.yexcr.2008.05.006
Kanai F, Liu H, Field SJ, et al (2001) The PX domains of p47phox and p40phox bind to lipid products of PI(3)K. Nat Cell Biol 3:675–8. doi: 10.1038/35083070
Kihara A (2001) Two Distinct Vps34 Phosphatidylinositol 3-Kinase Complexes Function in Autophagy and Carboxypeptidase Y Sorting in Saccharomyces cerevisiae. J Cell Biol 152:519–530. doi: 10.1083/jcb.152.3.519
Kim CG, Park D, Rhee SG (1996) The role of carboxyl-terminal basic amino acids in Gqalpha-dependent activation, particulate association, and nuclear localization of phospholipase C-beta1. J Biol Chem 271:21187–92.
Klein BM, Andrews JB, Bannan BA, et al (2008) Phospholipase C beta 4 in mouse hepatocytes: rhythmic expression and cellular distribution. Comp Hepatol 7:8. doi: 10.1186/1476-5926-7-8
Kokai E, Beck H, Weissbach J, et al (2014) Analysis of nuclear actin by overexpression of wild-type and actin mutant proteins. Histochem Cell Biol 141:123–35. doi: 10.1007/s00418-013-1151-4
Krause M, Leslie JD, Stewart M, et al (2004) Lamellipodin, an Ena/VASP ligand, is implicated in the regulation of lamellipodial Dynamics. Dev Cell 7:571–583. doi: 10.1016/j.devcel.2004.07.024
Lachyankar MB, Sultana N, Schonhoff CM, et al (2000) A Role for Nuclear PTEN in Neuronal Differentiation. J Neurosci 20:1404–1413.
Lalli E, Doghman M, Latre de Late P, et al (2013) Beyond steroidogenesis: novel target genes for SF-1 discovered by genomics. Mol Cell Endocrinol 371:154–9. doi: 10.1016/j.mce.2012.11.005
Larman MG, Saunders CM, Carroll J, et al (2004) Cell cycle-dependent Ca2+ oscillations in mouse embryos are regulated by nuclear targeting of PLCzeta. J Cell Sci 117:2513–21. doi: 10.1242/jcs.01109
Layerenza JP, González P, García de Bravo MM, et al (2013) Nuclear lipid droplets: a novel nuclear domain. Biochim Biophys Acta 1831:327–40. doi: 10.1016/j.bbalip.2012.10.005
Leblanc B, Read C, Moss T (1993) Recognition of the Xenopus ribosomal core promoter by the transcription factor xUBF involves multiple HMG box domains and leads to an xUBF interdomain interaction. EMBO J 12:513–25.

Lee DY, Hayes JJ, Pruss D, Wolffe AP (1993) A positive role for histone acetylation in transcription factor access to nucleosomal DNA. Cell 72:73–84.
Lee SB, Xuan Nguyen TL, Choi JW, et al (2008) Nuclear Akt interacts with B23/NPM and protects it from proteolytic cleavage, enhancing cell survival. Proc Natl Acad Sci U S A 105:16584–16589. doi: 10.1073/pnas.0807668105
Levine A, Yeivin A, Ben-Asher E, et al (1993) Histone H1-mediated inhibition of transcription initiation of methylated templates in vitro. J Biol Chem 268:21754–9.
Lewis AE, Sommer L, Arntzen MO, et al (2011) Identification of Nuclear Phosphatidylinositol 4,5-Bisphosphate-Interacting Proteins by Neomycin Extraction. Mol Cell Proteomics 10:M110.003376–M110.003376. doi: 10.1074/mcp.M110.003376
Li W, Laishram RS, Ji Z, et al (2012) Star-PAP control of BIK expression and apoptosis is regulated by nuclear PIPKIα and PKCδ signaling. Mol Cell 45:25–37. doi: 10.1016/j.molcel.2011.11.017
Lindsay Y, McCoull D, Davidson L, et al (2006) Localization of agonist-sensitive PtdIns(3,4,5)P3 reveals a nuclear pool that is insensitive to PTEN expression. J Cell Sci 119:5160–5168. doi: 10.1242/jcs.000133
Lioubin MN, Algate PA, Tsai S, et al (1996) p150Ship, a signal transduction molecule with inositol polyphosphate-5-phosphatase activity. Genes Dev 10:1084–95.
Liu N, Fukami K, Yu H, Takenawa T (1996) A new phospholipase C delta 4 is induced at S-phase of the cell cycle and appears in the nucleus. J Biol Chem 271:355–60.
Maag D, Maxwell MJ, Hardesty DA, et al (2011) Inositol polyphosphate multikinase is a physiologic PI3-kinase that activates Akt/PKB. Proc Natl Acad Sci U S A 108:1391–6. doi: 10.1073/pnas.1017831108
Mais C, Wright JE, Prieto J-L, et al (2005) UBF-binding site arrays form pseudo-NORs and sequester the RNA polymerase I transcription machinery. Genes Dev 19:50–64. doi: 10.1101/gad.310705
Mason D, Mallo G V, Terebiznik MR, et al (2007) Alteration of epithelial structure and function associated with PtdIns(4,5)P2 degradation by a bacterial phosphatase. J Gen Physiol 129:267–83. doi: 10.1085/jgp.200609656
McCartney AJ, Zhang Y, Weisman LS (2014) Phosphatidylinositol 3,5-bisphosphate: low abundance, high significance. Bioessays 36:52–64. doi: 10.1002/bies.201300012
Mellman DL, Gonzales ML, Song C, et al (2008) A PtdIns4,5P2-regulated nuclear poly(A) polymerase controls expression of select mRNAs. Nature 451:1013–1017. doi: 10.1038/nature06666
Metjian A, Roll RL, Ma AD, Abrams CS (1999) Agonists cause nuclear translocation of phosphatidylinositol 3-kinase gamma. A Gbetagamma-dependent pathway that requires the p110gamma amino terminus. J Biol Chem 274:27943–7.
Mills IG, Praefcke GJK, Vallis Y, et al (2003) EpsinR: an AP1/clathrin interacting protein involved in vesicle trafficking. J Cell Biol 160:213–22. doi: 10.1083/jcb.200208023
Miyamoto K, Pasque V, Jullien J, Gurdon JB (2011) Nuclear actin polymerization is required for transcriptional reprogramming of Oct4 by oocytes. Genes Dev 25:946–58. doi: 10.1101/gad.615211
Mizuno-Yamasaki E, Medkova M, Coleman J, Novick P (2010) Phosphatidylinositol 4-phosphate controls both membrane recruitment and a regulatory switch of the Rab GEF Sec2p. Dev Cell 18:828–840. doi: 10.1016/j.devcel.2010.03.016
Mondal N, Parvin JD (2001) DNA topoisomerase IIalpha is required for RNA polymerase II transcription on chromatin templates. Nature 413:435–8. doi: 10.1038/35096590
Morris JB, Hinchliffe KA, Ciruela A, et al (2000) Thrombin stimulation of platelets causes an increase in phosphatidylinositol 5-phosphate revealed by mass assay. FEBS Lett 475:57–60. doi: 10.1016/S0014-5793(00)01625-2
Mougey EB, Pape LK, Sollner-Webb B (1996) Virtually the entire Xenopus laevis rDNA multikilobase intergenic spacer serves to stimulate polymerase I transcription. J Biol Chem 271:27138–45.
Moulding DA, Blundell MP, Spiller DG, et al (2007) Unregulated actin polymerization by WASp causes defects of mitosis and cytokinesis in X-linked neutropenia. J Exp Med 204:2213–24. doi: 10.1084/jem.20062324

Nagashima M, Shiseki M, Miura K, et al (2001) DNA damage-inducible gene p33ING2 negatively regulates cell proliferation through acetylation of p53. Proc Natl Acad Sci U S A 98:9671–6. doi: 10.1073/pnas.161151798

Nalaskowski MM, Deschermeier C, Fanick W, Mayr GW (2002) The human homologue of yeast ArgRIII protein is an inositol phosphate multikinase with predominantly nuclear localization. Biochem J 366:549–56. doi: 10.1042/BJ20020327

Nalaskowski MM, Metzner A, Brehm MA, et al (2012) The inositol 5-phosphatase SHIP1 is a nucleo-cytoplasmic shuttling protein and enzymatically active in cell nuclei. Cell Signal 24:621–8. doi: 10.1016/j.cellsig.2011.07.012

Neri LM, Milani D, Bertolaso L, et al (1994) Nuclear translocation of phosphatidylinositol 3-kinase in rat pheochromocytoma PC 12 cells after treatment with nerve growth factor. Cell Mol Biol (Noisy-le-grand) 40:619–26.

Niebuhr K, Giuriato S, Pedron T, et al (2002) Conversion of PtdIns(4,5)P2 into PtdIns(5)P by the S.flexneri effector IpgD reorganizes host cell morphology. EMBO J 21:5069–5078. doi: 10.1093/emboj/cdf522

Nojima T, Hirose T, Kimura H, Hagiwara M (2007) The interaction between cap-binding complex and RNA export factor is required for intronless mRNA export. J Biol Chem 282:15645–51. doi: 10.1074/jbc.M700629200

O'Sullivan AC, Sullivan GJ, McStay B (2002) UBF binding in vivo is not restricted to regulatory sequences within the vertebrate ribosomal DNA repeat. Mol Cell Biol 22:657–68.

Oikawa T, Itoh T, Takenawa T (2008) Sequential signals toward podosome formation in NIH-src cells. J Cell Biol 182:157–169. doi: 10.1083/jcb.200801042

Okada M, Jang S-W, Ye K (2008) Akt phosphorylation and nuclear phosphoinositide association mediate mRNA export and cell proliferation activities by ALY. Proc Natl Acad Sci U S A 105:8649–8654. doi: 10.1073/pnas.0802533105

Osborne SL, Thomas CL, Gschmeissner S, Schiavo G (2001) Nuclear PtdIns(4,5)P2 assembles in a mitotically regulated particle involved in pre-mRNA splicing. J Cell Sci 114:2501–11.

Patki V, Lawe DC, Corvera S, et al (1998) A functional PtdIns(3)P-binding motif. Nature 394:433–4. doi: 10.1038/28771

Pikaard CS, McStay B, Schultz MC, et al (1989) The Xenopus ribosomal gene enhancers bind an essential polymerase I transcription factor, xUBF. Genes Dev 3:1779–88.

Posor Y, Eichhorn-Gruenig M, Puchkov D, et al (2013) Spatiotemporal control of endocytosis by phosphatidylinositol-3,4-bisphosphate. Nature 499:233–7. doi: 10.1038/nature12360

Putnam CD, Pikaard CS (1992) Cooperative binding of the Xenopus RNA polymerase I transcription factor xUBF to repetitive ribosomal gene enhancers. Mol Cell Biol 12:4970–80.

Ramel D, Lagarrigue F, Pons V, et al (2011) Shigella flexneri infection generates the lipid PI5P to alter endocytosis and prevent termination of EGFR signaling. Sci Signal 4:ra61. doi: 10.1126/scisignal.2001619

Rando OJ, Zhao K, Janmey P, Crabtree GR (2002) Phosphatidylinositol-dependent actin filament binding by the SWI/SNF-like BAF chromatin remodeling complex. Proc Natl Acad Sci U S A 99:2824–9. doi: 10.1073/pnas.032662899

Resnick AC, Snowman AM, Kang BN, et al (2005) Inositol polyphosphate multikinase is a nuclear PI3-kinase with transcriptional regulatory activity. Proc Natl Acad Sci U S A 102:12783–8. doi: 10.1073/pnas.0506184102

Richardson JP, Wang M, Clarke JH, et al (2007) Genomic tagging of endogenous type IIbeta phosphatidylinositol 5-phosphate 4-kinase in DT40 cells reveals a nuclear localisation. Cell Signal 19:1309–14. doi: 10.1016/j.cellsig.2007.01.010

Rutherford AC, Traer C, Wassmer T, et al (2006) The mammalian phosphatidylinositol 3-phosphate 5-kinase (PIKfyve) regulates endosome-to-TGN retrograde transport. J Cell Sci 119:3944–57. doi: 10.1242/jcs.03153

Salamon RS, Backer JM (2013) Phosphatidylinositol-3,4,5-trisphosphate: Tool of choice for class I PI 3-kinases. BioEssays 35:602–611. doi: 10.1002/bies.201200176

Sarkes D, Rameh LE (2010) A novel HPLC-based approach makes possible the spatial characterization of cellular PtdIns5P and other phosphoinositides. Biochem J 428:375–84. doi: 10.1042/BJ20100129

Sbrissa D, Ikonomov OC, Strakova J, Shisheva A (2004) Role for a novel signaling intermediate, phosphatidylinositol 5-phosphate, in insulin-regulated F-actin stress fiber breakdown and GLUT4 translocation. Endocrinology 145:4853–65. doi: 10.1210/en.2004-0489

Scassellati C, Albi E, Cmarko D, et al (2010) Intranuclear sphingomyelin is associated with transcriptionally active chromatin and plays a role in nuclear integrity. Biol Cell 102:361–75. doi: 10.1042/BC20090139

Shah ZH, Jones DR, Sommer L, et al (2013) Nuclear phosphoinositides and their impact on nuclear functions. FEBS J 280:6295–6310. doi: 10.1111/febs.12543

Shi Y, Lan F, Matson C, et al (2004) Histone demethylation mediated by the nuclear amine oxidase homolog LSD1. Cell 119:941–53. doi: 10.1016/j.cell.2004.12.012

Schill NJ, Anderson RA (2009) Two novel phosphatidylinositol-4-phosphate 5-kinase type Igamma splice variants expressed in human cells display distinctive cellular targeting. Biochem J 422:473–82. doi: 10.1042/BJ20090638

Schink KO, Raiborg C, Stenmark H (2013) Phosphatidylinositol 3-phosphate, a lipid that regulates membrane dynamics, protein sorting and cell signalling. BioEssays 35:900–912. doi: 10.1002/bies.201300064

Sindić A, Aleksandrova A, Fields AP, et al (2001) Presence and activation of nuclear phosphoinositide 3-kinase C2beta during compensatory liver growth. J Biol Chem 276:17754–61. doi: 10.1074/jbc.M006533200

Slessareva JE, Routt SM, Temple B, et al (2006) Activation of the Phosphatidylinositol 3-Kinase Vps34 by a G Protein α Subunit at the Endosome. Cell 126:191–203. doi: 10.1016/j.cell.2006.04.045

Smith CD, Wells WW (1983) Phosphorylation of rat liver nuclear envelopes. I. Characterization of in vitro protein phosphorylation. J Biol Chem 258:9360–9367.

Sobol M, Philimonenko V V, Marášek P, et al (2016) Nuclear PIP2 islets contribute to efficient DNA transcription.

Sobol M, Yildirim S, Philimonenko V V, et al (2013) UBF complexes with phosphatidylinositol 4,5-bisphosphate in nucleolar organizer regions regardless of ongoing RNA polymerase I activity. Nucleus 4:478–86. doi: 10.4161/nucl.27154

Spector DL, Lamond AI (2011) Nuclear speckles. Cold Spring Harb Perspect Biol 3:a000646–. doi: 10.1101/cshperspect.a000646

Strahl T, Hama H, DeWald DB, Thorner J (2005) Yeast phosphatidylinositol 4-kinase, Pik1, has essential roles at the Golgi and in the nucleus. J Cell Biol 171:967–979. doi: 10.1083/jcb.200504104

Sun Y, Thapa N, Hedman AC, Anderson RA (2013) Phosphatidylinositol 4,5-bisphosphate: Targeted production and signaling. BioEssays 35:513–522. doi: 10.1002/bies.201200171

Szivak I, Lamb N, Heilmeyer LMG (2006) Subcellular localization and structural function of endogenous phosphorylated phosphatidylinositol 4-kinase (PI4K92). J Biol Chem 281:16740–16749. doi: 10.1074/jbc.M511645200

Tabellini G, Bortul R, Santi S, et al (2003) Diacylglycerol kinase-θ is localized in the speckle domains of the nucleus. Exp Cell Res 287:143–154. doi: 10.1016/S0014-4827(03)00115-0

Tan X, Thapa N, Choi S, Anderson RA (2015) Emerging roles of PtdIns(4,5)P2 - beyond the plasma membrane. J Cell Sci 128:4047–56. doi: 10.1242/jcs.175208

Tanaka K, Horiguchi K, Yoshida T, et al (1999) Evidence That a Phosphatidylinositol 3,4,5-Trisphosphate-binding Protein Can Function in Nucleus. J Biol Chem 274 :3919–3922. doi: 10.1074/jbc.274.7.3919

Tollervey D, Lehtonen H, Jansen R, et al (1993) Temperature-sensitive mutations demonstrate roles for yeast fibrillarin in pre-rRNA processing, pre-rRNA methylation, and ribosome assembly. Cell 72:443–57.

Toska E, Campbell HA, Shandilya J, et al (2012) Repression of Transcription by WT1-BASP1 Requires

the Myristoylation of BASP1 and the PIP2-Dependent Recruitment of Histone Deacetylase. Cell Rep 2:462–469. doi: 10.1016/j.celrep.2012.08.005
Tóth B, Balla A, Ma H, et al (2006) Phosphatidylinositol 4-kinase IIIbeta regulates the transport of ceramide between the endoplasmic reticulum and Golgi. J Biol Chem 281:36369–77. doi: 10.1074/jbc.M604935200
Tsukazaki T, Chiang TA, Davison AF, et al (1998) SARA, a FYVE Domain Protein that Recruits Smad2 to the TGFβ Receptor. Cell 95:779–791. doi: 10.1016/S0092-8674(00)81701-8
Ungewickell A, Hugge C, Kisseleva M, et al (2005) The identification and characterization of two phosphatidylinositol-4,5-bisphosphate 4-phosphatases. Proc Natl Acad Sci U S A 102:18854–9. doi: 10.1073/pnas.0509740102
Vanhaesebroeck B, Leevers SJ, Ahmadi K, et al (2001) Synthesis and function of 3-phosphorylated inositol lipids. Annu Rev Biochem 70:535–602. doi: 10.1146/annurev.biochem.70.1.535
Vann LR, Wooding FB, Irvine RF, Divecha N (1997) Metabolism and possible compartmentalization of inositol lipids in isolated rat-liver nuclei. Biochem J 327 (Pt 2:569–576.
Viaud J, Boal F, Tronchère H, et al (2014) Phosphatidylinositol 5-phosphate: a nuclear stress lipid and a tuner of membranes and cytoskeleton dynamics. Bioessays 36:260–72. doi: 10.1002/bies.201300132
Viaud J, Mansour R, Antkowiak A, et al (2015) Phosphoinositides: Important lipids in the coordination of cell dynamics. Biochimie. doi: 10.1016/j.biochi.2015.09.005
Viiri K, Mäki M, Lohi O (2012) Phosphoinositides as regulators of protein-chromatin interactions. Sci Signal 5:pe19. doi: 10.1126/scisignal.2002917
Wang M, Bond NJ, Letcher AJ, et al (2010) Genomic tagging reveals a random association of endogenous PtdIns5P 4-kinases IIalpha and IIbeta and a partial nuclear localization of the IIalpha isoform. Biochem J 430:215–21. doi: 10.1042/BJ20100340
Wang Y, Li X, Hu H (2014) H3K4me2 reliably defines transcription factor binding regions in different cells. Genomics 103:222–8. doi: 10.1016/j.ygeno.2014.02.002
Wang YJ, Wang J, Sun HQ, et al (2003) Phosphatidylinositol 4 Phosphate Regulates Targeting of Clathrin Adaptor AP-1 Complexes to the Golgi. Cell 114:299–310. doi: 10.1016/S0092-8674(03)00603-2
Wickramasinghe V, Savill J, Chavali S, et al (2013) Human Inositol Polyphosphate Multikinase Regulates Transcript-Selective Nuclear mRNA Export to Preserve Genome Integrity. Mol Cell 51:737–750. doi: 10.1016/j.molcel.2013.08.031
Wilcox A, Hinchliffe KA (2008) Regulation of extranuclear PtdIns5P production by phosphatidylinositol phosphate 4-kinase 2alpha. FEBS Lett 582:1391–4. doi: 10.1016/j.febslet.2008.03.022
Wullschleger S, Wasserman DH, Gray A, et al (2011) Role of TAPP1 and TAPP2 adaptor binding to PtdIns(3,4)P2 in regulating insulin sensitivity defined by knock-in analysis. Biochem J 434:265–74. doi: 10.1042/BJ20102012
Xu Y, Hortsman H, Seet L, et al (2001) SNX3 regulates endosomal function through its PX-domain-mediated interaction with PtdIns(3)P. Nat Cell Biol 3:658–66. doi: 10.1038/35083051
Xuan Nguyen TL, Choi JW, Lee SB, et al (2006) Akt phosphorylation is essential for nuclear translocation and retention in NGF-stimulated PC12 cells. Biochem Biophys Res Commun 349:789–798. doi: 10.1016/j.bbrc.2006.08.120
Yamaga M, Fujii M, Kamata H, et al (1999) Phospholipase C-delta1 contains a functional nuclear export signal sequence. J Biol Chem 274:28537–41.
Yamaji T, Kumagai K, Tomishige N, Hanada K (2008) Two sphingolipid transfer proteins, CERT and FAPP2: their roles in sphingolipid metabolism. IUBMB Life 60:511–8. doi: 10.1002/iub.83
Ye J, Zhao J, Hoffmann-Rohrer U, Grummt I (2008) Nuclear myosin I acts in concert with polymeric actin to drive RNA polymerase I transcription. Genes Dev 22:322–30. doi: 10.1101/gad.455908
Yildirim S, Castano E, Sobol M, et al (2013) Involvement of phosphatidylinositol 4,5-bisphosphate in RNA polymerase I transcription. J Cell Sci 126:2730–9. doi: 10.1242/jcs.123661
Yoda A, Oda S, Shikano T, et al (2004) Ca2+ oscillation-inducing phospholipase C zeta expressed in

mouse eggs is accumulated to the pronucleus during egg activation. Dev Biol 268:245–57. doi: 10.1016/j.ydbio.2003.12.028

Yoo SH, Huh YH, Huh SK, et al (2014) Localization and projected role of phosphatidylinositol 4-kinases IIα and IIβ in inositol 1,4,5-trisphosphate-sensitive nucleoplasmic Ca^{2+} store vesicles. Nucleus 5:341–51. doi: 10.4161/nucl.29776

York JD, Majerus PW (1994) Nuclear phosphatidylinositols decrease during S-phase of the cell cycle in HeLa cells [published erratum appears in J Biol Chem 1994 Dec 9;269(49):31322]. J Biol Chem 269:7847–7850.

Yu H, Fukami K, Watanabe Y, et al (1998) Phosphatidylinositol 4,5-bisphosphate reverses the inhibition of RNA transcription caused by histone H1. Eur J Biochem 251:281–287.

Zhang Y, Zolov SN, Chow CY, et al (2007) Loss of Vac14, a regulator of the signaling lipid phosphatidylinositol 3,5-bisphosphate, results in neurodegeneration in mice. Proc Natl Acad Sci U S A 104:17518–23. doi: 10.1073/pnas.0702275104

Zhao K, Wang W, Rando OJ, et al (1998) Rapid and phosphoinositol-dependent binding of the SWI/SNF-like BAF complex to chromatin after T lymphocyte receptor signaling. Cell 95:625–636. doi: 10.1016/S0092-8674(00)81633-5

Zini N, Martelli AM, Cocco L, et al (1993) Phosphoinositidase C isoforms are specifically localized in the nuclear matrix and cytoskeleton of Swiss 3T3 cells. Exp Cell Res 208:257–69. doi: 10.1006/excr.1993.1245

Zini N, Ognibene A, Bavelloni A, et al (1996) Cytoplasmic and nuclear localization sites of phosphatidylinositol 3-kinase in human osteosarcoma sensitive and multidrug-resistant Saos-2 cells. Histochem Cell Biol 106:457–64.

Zou J, Marjanovic J, Kisseleva M V, et al (2007) Type I phosphatidylinositol-4,5-bisphosphate 4-phosphatase regulates stress-induced apoptosis. Proc Natl Acad Sci U S A 104:16834–16839. doi: 10.1073/pnas.0708189104